Traffic Modelling for Intelligent Transportation Systems

by

Zawar Khan
B.Sc., University of Engineering and Technology, Peshawar, Pakistan, 2006
M.S., George Washington University,Washington DC, USA, 2009

A Dissertation Submitted in Partial Fullfilment of the Requirements for the Degree of

DOCTOR OF PHILOSOPHY

in the Department of Electrical and Computer Engineering

Traffic Modelling for Intelligent Transportation Systems

by

Zawar Khan
B.Sc., University of Engineering and Technology, Peshawar, Pakistan, 2006
M.S., George Washington University,Washington DC, USA, 2009

Supervisory Committee

Dr. T. A. Gulliver, Supervisor
(Department of Electrical and Computer Engineering)

Dr. Mihai Sima, Departmental Member
(Department of Electrical and Computer Engineering)

Dr. Brad Buckham, Outside Member
(Department of Mechanical Engineering)

Supervisory Committee

Dr. T. A. Gulliver, Supervisor
(Department of Electrical and Computer Engineering)

Dr. Mihai Sima, Departmental Member
(Department of Electrical and Computer Engineering)

Dr. Brad Buckham, Outside Member
(Department of Mechanical Engineering)

ABSTRACT

In this dissertation, we study macroscopic traffic flow modeling for intelligent transportation systems. Based on the characteristics of traffic flow evolution, and the requirement to realistically predict and ameliorate traffic flow in high traffic regions, we consider traffic flow modeling for intelligent transportation systems. Four major traffic flow modeling issues, that is, accurately predicting the spatial adjustment of traffic density, the traffic behavior on a long infinite road and on a road having egress and ingress to the flow, affect of driver behavior on traffic flow, and the route merit are investigated. The spatial adjustment of traffic density is investigated from a velocity adjustment perspective. Then the traffic behavior based on the safe distance and safe time is studied on a long infinite road for a transition and uniform flow. The traffic flow transition behavior is also investigated for egress and ingress to the flow having a regulation value which characterizes the driver response. The variation of regulation value refines the traffic velocity and density distributions according to a slow or aggressive driver response. Further, the influence of driver behavior on traffic flow is studied. The driver behavior includes the physiological and psychological response. In this dissertation, route merits are also developed to reduce the trip time, pollution and fuel consumption. Performance results of the proposed models are presented.

Contents

List of Tables

List of Figures

ACKNOWLEDGEMENTS

First of all, I would like to thank Allah, the most Beneficent and Merciful, for giving me the patience, courage, intelligence, love and strength to make this work possible. I am really indebted to my Creator for being a great teacher and mentor.

I would like to thank my supervisor, Dr. T. A. Gulliver, for giving me the opportunity to work under his supervision in the field of intelligent transportation systems, and for his continuous support, patience, encouragement, always availability even after 5 pm and self fostering research environment provided during my PhD studies.

I would present thanks to Dr. Mihia Sima from UVIC ECE department and Dr. Brad Buckham from UVIC Mechanical department, for their valuable feedback while serving as my PhD advisory committee members. I am also indebted to Dr. Shahram Payandeh from Simon Fraser university for serving as external examiner.

I would like to express my special thanks to Dr. Ahmed Altamimi, Khurrum Khattak from GWU, Muhammad Hanif, Dr. Ning, Ahsan, Arash Ghayoori, Dr. Kenza and Manzoor Abro for being friends and sharing their experience without any hesitation.

I am also indebted to all my teachers and mentors whose hard efforts made this encouragement possible.

Many thanks and love to my family members, specially my wife and three young daughters who patiently supported me during my doctoral program. I believe my wife deserves an honorary PhD degree. I remember the days when my kids used to wait for me late in the evenings, to play around, when I would be free from my studies. I would express my gratitude to my brother (Fawad Khan), uncles (Shamim Khan, Dr. Iftikhar Ahmad) and aunt (Shaheen Bibi) for their continuous encouragement and support.

For each new morning with its light,
For rest and shelter of the night,
For health and food, for love and friends,
For everything Thy goodness sends
Ralph Waldo Emerson

DEDICATION

To
Sultan Khan and Kausar Begum (my parents),
Shumaila Khan (my wife)
and
Shaima, Zarina and Hibba (my sweet daughters)

List of Acronyms

Acronym	Definition
AR model	AW and Rascle model
BMW model	Berg, Mason and Woods model
CFL condition	Courant-Friedrichs-Levy condition
KG model	Khan and Gulliver model
LWR model	Lighthill, Witham and Richards model
PW model	Payne and Witham model
ρ	Average traffic density
v	Average velocity
ρv	Traffic flow
ρ_m	Maximum traffic density
v_m	Maximum velocity
$v(\rho)$	Equilibrium velocity distribution
G	Vector of data variables
$f(G)$	Vector of the functions of the data variables
$A(G)$	Jacobian matrix
$S(G)$	Vector of source terms
δt	Time step
δx	Segment length
ΔG	Change in data variables
Δf	Change in the functions of data variables
N	Number of road segments
M	Number of time steps
t_M	Total simulation time
λ_k	Eigenvalues
Λ	Diagonal matrix of the eigenvalues

C_0	Velocity constant
τ	Relaxation time
d_{tr}	Transition distance
d_r	Reaction distance
l_s	Distance between vehicles at stand still position
e	Eigenvector
ρ_0	Initial density at zero time
$\rho_{i+\frac{1}{2}}$	Average density at the boundary of segments
$v_{i+\frac{1}{2}}$	Average velocity at the boundary of segments
$a(\rho)$	Acceleration distribution
d_s	Safe distance
t_s	Safe time
v_a	Velocity at transitions
v_s	Safe velocity
ζ	Sensitivity
b	Regulation value
p	Pressure
V	Volume
R_s	Specific gas constant
z	Molar mass
$\tau(\rho)$	Perception time
β	Driver attitude
L_d	Traffic constant
S	Driver awareness
M_n	Mach number
T_{tr}	Relative trip time
R	Traffic resistance
R_r	Minimum resistance of a route
P_r	Probability of a route

Chapter 1

Introduction

1.1 Motivation and Background

Traffic modeling has gained significant importance since the appearance of traffic jams in the last decades. Traffic modeling is the characterization of traffic behavior. Congested areas of traffic are those regions where volume of traffic due to traffic density is high. It is envisioned that if a model accurately characterizes traffic behavior for initial set of data, then employment of such model at congested areas will ameliorate the traffic flow. Development of high traffic density over the distance along the road is due to slow moving vehicles, accidents and traffic control elements. Employment of models which accurately characterize traffic behavior will improve utilization of road infrastructure as well as mitigate congestion and pollution. These models will also reduce trip time and travelling cost. Traffic will take form of a pre-controlled system by adjusting the traffic characteristics in advance. Examples include the dynamic changes in traffic signs, overhead vehicle velocity monitored devices and synchronized flow with traffic lamps. In this dissertation, new models are proposed to accurately characterize the traffic flow behavior to improve the traffic conditions.

Traffic flow is categorized on the basis of traffic conditions on the road. The terms used for traffic flow are homogeneous, inhomogeneous, equilibrium and non-equilibrium flow. Inhomogeneous flow corresponds to traffic flow on a road with different parameters at different locations, other wise flow is homogeneous.

Equilibrium flow is defined as the traffic flow whose velocity is a unique function of density, otherwise flow is non-equilibrium. The velocity at equilibrium flow is known as equilibrium velocity. Several models have been proposed for equilibrium velocity

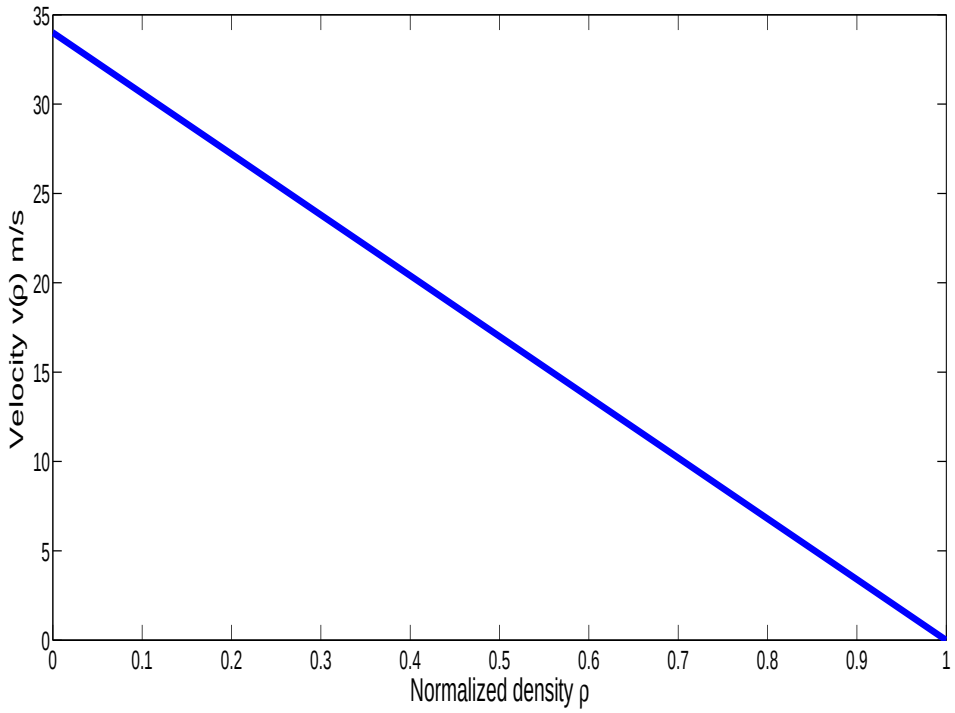

Figure 1.1: Greenshilelds equilibrium velocity distribution.

in the literature. The most commonly employed model is the Greenshields model [60] which is given by

$$v(\rho) = v_m \left(1 - \frac{\rho}{\rho_m}\right), \tag{1.1}$$

where ρ_m and ρ are the maximum and average traffic densities, respectively, and v_m is the maximum velocity on the road. This shows that the density and velocity are inversely related, so that velocity increases as the traffic density decreases and vice versa.

Figure 1.1 demonstrates (1.1) with $\rho_m = 1$ and $v_m = 34$ m/s. The average normalized density ρ is varied from zero to $\rho_m = 1$. For minimum traffic density, traffic has maximum velocity. At higher densities, velocity reduces and ultimately reaches to zero m/s for 100% density on the road.

The traffic flow ρv based on equilibrium velocity distribution is given by Figure 1.2, which gives the flow information with change in density. It shows that flow of traffic is maximum at 0.5 normalized density. 0.5 is the critical density, beyond which the traffic flow reduces with the rise in density and traffic moves to congested zone.

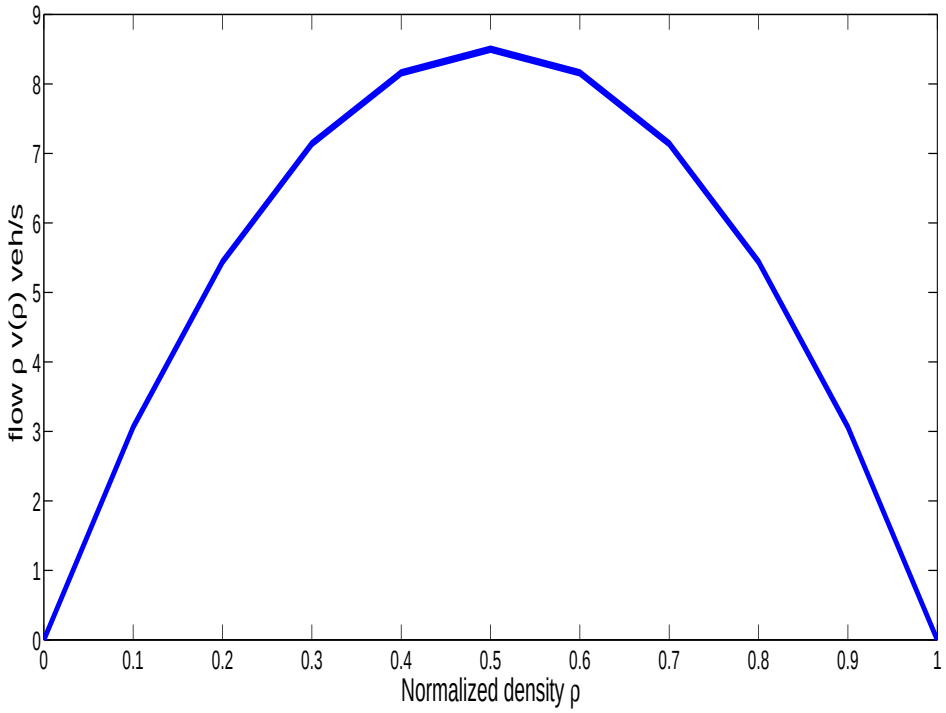

Figure 1.2: Traffic flow based on Greenshields velocity distribution.

There are three main types of traffic models. Macroscopic models consider the collective flow of vehicles, whereas microscopic models are used to examine the temporal and spatial behavior of drivers based on the influence of vehicles in their proximity. Mesoscopic models share the properties of macroscopic and microscopic traffic models as the time-space traffic flow behavior is modelled using probability distributions and queuing theory. In this case, vehicles are modeled at an individual level and the aggregate behavior is approximated. Thus, small groups of vehicles and their interactions are considered. Examples include lane changing decisions based on velocity and density distributions, and traffic acceleration based on velocity distributions. Macroscopic models are the most commonly employed because of their low complexity and good overall performance.

In macroscopic models, the velocity and density are used to determine the cumulative behavior of the traffic. The density ρ is the average number of vehicles on a road segment per unit length, and the traffic flow is the product of velocity v and density ρ, and so is measured in terms of vehicles per unit time. Lighthill, Whitham and Richards [2, 41] developed a macroscopic traffic flow model (known as the LWR model), which is based on the equilibrium flow of vehicles. They assumed vehicles adjust their velocity in zero time [55], and ignored transitions in the traffic flow.

Some of the deficiencies of the LWR model are overcome by the Payne model [1], which is a two equation model. The first equation is based on the continuity equation for the conservation of vehicles on a road. The second equation models the acceleration behavior of traffic based on driver anticipation, relaxation and traffic inertia. Driver anticipation results from a presumption of changes in the forward traffic density, while relaxation is the tendency of traffic to adjust its velocity to a desirable velocity [53]. Inertia encompasses the spatial and temporal changes in traffic acceleration. Witham independently developed a similar model [7] which is known as the Payne-Witham (PW) model. This model is based on the assumption that vehicles on a road have similar behavior. Smooth traffic velocities and density distributions are assumed [3], i.e. the traffic velocity and density vary continuously in space and time. Unfortunately, this can result in unrealistic velocity and density behavior for abrupt changes (discontinuities) in the traffic flow [55]. Del Castillo et al. [4] improved the PW model by incorporating the anticipation and reaction time for small changes in density and velocity. The anticipation term characterizes driver behavior such as the response to changes in the forward traffic density. However, Daganzo [3] criticized the Del Castillo et al. model because the anticipation term is

too large and so does not accurately model the physical behavior of traffic. Aw and Rascle [8] provided an improved traffic model in which driver perception of temporal and spatial changes in the traffic is assumed to be an increasing function of the traffic density. However, the velocity profile of the traffic is not considered. It is assumed that greater braking and acceleration occurs for a higher forward density regardless of the velocity profile of the traffic.

The PW model was also improved by Berg, Mason and Woods, who developed the BMW model [10] based on the headway developed between vehicles. At abrupt changes in traffic flow, the spatial adjustment of traffic results in large traffic density variations which evolve in space and time. A noise term based on the density is used to reduce these variations and smooth the traffic flow so that it is more realistic. Other macroscopic traffic models incorporate a similar term based on the second derivative of the traffic velocity or density.

Some scientists looked into the traffic velocity in traffic flow modelling as metric of fuel consumption and emission of pollutants to air [19], while others defined it as route merit. A route merit is also defined as a trade off between distance, time, congestion, difficulty and toll [24]. This route merit can also be on the basis of travel time [26], [24] or distance [27]. The route merit is also based on the drivers familiarity to the route and the delay occurred at traffic lamps [23].

From thorough investigation of the field, it is found that there are still some significant improvements to be made. The most important is the adjustment of traffic flow behavior based on the anticipated traffic conditions.

In this dissertation, we study the macroscopic traffic class to accurately model the average behavior of traffic which fit well with the reality. More specifically, spatial adjustment of traffic density in proportion to the anticipated traffic changes, affect of driver response, distribution of traffic flow to achieve the anticipated changes and a route merit will be systematically examined.

To evaluate the performance, Roe decomposition technique is used to implement the two equation traffic flow models, whereas the Godunov scheme is used to implement the single equation traffic flow model, in this dissertation. The Roe technique is presented in Section 1.2.

1.2 Roe Decomposition Technique

The traffic models are discretized using Roe decomposition technique [11] to evaluate their performance. This technique can be used to approximate a nonlinear system of equations

$$G_t + f(G)_x = S(G), \tag{1.2}$$

where G denotes the vector of data variables, $f(G)$ denotes the vector of functions of the data variables, and $S(G)$ is the vector of source terms. The subscripts t and x denote the partial derivatives with respect to time and distance, respectively. Equation (1.2) can be expressed as

$$\frac{\partial G}{\partial t} + \frac{\partial f}{\partial G}\frac{\partial G}{\partial x} = S(G), \tag{1.3}$$

where $\frac{\partial f}{\partial G}$ is the gradient of the function of data variables with respect to these variables. Let $A(G)$ be the Jacobian matrix of the system. Then (1.3) can then be written as

$$\frac{\partial G}{\partial t} + A(G)\frac{\partial G}{\partial x} = S(G). \tag{1.4}$$

Setting the source term in (1.4) to zero gives the quasilinear form

$$\frac{\partial G}{\partial t} + A(G)\frac{\partial G}{\partial x} = 0. \tag{1.5}$$

The data variables are density ρ and flow ρv in both the PW and improved models. Roe's technique is used to linearize the Jacobian matrix $A(G)$ by decomposing it into eigenvalues and eigenvectors. It is based on the concept that the data variables, eigenvalues and eigenvectors remain conserved for small changes in time and distance. This technique is widely employed because it is able to capture the effects of abrupt changes in the data variables.

Consider a road divided into N equidistant segments and M equal duration time steps. The total length is x_N so a segment has length $\delta x = x_N/N$, and the total time duration is t_M so a time step is $\delta t = t_M/M$. The Jacobian matrix is approximated for road segments $(x_i + \frac{\delta x}{2}, x_i - \frac{\delta x}{2})$. This matrix is obtained for all N segments in every time interval (t_{m+1}, t_m), where $t_{m+1} - t_m = \delta t$.

Let $\triangle G$ denote the change in the data variables G and $\triangle f$ the corresponding change in the functions of the data variables. Further, let G_i be the average values of the data variables in the ith segment. The change in flux at the boundary between

the ith and $(i+1)$th segments is given by

$$\triangle f_{i+\frac{1}{2}} = A(G_{i+\frac{1}{2}})\triangle G, \tag{1.6}$$

where $A(G_{i+\frac{1}{2}})$ is the Jacobian matrix at the segment boundary, and $G_{i+\frac{1}{2}}$ is the vector of data variables at the boundary obtained using Roe's technique. The flux approximates the change in traffic density and flow at the segment boundary.

Then

$$\triangle f_{i+\frac{1}{2}} = A(G_{i+\frac{1}{2}})\left(G_{i+1} - G_i\right), \tag{1.7}$$

where the approximation $\triangle G = (G_{i+1} - G_i)$ is used. The flux at the boundary between segments i and $i+1$ at time m is then approximated by

$$f^m_{i+\frac{1}{2}}(G^m_i, G^m_{i+1}) = \frac{1}{2}\left(f(G^m_i) + f(G^m_{i+1})\right) - \frac{1}{2}\triangle f_{i+\frac{1}{2}}, \tag{1.8}$$

where $f(G^m_i)$ and $f(G^m_{i+1})$ denote the values of the functions of the data variables in road segments i and $i+1$, respectively, at time m. Substituting (1.7) into (1.8) gives

$$f^m_{i+\frac{1}{2}}(G^m_i, G^m_{i+1}) = \frac{1}{2}\left(f(G^m_i) + f(G^m_{i+1})\right) - \frac{1}{2}A(G_{i+\frac{1}{2}})\left(G^m_{i+1} - G^m_i\right). \tag{1.9}$$

This approximates the change in density and flow without considering the source. The updated data variables are obtained by including the source term which gives

$$G^{m+1}_i = G^m_i - \frac{\delta t}{\delta x}\left(f^m_{i+\frac{1}{2}} - f^m_{i-\frac{1}{2}}\right) + \delta t S(G^m_i). \tag{1.10}$$

1.3 Entropy Fix

Entropy fix is applied to Roe's technique to smooth any discontinuities at the segment boundaries [52]. The Jacobian matrix $A(G_{i+\frac{1}{2}})$ is decomposed into its eigenvalues and eigenvectors to approximate the flux in the road segments (1.9). Thus, the Jacobian matrix for the road segments is replaced with the entropy fix solution given by

$$e|\Lambda|e^{-1},$$

where $|\Lambda| = \left[\hat{\lambda}_1, \hat{\lambda}_2, \ldots, \hat{\lambda}_k, \ldots, \hat{\lambda}_n\right]$ is a diagonal matrix which is a function of the eigenvalues λ_k of the Jacobian matrix, and e is the corresponding eigenvector matrix.

The Harten and Hayman entropy fix scheme [59] is employed here and is given by

$$\hat{\lambda}_k = \begin{cases} \hat{\delta}_k & \text{if} \quad |\lambda_k| < \hat{\delta}_k \\ |\lambda_k| & \text{if} \quad |\lambda_k| \geq \hat{\delta}_k \end{cases} \tag{1.11}$$

with

$$\hat{\delta}_k = \max\left(0, \quad \lambda_{i+\frac{1}{2}} - \lambda_i, \quad \lambda_{i+1} - \lambda_{i+\frac{1}{2}}\right). \tag{1.12}$$

This ensures that the $\hat{\lambda}_k$ are not negative and similar at the segment boundaries.

1.4 Dissertation Organization

This chapter served as introduction to traffic modelling for intelligent transportation systems. The rest of dissertation is organized as follows:

Chapter 2 In this chapter, the characterization of spatial changes in traffic density is investigated to smoothly align the traffic flow with forward traffic conditions. The commonly employed Payne Witham (PW) model adjusts the traffic with a constant velocity regardless of the transitions on a road. As a consequence, the traffic can oscillate with velocities that exceed the maximum or go below zero. In this chapter, the PW model is improved so that the velocity during traffic adjustments is inversely proportional to the traffic density. This is based on the fact that traffic adapts quicker for a smaller forward traffic density and vice versa. A discontinuous traffic density distribution caused by a bottleneck along both straight and circular roads is used to show that this new model eliminates the unrealistic oscillatory behavior of the PW model.

Chapter 3 Traffic flow is known to align itself to forward traffic conditions, and the time and distance required for alignment has a significant affect on the traffic density. Thus, in this chapter, the well-known Lighthill, Witham and Richards (LWR) model is improved to account for traffic behavior during this transition period. A model for the inhomogeneous traffic flow during transitions is proposed which can be used to determine how the traffic density distribution changes. Later in the chapter, both the proposed and LWR models are evaluated.

Chapter 4 Traffic flow will align itself to forward conditions. The time and distance

required for alignment can have a significant affect on the traffic density. The flow can evolve into clusters of vehicles or become uniform depending on parameters such as the safe time and safe distance. In this chapter, a new model is presented to provide a realistic characterization of traffic behavior during the alignment period. Results are presented for a discontinuous density distribution on a circular road which shows that this model produces more realistic traffic behavior than other models in the literature.

Chapter 5 A new macroscopic traffic flow model is proposed to accurately represent traffic behavior. This model is based on analogies with the ideal gas law. As with the ideal gas constant, a traffic constant is developed for the characterization of driver response. This response includes both physiological and psychological behavior. The physiological behavior includes the time taken to perceive and process traffic situations and the resulting actions. The psychological behavior is the response to a situation based on driver attitude and awareness. Thus, this constant encompasses the perception, awareness, attitude and reaction of a driver. The proposed model is evaluated for a transition caused by a bottleneck on a road and is compared with the well known Payne-Witham (PW) model. It is shown that including the driver response results in a more realistic traffic model.

Chapter 6 In this chapter, route merits such as Mach number, relative trip time and traffic resistance are proposed to minimize the trip time, improve fuel consumption and smooth the traffic flow. In this chapter, Mach number is developed as an indicator of velocity fluctuation in traffic. Relative trip time gives the comparison of trip time of a route when followed with different velocity. The traffic resistance is developed from the analogies of fluid pressure. Just like fluid pressure, traffic resistance depends on acceleration and density. This traffic resistance identifies a route with smaller transitions. The traffic resistance based on electric circuit theory is noteworthy.

Chapter 7 concludes the dissertation. This chapter provides brief summary of the dissertation contributions and extension and employment of this dissertation work in future.

Chapter 2

Traffic flow Model based on Anticipation

The realistic characterization of traffic density on a road is of significant importance in traffic modelling. This characterization is required for proper alignment with forward traffic conditions. To realistically predict the traffic density evolution, it is essential that the velocity stay within the maximum and minimum values. The traffic density evolves according to changes in velocity, and a density distribution with a low variance is expected at smaller velocities and vice versa. Traffic cannot align to forward traffic conditions instantaneously. The time required for traffic alignment is known as the transition time, t_{tr}. The distance required for alignment is the transition distance, d_{tr}, which is covered during the transition time. The transition distance is the distance required to achieve the equilibrium velocity distribution when a change in traffic flow is observed. Therefore, a traffic flow model is proposed which characterizes the evolution of the traffic density during a transition on the road which is based on the velocity.

In this chapter, an improvement to the PW model is proposed so that the spatial alignment of the traffic density occurs with a variable velocity. The PW model is known to produce unrealistic oscillatory behavior at traffic discontinuities. This behavior corresponds to a stop and go traffic flow and is due to an inadequate characterization of spatial changes in the traffic density during transitions. Traffic adjustments are assumed to occur with a constant velocity, which can result in the velocity at discontinuities exceeding the maximum or below zero, which is impossible. Driver anticipation depends on the average traffic velocity at the transition v,

the equilibrium velocity distribution $v(\rho)$ and the transition distance d_{tr}. An anticipation term is introduced which eliminates the PW model inconsistencies present due to the smooth density and velocity distributions [43] assumed for vehicle flow. To investigate the oscillatory behavior of the PW model and the effect of the model improvement, an inactive bottleneck on straight and circular roads is considered. An inactive bottleneck is defined as congestion resulting from either a large density or slow moving vehicles, and thus creates a transition in the traffic.

The rest of the chapter is organized as follows. Section 2.1 presents the PW and improved PW models. Section 2.2 gives the decomposition of the models with Roe's technique. A comparison of the PW and proposed models is presented in Section 2.3. Finally, some concluding remarks are given in Section 2.4.

2.1 Traffic Flow Models

Payne [1] and Whitham [7] independently developed a two equation model for traffic flow which is known as the Payne-Whitham (PW) model. The first equation models traffic conservation on the road with a constant number of vehicles. The second equation models the traffic acceleration. The PW model can be expressed as

$$\frac{\partial \rho}{\partial t} + \frac{\partial(\rho v)}{\partial x} = 0, \tag{2.1}$$

$$\frac{\partial v}{\partial t} + \frac{v \partial v}{\partial x} = -\frac{C_o^2}{\rho}\frac{\partial \rho}{\partial x} + \left(\frac{v(\rho) - v}{\tau}\right). \tag{2.2}$$

The model parameters are summarized in Table 2.1. C_o is the velocity constant and τ is the relaxation time to align the traffic velocities. $\frac{v(\rho)-v}{\tau}$ is the relaxation term and accounts for the alignment in velocity. The anticipation term is

$$\frac{C_o^2}{\rho}\frac{\partial \rho}{\partial x},$$

and accounts for spatial changes in the traffic density. It is a function of the spatial gradient of density $\frac{\partial \rho}{\partial x}$. According to the relaxation term, traffic adjusts to the equilibrium velocity distribution. Once traffic attains the equilibrium velocity distribution, the flow is homogeneous. Several models have been proposed for $v(\rho)$ which is determined by the density distribution [32]. A commonly employed model is the

Table 2.1: PW Model Parameters

Term	Description
ρ	Density
$v(\rho)$	Equilibrium velocity distribution
ρv	Flow (Momentum)
$\frac{C_o^2}{\rho}\frac{\partial \rho}{\partial x}$	Anticipation term
$\frac{v(\rho)-v}{\tau}$	Relaxation term
τ	Relaxation time
$\frac{v\partial v}{\partial x}$	Convective acceleration
$\frac{\partial v}{\partial t}$	Unsteady acceleration
$\frac{\partial v}{\partial t} + \frac{v\partial v}{\partial x}$	Inertial term
C_0	Velocity constant

Greenshields model [60, 33] which is given by

$$v(\rho) = v_m \left(1 - \frac{\rho}{\rho_m}\right), \tag{2.3}$$

where ρ_m and ρ are the maximum and average traffic densities, respectively, and v_m is the maximum velocity on the road. This shows that the density and velocity are inversely related, so that velocity increases as the traffic density decreases and vice versa. The inertial term $\frac{\partial v}{\partial t} + \frac{v \partial v}{\partial x}$ accounts for the unsteady acceleration (with respect to time) and convectional acceleration (with respect to changes in vehicle positions). It is a function of the spatial change in density and the relaxation term.

In the PW model, the spatial change in density is multiplied by a constant coefficient, C_o^2, having units m^2/s^2. However, this constant can only account for small changes in the forward traffic density, so large changes result in unrealistic behavior. At traffic density discontinuities, the anticipation term can be very large. Thus, a variable anticipation term should be employed which is a function of the transition velocity.

The well known kinematic equation of motion is

$$a = \frac{V_f^2 - V_i^2}{2d}, \tag{2.4}$$

where a is acceleration, V_f is the final velocity, V_i is the initial velocity, and d is the distance covered. As V_f is the velocity to be attained, it is replaced with the equilibrium velocity distribution $v(\rho)$. Further, V_i is replaced with v, and d with the transition distance d_{tr}. The transition distance is given by

$$d_{tr} = \tau v_m + l_s, \tag{2.5}$$

where l_s is the distance between the vehicles at stand still position [54]. Then (2.4) takes the form

$$a(\rho) = \frac{v^2(\rho) - v^2}{2d_{tr}}, \tag{2.6}$$

having units m/s^2 which characterizes the variation in velocity during transitions. The change in velocity during a transition over a distance x is then given by

$$\frac{\partial}{\partial x} a(\rho) = \frac{\partial}{\partial x} \left(\frac{v^2(\rho) - v^2}{2d_{tr}}\right). \tag{2.7}$$

The term C_o^2 in (2.2) can be replaced with (2.7) to account for changes in the traffic density when a transition occurs. Then, driver response to a discontinuity is such that the velocity is lower for a large density and vice versa. Further, density changes will be larger for smaller transition distances. Traffic velocity does not change if there is no transition in the traffic flow, in which case $v = v(\rho)$, so that $a(\rho) = 0$. Hence in this case, the coefficient of $\frac{\partial \rho}{\partial x}$ is zero.

2.2 The Decomposition of Traffic Flow Models

In order to evaluate the performance of the PW and improved PW models, they are decomposed using Roe's technique to approximate the macroscopic traffic flow. This approach is described in Section 1.2.

2.2.1 Jacobian Matrix

In this section, the Jacobian matrix $A(G)$ is derived. We first consider the PW model and convert it into conservation form. To achieve this, multiply (2.1) by v to obtain

$$v\rho_t + v(\rho v)_x = 0, \tag{2.8}$$

where the subscripts t and x denote the partial derivatives with respect to time and distance, respectively. $(\rho v)_t$ can be written as

$$(\rho v)_t = \rho v_t + v\rho_t, \tag{2.9}$$

and rearranging gives

$$v\rho_t = (\rho v)_t - \rho v_t, . \tag{2.10}$$

Substituting (2.10) into (2.8), we obtain

$$\rho v_t = v(\rho v)_x + (\rho v)_t. \tag{2.11}$$

Multiplying (2.2) by ρ gives

$$\rho v_t + \rho v v_x + C_0^2 \rho_x = \rho \frac{v(\rho) - v}{\tau}, \tag{2.12}$$

and substituting (2.11) in (2.12) results in

$$v(\rho v)_x + (\rho v)_t + \rho v v_x + C_0^2 \rho_x = \rho \frac{v(\rho) - v}{\tau}. \tag{2.13}$$

We have that

$$(\rho v v)_x = v(\rho v)_x + \rho v v_x, \tag{2.14}$$

and rearranging gives

$$v(\rho v)_x = (\rho v v)_x - \rho v v_x. \tag{2.15}$$

Substituting (2.15) in (2.13), we obtain

$$(\rho v v)_x + (\rho v)_t + C_0^2 \rho_x = \rho \frac{v(\rho) - v}{\tau}. \tag{2.16}$$

Now, using the fact that

$$(\rho v v)_x = \left(\frac{(\rho v)^2}{\rho} \right)_x,$$

(2.16) can be written as

$$(\rho v)_t + \left(\frac{(\rho v)^2}{\rho} + C_0^2 \rho \right)_x = \rho \left(\frac{v(\rho) - v}{\tau} \right), \tag{2.17}$$

which is in conservation form. The source term can be considered as traffic movement into and out of the flow. If the source term is assumed to be zero and traffic mobility is conserved, then the RHS of (2.17) is zero which gives

$$(\rho v)_t + \left(\frac{(\rho v)^2}{\rho} + C_0^2 \rho \right)_x = 0. \tag{2.18}$$

The model in quasilinear form is then

$$G = \begin{pmatrix} \rho \\ \rho v \end{pmatrix}, f(G) = \begin{pmatrix} f_1 \\ f_2 \end{pmatrix} = \begin{pmatrix} \rho v \\ \frac{(\rho v)^2}{\rho} + C_0^2 \rho \end{pmatrix} \text{ and } S(G) = \begin{pmatrix} 0 \\ 0 \end{pmatrix}, \tag{2.19}$$

The Jacobian matrix $A(G) = \frac{\partial f}{\partial G}$ from (2.19) is

$$A(G) = \begin{pmatrix} 0 & 1 \\ -\frac{(\rho v)^2}{\rho^2} + C_0^2 & \frac{2\rho v}{\rho} \end{pmatrix}, \tag{2.20}$$

which gives

$$A(G) = \begin{pmatrix} 0 & 1 \\ -v^2 + C_0^2 & 2v \end{pmatrix}. \tag{2.21}$$

The eigenvalues λ_i of the Jacobian matrix are required to obtain the flux in (1.9), and are obtained from (2.21) as the solution of

$$\Big|A(G) - \lambda I\Big| = \begin{vmatrix} -\lambda & 1 \\ -v^2 + C_0^2 & 2v - \lambda \end{vmatrix} = 0, \tag{2.22}$$

which gives

$$\lambda^2 - 2v\lambda + v^2 - C_0^2 = 0. \tag{2.23}$$

The eigenvalues are then

$$\lambda_{1,2} = \frac{2v \pm \sqrt{4v^2 - 4(v^2 - C_0^2)}}{2} = v \pm \sqrt{C_0^2}. \tag{2.24}$$

For the PW model

$$\lambda_{1,2} = v \pm C_0. \tag{2.25}$$

For the improved PW model, we have

$$C_0^2 = \frac{\partial}{\partial x}\left(\tfrac{v^2(\rho) - v^2}{2d_{tr}}\right)$$

and substituting this in (2.16) for C_0^2 gives the eigenvalues

$$\lambda_{1,2} = v \pm \sqrt{\frac{v^2(\rho) - v^2}{2d_{tr}}}. \tag{2.26}$$

The eigenvectors are obtained by solving

$$|A(G) - \lambda I|x = 0, \tag{2.27}$$

where

$$x = \begin{pmatrix} 1 \\ x_2 \end{pmatrix}. \tag{2.28}$$

For the PW model, using (2.21) and $\lambda_1 = v + C_0$ from (2.25), the eigenvectors obtained

from (2.27) are

$$e_1 = \begin{pmatrix} 1 \\ v + C_0 \end{pmatrix}, \tag{2.29}$$

and

$$e_2 = \begin{pmatrix} 1 \\ v - C_0 \end{pmatrix}. \tag{2.30}$$

For the improved PW model, using (2.21) and $\lambda_1 = v + \sqrt{\frac{v^2(\rho)-v^2}{2d_{tr}}}$ from (2.26), (2.27) takes the form

$$\begin{pmatrix} -v - \sqrt{\frac{v^2(\rho)-v^2}{2d_{tr}}} & 1 \\ \frac{v^2(\rho)-v^2}{2d_{tr}} - v^2 & v - \sqrt{\frac{v^2(\rho)-v^2}{2d_{tr}}} \end{pmatrix} \begin{pmatrix} 1 \\ x_2 \end{pmatrix} = 0, \tag{2.31}$$

so the eigenvectors are

$$e_1 = \begin{pmatrix} 1 \\ v + \sqrt{\frac{v^2(\rho)-v^2}{2d_{tr}}} \end{pmatrix}, \tag{2.32}$$

and

$$e_2 = \begin{pmatrix} 1 \\ v - \sqrt{\frac{v^2(\rho)-v^2}{2d_{tr}}} \end{pmatrix}. \tag{2.33}$$

To obtain the average velocity for the improved PW model, using (1.6) and (2.21), Δf can be expressed as

$$\triangle f = \begin{pmatrix} \triangle f_1 \\ \triangle f_2 \end{pmatrix} = A(G) \triangle G = \begin{pmatrix} 0 & 1 \\ \frac{v^2(\rho)-v^2}{2d_{tr}} - v^2 & 2v \end{pmatrix} \begin{pmatrix} \triangle \rho \\ \triangle \rho v \end{pmatrix}. \tag{2.34}$$

From (2.34), we have

$$\triangle f_2 = \left(\frac{v^2(\rho)-v^2}{2d_{tr}} - v^2 \right) \triangle \rho + 2v \triangle \rho v, \tag{2.35}$$

and substituting $C_0^2 = \int \frac{\partial}{\partial x} \left(\frac{v^2(\rho)-v^2}{2d_{tr}} \right) \mathrm{d}x$ in (2.19) gives

$$f(G) = \begin{pmatrix} f_1 \\ f_2 \end{pmatrix} = \begin{pmatrix} \rho v \\ \frac{(\rho v)^2}{\rho} + \rho \frac{v^2(\rho)-v^2}{2d_{tr}} \end{pmatrix}, \tag{2.36}$$

so then

$$\triangle f(G) = \begin{pmatrix} \triangle f_1 \\ \triangle f_2 \end{pmatrix} = \begin{pmatrix} \triangle(\rho v) \\ \triangle\left(\frac{(\rho v)^2}{\rho} + \rho\frac{v^2(\rho)-v^2}{2d_{tr}}\right) \end{pmatrix}. \tag{2.37}$$

Equating (2.35) with $\triangle f_2$ from (2.37), we obtain

$$\overline{v}^2\triangle\rho - 2\overline{v}\triangle\rho v + \triangle\rho v^2 = 0, \tag{2.38}$$

and taking the positive root gives the average velocity of the improved model as

$$\overline{v} = \frac{2\triangle\rho v + 2\sqrt{(\triangle\rho v)^2 - (\triangle\rho)(\triangle\rho v^2)}}{2\triangle\rho}, \tag{2.39}$$

Substituting $\triangle\rho v = \rho_{i+1}v_{i+1} - \rho_i v_i$, $\triangle\rho v^2 = \rho_{i+1}v_{i+1}^2 - \rho_i v_i^2$, and $\triangle\rho = \rho_{i+1} - \rho_i$ in (2.39), the average velocity at the boundary of segments i and $i+1$ is

$$v_{i+\frac{1}{2}} = \frac{v_{i+1}\sqrt{\rho_{i+1}} + v_i\sqrt{\rho_i}}{\sqrt{\rho_{i+1}} + \sqrt{\rho_i}}. \tag{2.40}$$

To obtain the average velocity for the PW model, using (1.6) and (2.21), Δf can be expressed as

$$\triangle f = \begin{pmatrix} \triangle f_1 \\ \triangle f_2 \end{pmatrix} = A(G)\triangle G = \begin{pmatrix} 0 & 1 \\ C_0^2 - v^2 & 2v \end{pmatrix}\begin{pmatrix} \triangle\rho \\ \triangle\rho v \end{pmatrix}. \tag{2.41}$$

From (2.41), we obtain

$$\triangle f_2 = (-v^2 + C_0^2)\triangle\rho + 2v\triangle\rho v, \tag{2.42}$$

and using (2.19) gives

$$f(G) = \begin{pmatrix} f_1 \\ f_2 \end{pmatrix} = \begin{pmatrix} (\rho v) \\ \left(\frac{(\rho v)^2}{\rho} + C_0^2\rho\right) \end{pmatrix}, \tag{2.43}$$

so then

$$\triangle f(G) = \begin{pmatrix} \triangle f_1 \\ \triangle f_2 \end{pmatrix} = \begin{pmatrix} \triangle(\rho v) \\ \triangle\left(\frac{(\rho v)^2}{\rho} + C_0^2\rho\right) \end{pmatrix}. \tag{2.44}$$

Equating (2.42) with $\triangle f_2$ in (2.44) results in

$$\overline{v}^2 \triangle \rho - 2\overline{v} \triangle \rho v + \triangle \rho v^2 = 0, \tag{2.45}$$

which is the same as for the improved PW model given in (2.38). Therefore, both models have the same average velocity at the segment boundaries.

The average density $\rho_{i+\frac{1}{2}}$ at the boundary of segments i and $i+1$ is given by the geometric mean of the densities in these segments

$$\rho_{i+\frac{1}{2}} = \sqrt{\rho_{i+1}\rho_i}. \tag{2.46}$$

The improved PW model eigenvalues of the Jacobian matrix $A(G_{i+\frac{1}{2}})$ are

$$\lambda_{1,2} = v_{i+\frac{1}{2}} \pm \sqrt{\frac{v^2(\rho_{i+\frac{1}{2}}) - v^2_{i+\frac{1}{2}}}{2d_{tr}}}, \tag{2.47}$$

which show that when a transition occurs, the velocity changes according to the equilibrium velocity distribution and the average velocity.

For a traffic flow system to be strictly hyperbolic, the eigenvectors must be distinct and real [47]. The eigenvectors of the improved model given in (2.47) are distinct and real when the equilibrium velocity is greater than the average velocity, i.e.

$$v(\rho_{i+\frac{1}{2}}) > v_{i+\frac{1}{2}}.$$

However, the eigenvectors are imaginary when

$$v(\rho_{i+\frac{1}{2}}) < v_{i+\frac{1}{2}}.$$

Therefore, to maintain the hyperbolicity of the improved PW model, the absolute value of the numerator under the radical sign in (2.47) is employed, which gives

$$\lambda_{1,2} = v_{i+\frac{1}{2}} \pm \sqrt{\frac{|v^2(\rho_{i+\frac{1}{2}}) - v^2_{i+\frac{1}{2}}|}{2d_{tr}}}, \tag{2.48}$$

The corresponding eigenvectors are

$$e_{1,2} = \begin{pmatrix} 1 \\ v_{i+\frac{1}{2}} \pm \sqrt{\frac{|v^2(\rho_{i+\frac{1}{2}}) - v^2_{i+\frac{1}{2}}|}{2d_{tr}}} \end{pmatrix}. \tag{2.49}$$

The eigenvalues of the Jacobian matrix for the PW model are

$$\lambda_{1,2} = v_{i+\frac{1}{2}} \pm C_o, \tag{2.50}$$

which shows that the change in velocity due to a transition is constant. The corresponding eigenvectors are

$$e_{1,2} = \begin{pmatrix} 1 \\ v_{i+\frac{1}{2}} \pm C_o \end{pmatrix}. \tag{2.51}$$

2.2.2 Entropy Fix

Entropy fix as described in Section 1.2.1 is applied to the Jacobian matrix of the improved and PW models. For the improved PW model, we obtain

$$e|\Lambda|e^{-1} = \begin{pmatrix} 1 & 1 \\ v_{i+\frac{1}{2}} + \sqrt{\frac{|v^2(\rho_{i+\frac{1}{2}}) - v^2_{i+\frac{1}{2}}|}{2d_{tr}}} & v_{i+\frac{1}{2}} - \sqrt{\frac{|v^2(\rho_{i+\frac{1}{2}}) - v^2_{i+\frac{1}{2}}|}{2d_{tr}}} \end{pmatrix} \times$$
$$\begin{pmatrix} \left| v_{i+\frac{1}{2}} + \sqrt{\frac{|v^2(\rho_{i+\frac{1}{2}}) - v^2_{i+\frac{1}{2}}|}{2d_{tr}}} \right| & 0 \\ 0 & \left| v_{i+\frac{1}{2}} - \sqrt{\frac{|v^2(\rho_{i+\frac{1}{2}}) - v^2_{i+\frac{1}{2}}|}{2d_{tr}}} \right| \end{pmatrix} \times \begin{pmatrix} v_{i+\frac{1}{2}} - \sqrt{\frac{|v^2(\rho_{i+\frac{1}{2}}) - v^2_{i+\frac{1}{2}}|}{2d_{tr}}} & -1 \\ -v_{i+\frac{1}{2}} - \sqrt{\frac{|v^2(\rho_{i+\frac{1}{2}}) - v^2_{i+\frac{1}{2}}|}{2d_{tr}}} & 1 \end{pmatrix} \times$$
$$\frac{-1}{2\sqrt{\frac{|v^2(\rho_{i+\frac{1}{2}}) - v^2_{i+\frac{1}{2}}|}{2d_{tr}}}},$$

and for the PW model we have

$$e|\Lambda|e^{-1} = \begin{pmatrix} 1 & 1 \\ v_{i+\frac{1}{2}} + C_o & v_{i+\frac{1}{2}} - C_o \end{pmatrix} \times$$
$$\begin{pmatrix} \left| v_{i+\frac{1}{2}} + C_o \right| & 0 \\ 0 & \left| v_{i+\frac{1}{2}} - C_o \right| \end{pmatrix} \times \begin{pmatrix} v_{i+\frac{1}{2}} - C_o & -1 \\ -v_{i+\frac{1}{2}} - C_o & 1 \end{pmatrix} \frac{-1}{2C_0}.$$

The corresponding flux is obtained from (1.9) using $f(G_i)$ and $f(G_{i+1})$ and substituting $e|\Lambda|e^{-1}$ for $A(G_{i+\frac{1}{2}})$. The updated data variables, ρ and ρv, are then obtained at time m using (1.10).

2.3 Simulation Results

The performance of the improved and PW models are evaluated in this section using the parameters given in Table 2.2. Non-reflective boundary conditions are used for the first example to evaluate the traffic evolution on a straight road for 1.2 s. The second example employs periodic boundary conditions for traffic on a circular road for 6 s. The traffic target is Greenshields equilibrium velocity distribution $v(\rho)$ given by (2.3) with $v_m = 25$ m/s, $l_s = 7.5$ m, and $d_{tr} = 20$ m. Both models are evaluated using a relaxation time $\tau = 0.5$ s which is suitable for transitions over small distances [57]. Further, a small value of δx is required to ensure accurate numerical results. Therefore, the road of length $x_N = 100$ m is divided into $N = 100$ equal segments with $\delta x = 1$ m for both examples. Based on this value of δx, to satisfy the CFL condition [46] $\delta t = 0.006$ s is chosen. Therefore, the time $t_M = 1.2$ s for the first example is divided into $M = 200$ intervals, and the time $t_M = 6$ s for the second example is divided into $M = 1000$ intervals. The initial density ρ_0 at time $t = 0$ s has the following distribution

$$\rho_0 = \begin{cases} 0.01, & \text{for} \quad x \leq 30; \\ 0.3, & \text{for} \quad 30 < x < 60; \\ 0.1, & \text{for} \quad x > 60, \end{cases} \tag{2.52}$$

which spans the first 100 m of the road. The maximum density on the road is $\rho_m = 1$ which means that it is 100% occupied. The values of the velocity constant used in the literature for the PW model varies between 2.4 m/s and 57 m/s to evaluate the performance in varying traffic densities [32, 58, 56]. Thus the values of C_0 considered here are 25 m/s and 5 m/s.

2.3.1 Example 1

The velocity behavior for the PW model with $C_0 = 25$ m/s on a straight road is given in Figure 2.1, while the corresponding behavior for the improved PW model is given

Table 2.2: Simulation Parameters

Name	Parameter	Value
maximum velocity	v_m	25 m/s
equilibrium velocity distribution	$v(\rho)$	Greenshields distribution
relaxation time	τ	0.5 s
velocity constant	C_o	25, 5 m/s
length of road	x_N	100 m
road step	δx	1 m
time step	δt	0.006 s
distance between the vehicles at stand still	l_s	7.5 m
transition distance	d_{tr}	20 m
maximum normalized density	ρ_m	1
total simulation time for Example 1	t_M	1.2 s
number of time steps for Example 1	M	200
total simulation time for Example 2	t_M	6 s
number of time steps for Example 2	M	1000
number of road steps	N	100

in Figure 2.2. These results show that the PW model does not respond realistically to abrupt changes in the traffic density. In particular, oscillatory behavior is observed with velocities as high as 400 m/s and down to -120 m/s, which is impossible. Conversely, the improved PW model results in realistic velocities between 0 m/s and 25 m/s.

The improved PW model density behavior is shown in Figure 2.3. Initially, the density is 0.01 from 0 to 30 m on the road, and the corresponding velocity is 24.7 m/s from Figure 2.2. The density is 0.3 from 30 m to 60 m, and the corresponding velocity is 17.5 m/s. As there are no vehicles at 60 m, the velocity is 25 m/s, which is the maximum allowed. The traffic velocity is 22.4 m/s beyond 60 m. As time passes the traffic moves forward so that after 1.2 s there are no vehicles on the first 20 m of the road, as shown in Figure 2.3. Further, the discontinuity advances and becomes smoother, as expected. In particular, the discontinuity moves from 30 to 45 m in 1.2 s, and the density at the discontinuity is reduced from 0.3 from 0.27. It is evident from the results in Figures 2.2 and 2.3 that the improved PW model does not exhibit oscillatory behavior, and the density and velocity stay within the maximum and minimum limits.

The PW model density behavior is shown in Figure 2.4. In this case, the discontinuity results in traffic oscillations. The traffic should move forward and leave an empty road behind, but the figure indicates that there is traffic well behind the transition. Further, the density after 1.2 s goes down to -0.05, which is impossible. The density between 30 and 80 m on the road should be below the maximum initial value of 0.3 after 1.2 s, but it actually increases to 0.35 at 70 m. This is unrealistic behavior caused by the fact that the PW model density does not evolve according to changes in the velocity.

The PW model traffic flow behavior is given in Figure 2.5. This figure also indicates vehicles behind the transition, although traffic should move forward. The traffic flow also goes below zero to -2 veh/s. The corresponding traffic flow behavior for the improved PW model is given in Figure 2.6, and shows a smooth traffic flow. At 1.2 s, there is no traffic flow on the road up to 20 m, i.e. in this region $\rho v = 0$ veh/s. Further, the traffic flow at $t = 0$ when the density is 0.3 is 5.25 veh/s, and this decreases over both distance and time, as expected.

The PW model velocity behavior with $C_0 = 5$ m/s on a straight road for a period of 7.8 s is shown in Figure 2.7. The maximum and minimum velocities observed are 1200 m/s and -10 m/s, respectively, which indicates that even with a small value of

C_0 the performance is unrealistic.

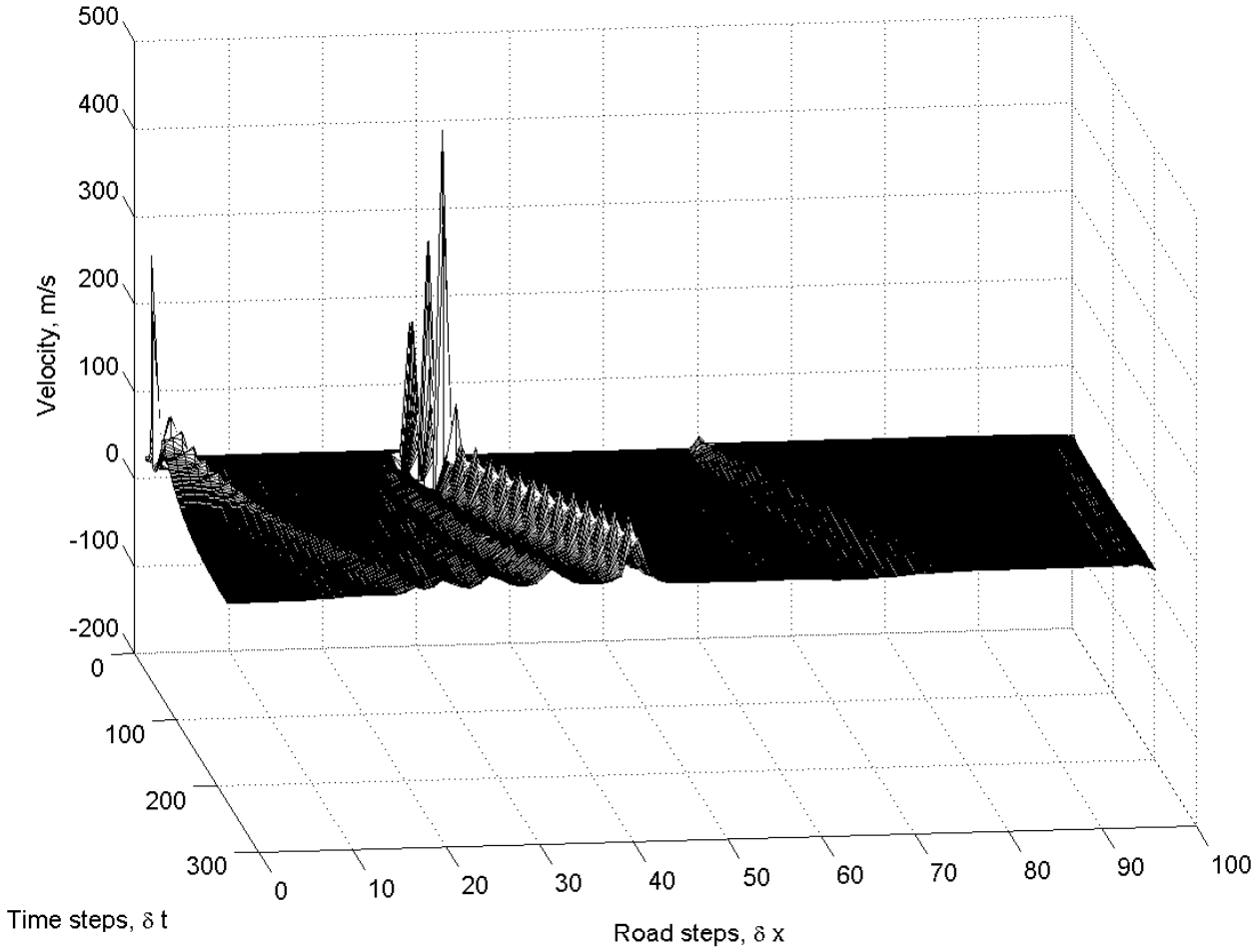

Figure 2.1: The PW model velocity behavior on a straight road with $C_0 = 25$ m/s.

2.3.2 Example 2

Figures 2.8, 2.9, 2.10 and 2.11, 2.12, 2.13 show the performance of the improved and PW models, respectively, on a circular road. The improved PW model density behavior is given in Figure 2.8. From 75 to 100 m and then from 0 to 10 m, the traffic density at $t = 6$ s is approximately uniform at 0.1. There is a cluster of vehicles between 10 and 75 m. The density of this cluster varies from 0.08 at 27 m to 0.2 at 40 m. The improved PW model velocity behavior is shown in Figure 2.9. From 75 to 100 m and then from 0 to 10 m, at $t = 6$ s the velocity is approximately uniform at 22.5 m/s. The velocity within the cluster varies from 20 to 23.3 m/s. This is realistic traffic behavior which is within the maximum and minimum velocities. The

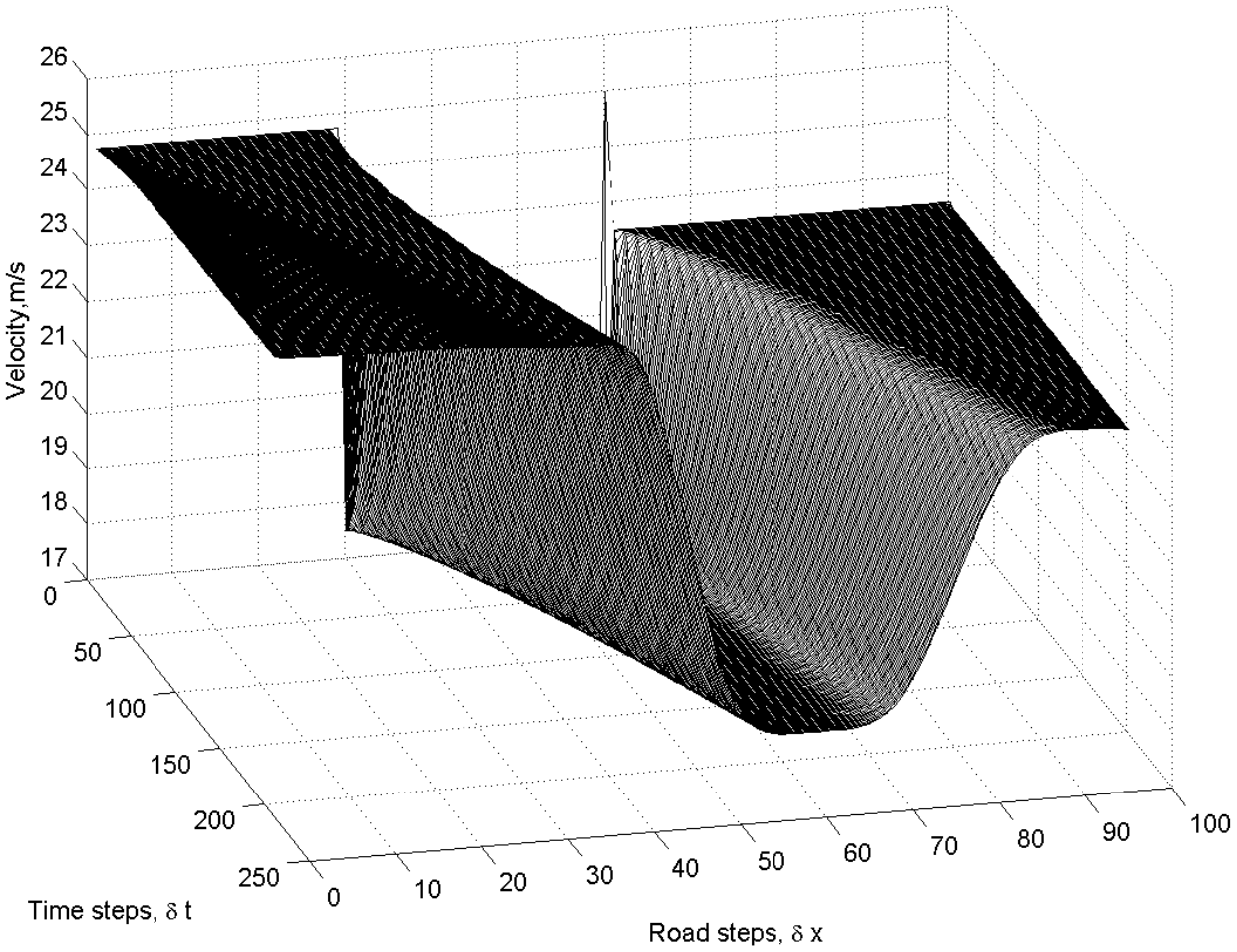

Figure 2.2: The improved PW model velocity behavior on a straight road.

corresponding traffic flow behavior is shown in Figure 2.10. At $t = 6$ s, the traffic between 75 to 100 m and then from 0 to 10 m has an approximately uniform flow of 2.25 veh/s. The flow within the cluster varies from 1.7 veh/s at 27 m to 4.2 veh/s close to 40 m. As expected, the traffic flow is large where the density is high and vice versa.

The PW model produces an oscillatory traffic flow on the circular road as shown in Figures 2.11, 2.12 and 2.13. The corresponding density behavior is given in Figure 2.11 and indicates that the traffic is divided into nine small clusters of span approximately 10 m, which is very close. The minimum density of 0.01 occurs at 20 m on the road, but the density is very small between the clusters. The PW model velocity behavior is given in Figure 2.12. This shows that the velocity ranges from 1400 m/s to -120 m/s after 0.4 s, which is impossible. Further, at 6 s the average velocity is 64 m/s

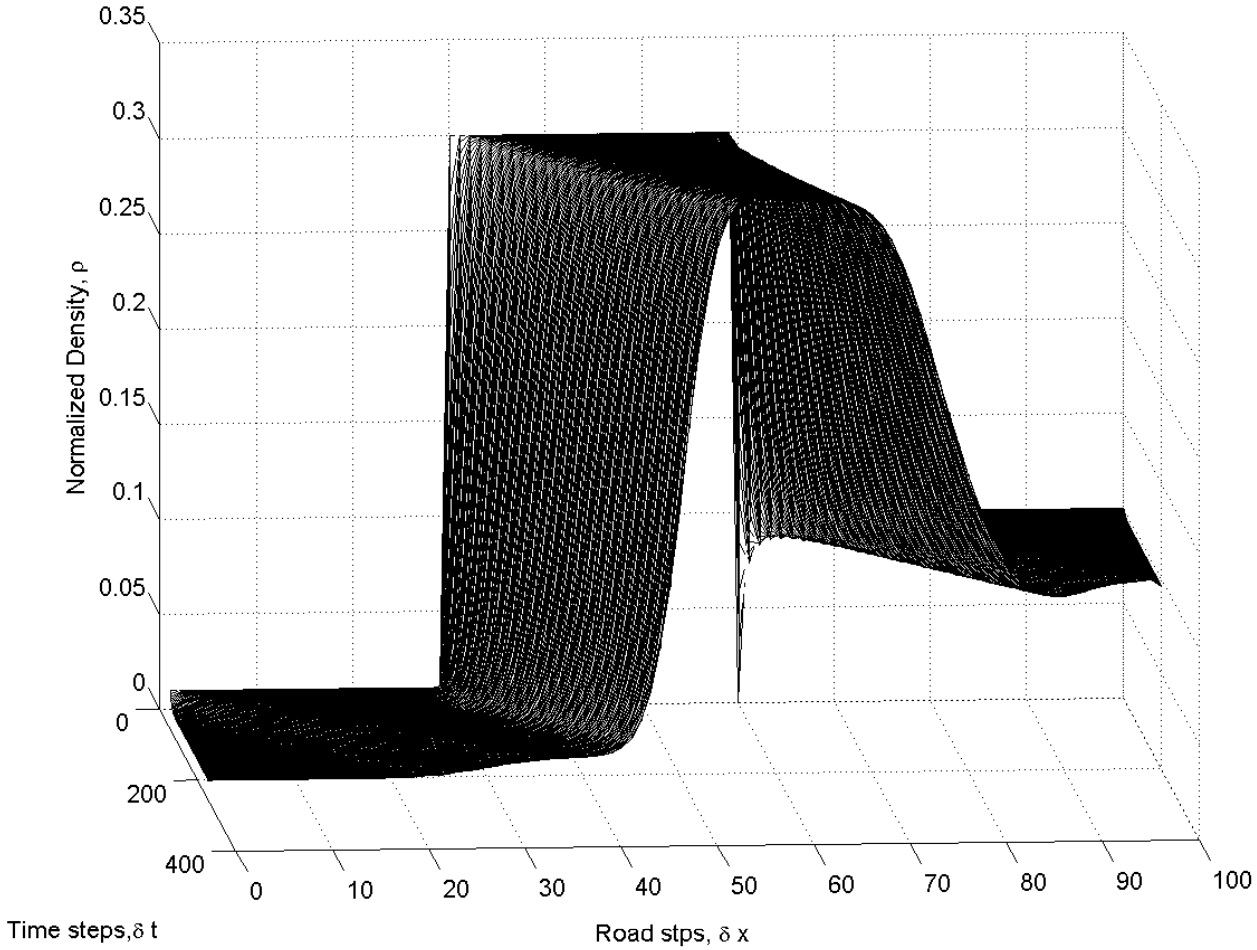

Figure 2.3: The improved PW model density behavior on a straight road.

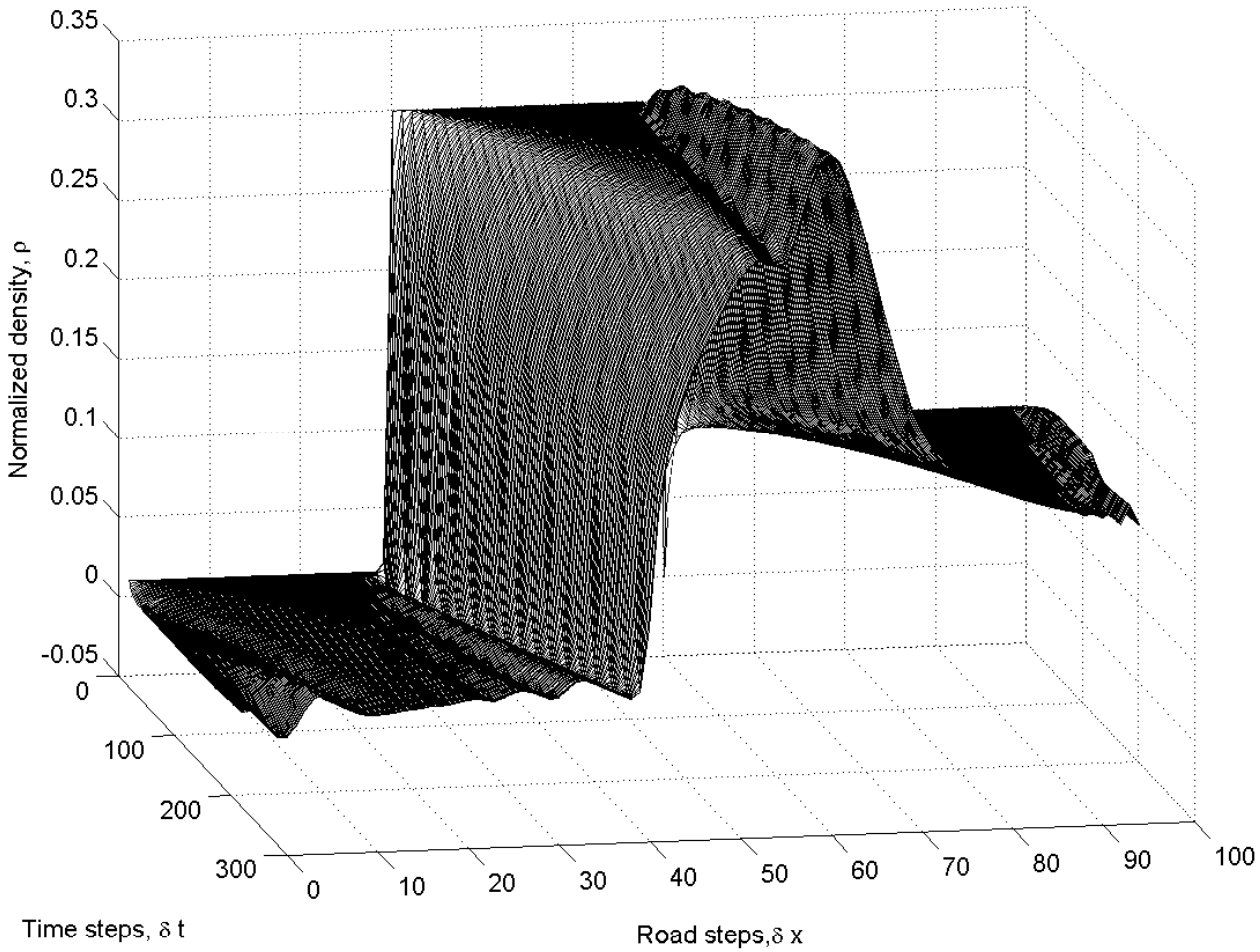

Figure 2.4: The PW model density behavior with on a straight road with $C_0 = 25$ m/s.

which is higher than the maximum velocity of 25 m/s, and there are abrupt changes in velocity. On average, within the clusters the velocity varies by 30 m/s within a distance of 5 m, which is unrealistic. The worst case occurs near 20 m when the velocity changes sharply from 23 m/s to 64 m/s and then falls to 14 m/s close to 25 m. The traffic flow behavior of the PW model is shown in Figure 2.13. The flow within the clusters varies by 2.5 veh/s over a span of 10 m, which is very large given the small distance. The results given show that the improved model has realistic behavior even when there is an abrupt change in density. Conversely, the PW model produces oscillatory traffic flow behavior under the same conditions.

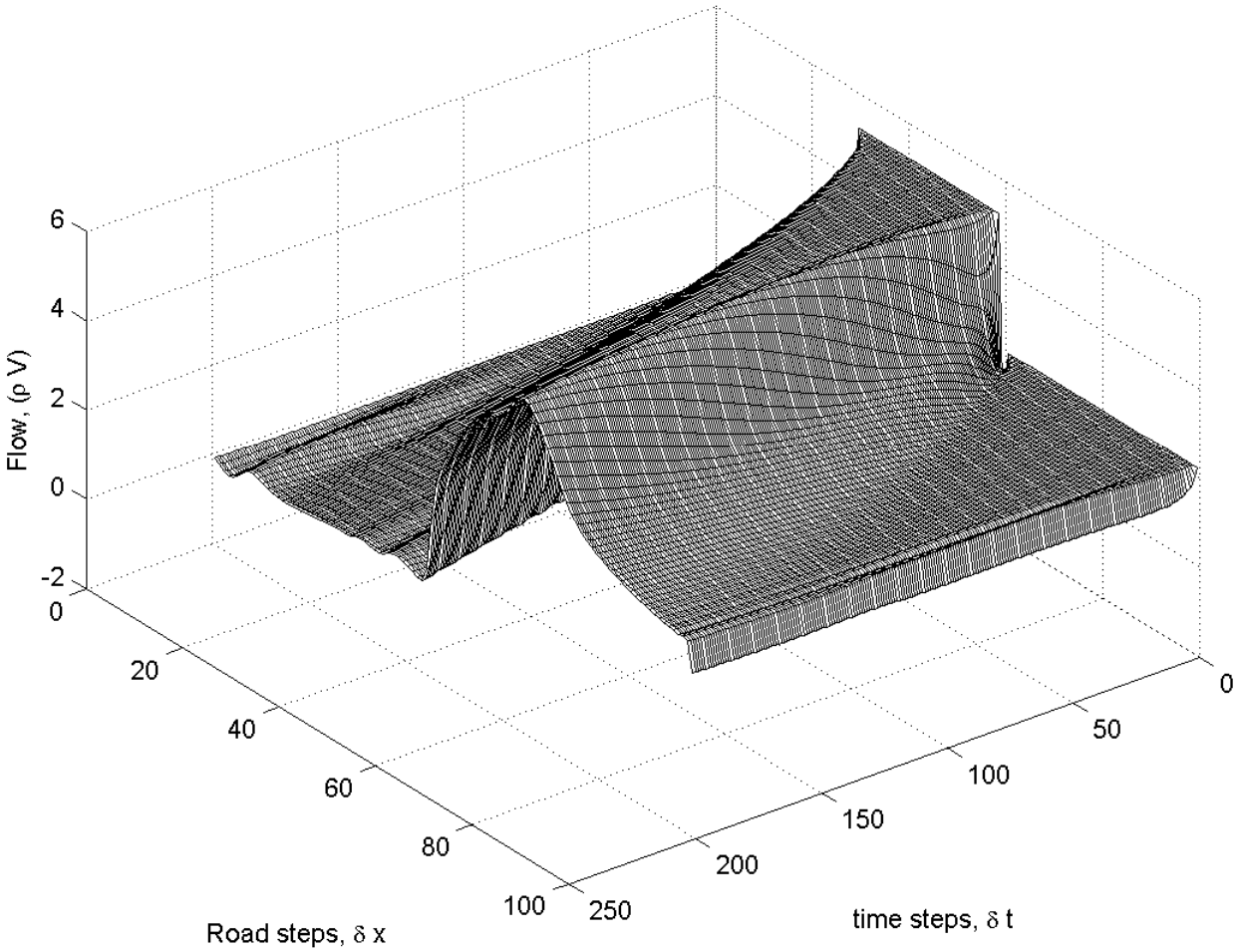

Figure 2.5: The PW model flow behavior on a straight road with $C_0 = 25$ m/s.

2.4 Summary

It was observed that the PW model produces oscillatory traffic behavior at density discontinuities. Further, the velocity oscillations go well above the maximum and below the minimum, and changes in both the velocity and density are very rapid. These unrealistic results are due to the PW model adjusting the traffic with a constant velocity regardless of the transitions on the road. An improved PW model was presented in which the traffic flow is dependent on the difference between the equilibrium velocity and current velocity. This model performs much better at traffic discontinuities. It eliminates the oscillatory behavior that occurs with the PW model and limits the velocity to realistic values.

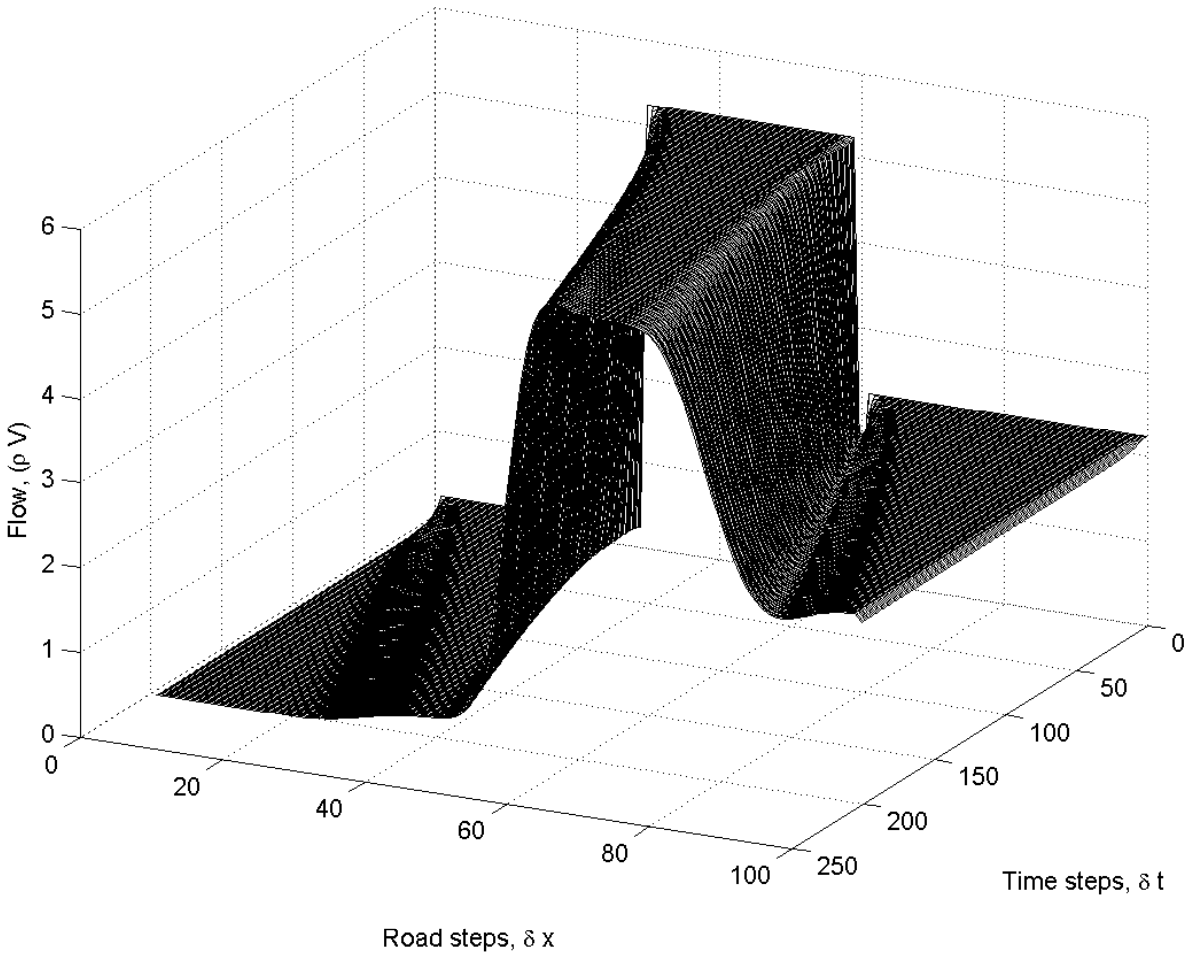

Figure 2.6: The improved PW model flow behavior a straight road.

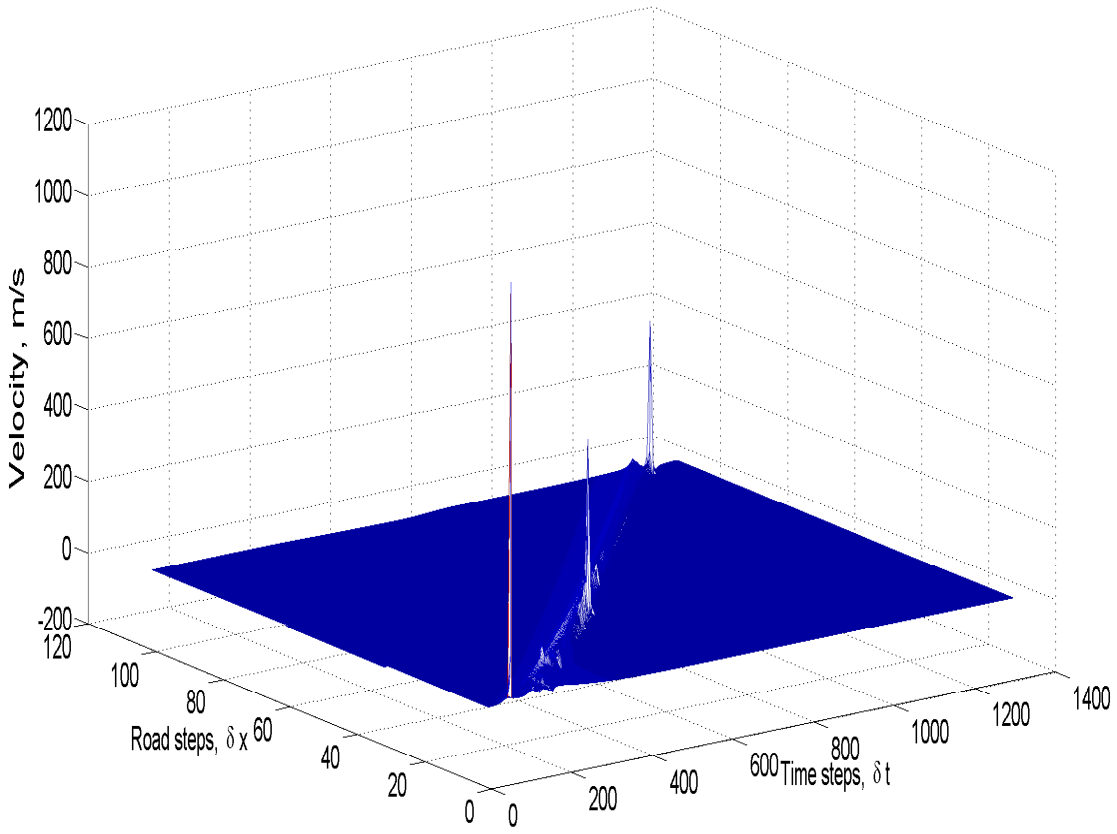

Figure 2.7: The PW model velocity behavior on a straight road with $C_0 = 5$ m/s.

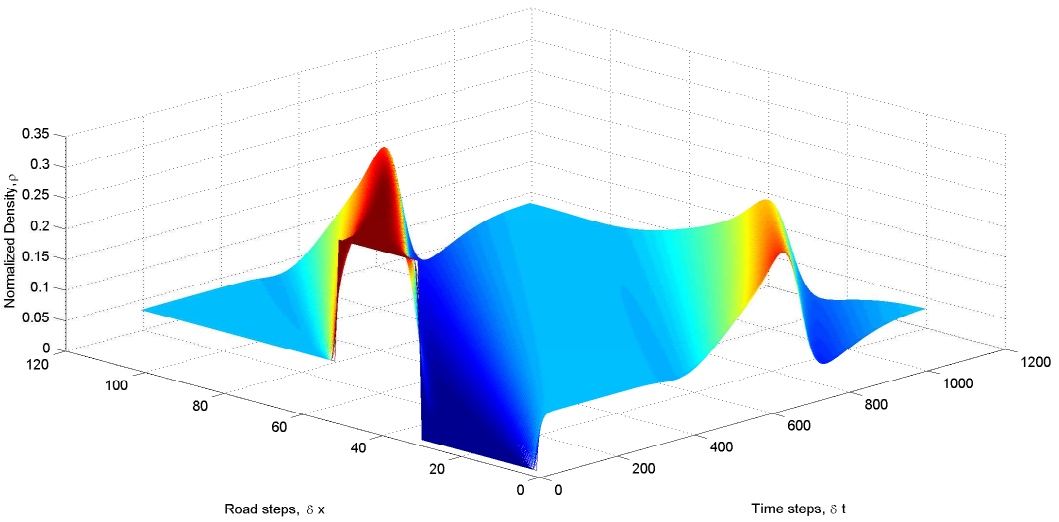

Figure 2.8: The improved PW model density behavior on a circular road.

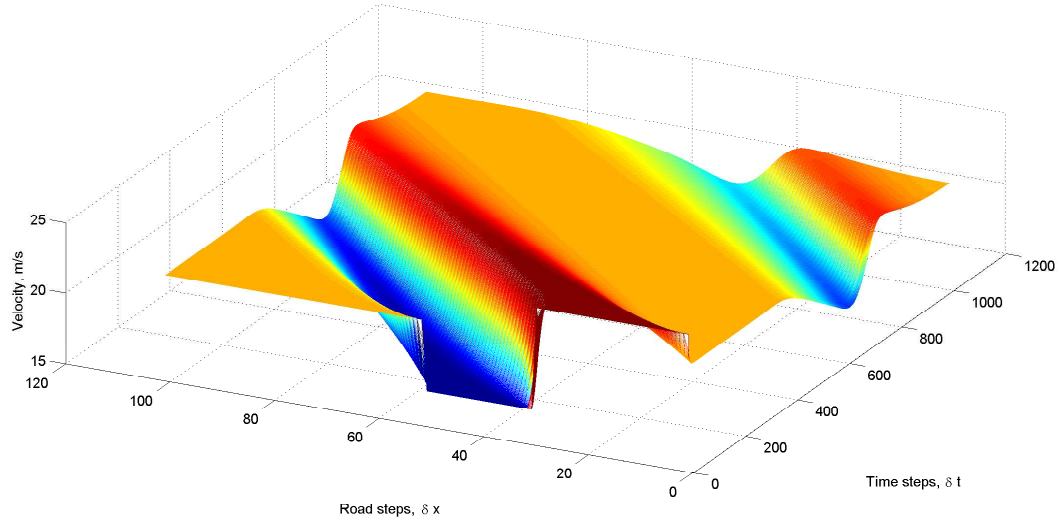

Figure 2.9: The improved PW model velocity behavior on a circular road.

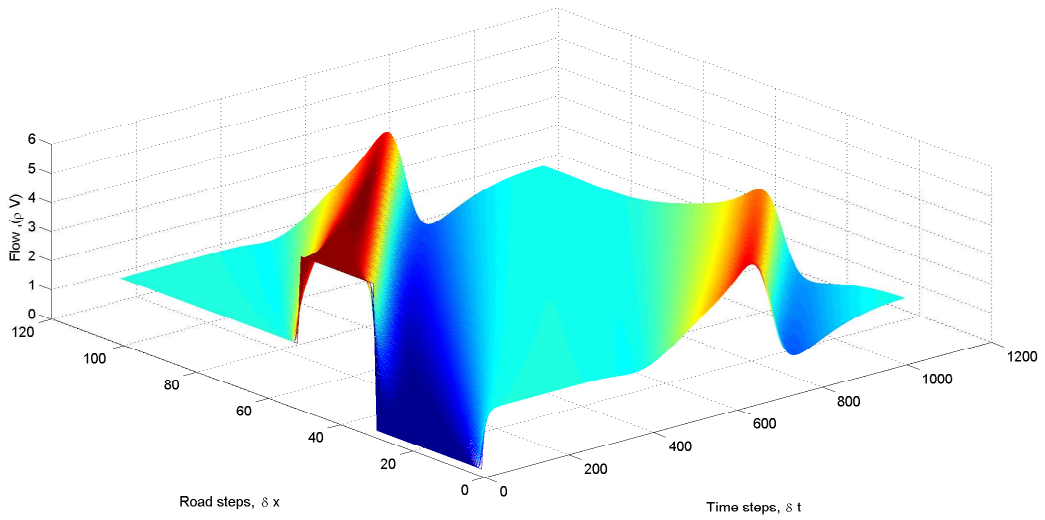

Figure 2.10: The improved PW model flow behavior on a circular road.

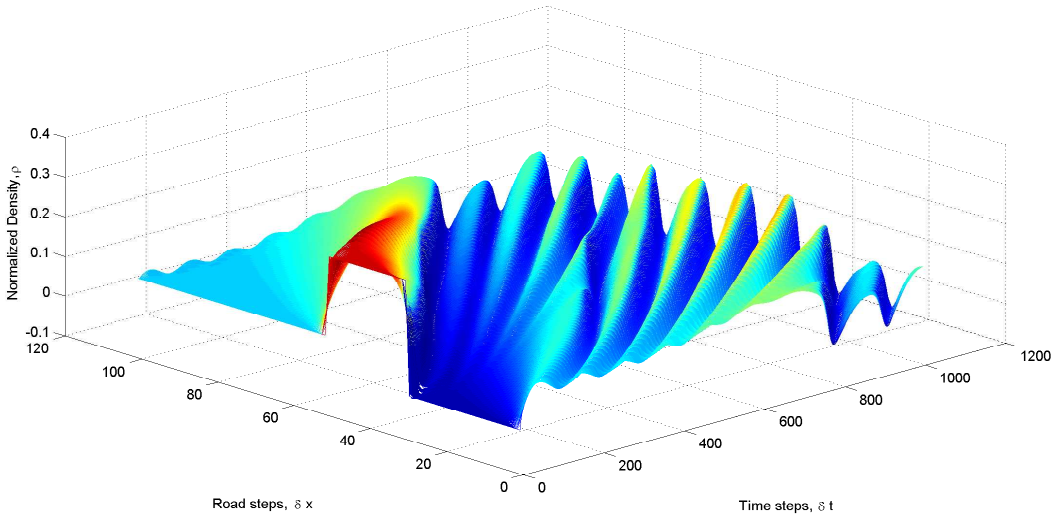

Figure 2.11: The PW model density behavior on a circular road with $C_0 = 25$ m/s.

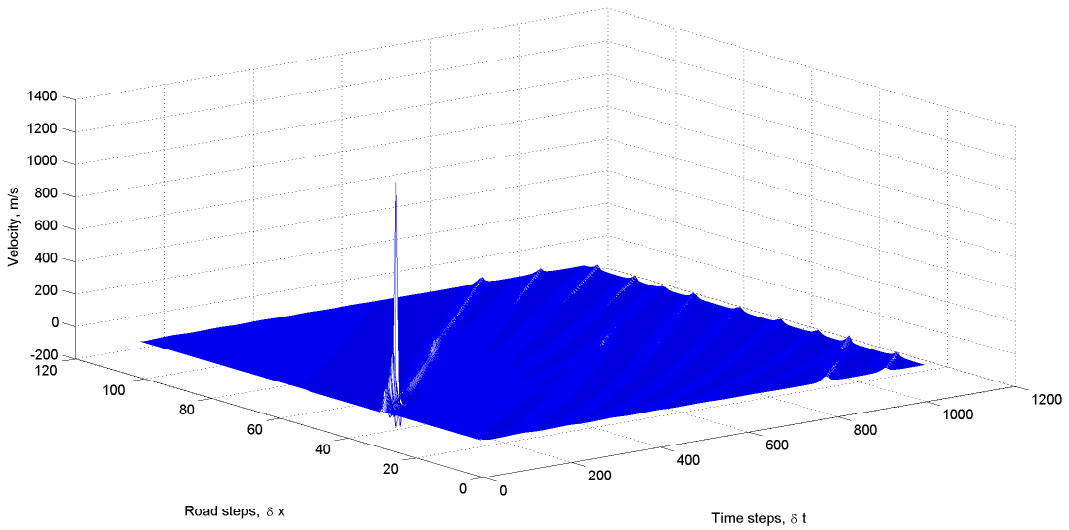

Figure 2.12: The PW model velocity behavior on a circular road with $C_0 = 25$ m/s.

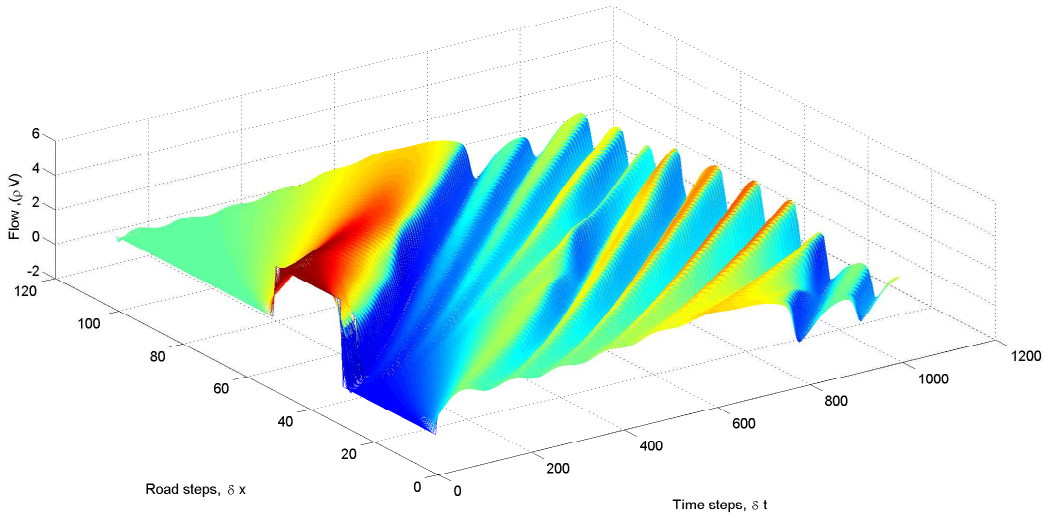

Figure 2.13: The PW model flow behavior on a circular road with $C_0 = 25$ m/s.

Chapter 3

Traffic Flow models based on Front Traffic Stimuli

This chapter considers the time and distance required for vehicles to become aligned with forward traffic conditions. The time for traffic flow adjustment is based on the front traffic stimuli, i.e. the time needed to react and align to the forward traffic. The time to react to this stimuli is known as the reaction time, and the subsequent time required for traffic alignment is known as the transition time. Thus, the reaction distance is the distance travelled during the reaction time, whereas the transition distance is the distance covered during the transition time. The sum of the transition and reaction times is known as the safe time. This is the time required for the safe adjustment of velocity and can be considered the minimum time needed to avoid accidents. The distance travelled during the safe time is known as the safe distance. The safe distance includes the reaction and transition distances. The equilibrium velocity distribution corresponds to a homogeneous traffic flow with no transitions. This distribution is dependent on the traffic density as well as driver behavior and road characteristics, and will result in a homogeneous traffic flow [4].

Parameters such as the safe distance and time, and the maximum density and velocity, determine the transition behavior of the traffic. A simple, practical approach is proposed to model traffic flow so that this behavior can be investigated with respect to variations in these parameters. This will lead to better control of traffic behavior to mitigate congestion, reduce pollution levels, and improve public safety. For example, real-time information can be stored in roadside units for communication to nearby vehicles to warn of congestion ahead and reduce the potential for accidents. Sugges-

tions can be provided to drivers to adjust their vehicle speed and/or take alternative routes.

In this chapter, a new model which includes the transition behavior of traffic is proposed. This model is based on a variable safe distance and safe time which improves the LWR model. The safe distance and time are based on the anticipated velocity. With a larger safe distance, traffic will move slower. Further, the traffic density distribution differs according to the safe distance, and has a greater variance at lower safe distances. Changes in this distribution during traffic transitions depend on the change in velocity required to achieve a homogeneous flow and maintain the safe distance. Transitions occur because of traffic bottlenecks, ramps and traffic lights which control traffic, and result in inhomogeneous traffic flow. Conversely, if a transition does not occur, traffic moves according to the equilibrium velocity distribution and has a homogeneous flow.

The rest of this chapter is organized as follows. Section 3.1 presents the LWR model, and the new model is introduced in Section 3.2. In Section 3.3, the Godunov technique is used to evaluate the performance of these models. A comparison of the LWR and improved LWR models is presented in Section 3.4. Finally, some concluding remarks are given in Section 3.5.

3.1 The LWR Model

The LWR model is the first macroscopic traffic model which was widely accepted. It is based on the principle of conservation of matter and is given by [2, 41]

$$(\rho)_t + (\rho v(\rho))_x = 0, \tag{3.1}$$

where ρ is the density distribution and $v(\rho)$ is the equilibrium velocity distribution. The subscripts t and x denote partial derivative with respect to time and space, respectively. The LWR model maintains vehicle conservation on the road, so it assumes there are no exits or entrances. A smooth traffic density distribution on the road is also assumed. Traffic following an equilibrium velocity distribution results in a homogeneous traffic flow. This distribution is uniquely determined by the density distribution. This distribution characterizes traffic behavior on a very long or infinite length idealized road [34]. An idealized road does not have any disturbances to the homogeneous flow of traffic. The problem with this model is that vehicles adjust their

velocity in zero time which is unrealistic. As a consequence, the LWR model does not consider the transition behavior of traffic. During a transition, the traffic density distribution changes as traffic adjusts its velocity. This adjustment occurs during the safe time period, and results in an inhomogeneous traffic flow, which is not possible with the LWR model [55].

3.2 The Improved LWR Model

A new traffic model is now presented which incorporates the traffic behavior during transitions. Traffic adapts to the equilibrium velocity distribution according to the anticipated change in velocity. This change in velocity results in an acceleration given by

$$a(\rho) = \frac{v(\rho)^2 - v_a^2}{2d_s}, \tag{3.2}$$

where $v(\rho)$ is the equilibrium velocity distribution, v_a is the average velocity of traffic at the transition, and $a(\rho)$ is the acceleration distribution as vehicles move through the safe distance d_s during the safe time t_s. $v(\rho)$ is the velocity distribution the traffic tries to achieve when a transition occurs. For the LWR model, the velocity distribution can be expressed as

$$v(\rho) = a(\rho)t_s. \tag{3.3}$$

Substituting (3.3) in (3.1) gives

$$(\rho)_t + (\rho a(\rho)t_s)_x = 0, \tag{3.4}$$

Now substituting (3.2) in (3.4) results in

$$(\rho)_t + \left(\rho\left(\frac{(v(\rho)^2 - v_a^2)}{2d_s}\right)t_s\right)_x = 0. \tag{3.5}$$

Substituting the equilibrium velocity distribution (1.1) into (3.5) gives

$$(\rho)_t + \left(\rho\left(\left((v_m(1 - \frac{\rho}{\rho_m})\right)^2 - v_a^2\right)\frac{t_s}{2d_s}\right)_x = 0. \tag{3.6}$$

The safe velocity is $v_s = \frac{d_s}{t_s}$, so that (3.6) can be written as

$$(\rho)_t + \left(\left(\left((v_m(1 - \frac{\rho}{\rho_m}) \right)^2 - v_a^2 \right) \frac{\rho}{2v_s} \right)_x = 0. \tag{3.7}$$

Define the traffic flow during a transition as

$$q(\rho) = \left(\left((v_m(1 - \frac{\rho}{\rho_m}) \right)^2 - v_a^2 \right) \frac{\rho}{2v_s}, \tag{3.8}$$

which is a function of the safe velocity. For a smaller safe velocity, the transition will be faster and vice versa. That is, vehicles maintaining a large safe distance will have slow transitions and less interaction between vehicles, whereas a smaller safe distance results in fast transitions and high interaction between vehicles. If there is no transition, v_a can be considered to be zero so the traffic flow (3.8) becomes

$$q(\rho) = \left((v_m(1 - \frac{\rho}{\rho_m}) \right)^2 \frac{\rho}{2v_s}. \tag{3.9}$$

This shows that traffic flow at the equilibrium velocity distribution depends on the safe velocity, which is not accounted for in the LWR model. The traffic flow reduces to the LWR model flow if the safe velocity is half the equilibrium velocity distribution as substituting $v_s(\rho) = \frac{v(\rho)}{2}$ in (3.9) gives

$$q(\rho) = \left(v_m(1 - \frac{\rho}{\rho_m}) \right) \rho, \tag{3.10}$$

and using (1.1) results in

$$q(\rho) = \rho v(\rho), \tag{3.11}$$

so that using (3.10) and (3.11) with (3.7) gives the LWR model

$$(\rho)_t + (\rho v(\rho))_x = 0. \tag{3.12}$$

Hence, the improved LWR model can account for both homogeneous and inhomogeneous traffic flows.

3.3 Performance Evaluation

Consider a road divided into N equidistant segments and M equal duration time steps. The total length is x_N so a segment has length $h = x_N/N$, and the total time duration is t_M so a time step is $k = t_M/M$. For the nth road segment denoted $x_{n-\frac{h}{2}}$ to $x_{n+\frac{h}{2}}$ over time t_m to t_{m+1}, the average traffic density ρ and flow $q(\rho)$ are evaluated using the technique developed by Godunov [46]. The number of vehicles present in the nth segment at time t is given by

$$l_n(t) = \int_{x_{n-\frac{h}{2}}}^{x_{n+\frac{h}{2}}} \rho(x,t)dx, \tag{3.13}$$

and the traffic flow through this segment at time t is

$$\Delta l_n(t) = q(\rho(x_{n-\frac{h}{2}},t)) - q(\rho(x_{n+\frac{h}{2}},t)). \tag{3.14}$$

The traffic flow through the nth segment during the time interval (t_m, t_{m+1}) is then

$$l_n(t_m+1) - l_n(t_m) = \int_{t_m}^{t_{m+1}} \Delta l_n(t)dt = \int_{t_m}^{t_{m+1}} \left(q(\rho(x_{n-\frac{h}{2}},t)) - q(\rho(x_{n+\frac{h}{2}},t))\right) dt. \tag{3.15}$$

Using (3.13), (3.15) takes the form

$$\int_{x_{n-\frac{h}{2}}}^{x_{n+\frac{h}{2}}} \rho(x,t_m+1)dx - \int_{x_{n-\frac{h}{2}}}^{x_{n+\frac{h}{2}}} \rho(x,t_m)dx = \int_{t_m}^{t_{m+1}} \left(q(\rho(x_{n-\frac{h}{2}},t)) - q(\rho(x_{n+\frac{h}{2}},t))\right) dt. \tag{3.16}$$

The average density at time step m for the nth segment is

$$\rho(n,m) = \frac{1}{h}\int_{x_n-\frac{1}{2}}^{x_n+\frac{1}{2}} \rho(x,t_m)dx, \tag{3.17}$$

and the corresponding flow is

$$q(n,m) = \frac{1}{k}\int_{t_m}^{t_{m+1}} q(\rho(x_{n-\frac{h}{2}},t))dt. \tag{3.18}$$

Substituting (3.17) and (3.18) into (3.16) gives

$$\rho(n,m+1) - \rho(n,m) = \frac{k}{h}\left(q(n,m) - q(n+1,m)\right), \tag{3.19}$$

For the LWR model, $q(\rho) = \rho v(\rho)$, and for the improved LWR model $q(\rho)$ is given by (3.8). The traffic flow has initial density distribution $\rho_0(x)$ at $t = 0$, and this is used to determine the initial average densities at $t = 0$.

For the time period (t_m, t_{m+1}) set

$$\rho(x,t) = \rho(n,m) \quad \text{for} \quad x_{n-\frac{1}{2}h} < x < x_{n+\frac{1}{2}h} \tag{3.20}$$

To account for both increasing and decreasing flows $q(\rho(x,t))$ is approximated as

$$q(\rho(x,t)) = \begin{cases} q\left(\min\left(\rho(n-1,m), \rho(n,m)\right)\right), & \text{if} \quad \rho(n-1,m) \leq \rho(n,m) \\ q\left(\max\left(\rho(n,m), \rho(n-1,m)\right)\right), & \text{if} \quad \rho(n-1,m) > \rho(n,m). \end{cases} \tag{3.21}$$

The time step should be chosen such that the maximum distance the traffic covers during this time is not greater than h

$$|q'(\rho)|_{max} \times k < h, \tag{3.22}$$

where $|q'(\rho)|_{max}$ is the maximum rate of change at $t = 0$ given by

$$\max\left(\frac{q(\Delta\rho)}{\Delta\rho}\right) = \max\left(\frac{q(\rho(n,0)) - q(\rho(n-1,0)}{\Delta\rho}\right). \tag{3.23}$$

The time step k is then set to

$$k = 0.5 \times \frac{h}{|q'(\rho)|_{max}}, \tag{3.24}$$

which ensures that the solution converges [46].

3.4 Simulation Results

The simulation parameters are summarized in Table 3.1. Traffic is observed over a period of three seconds while traversing a road from -20 m to 200 m. The road begins at -20 m so that the traffic can begin uniformly distributed about zero, and the length of road considered is $x_N = 220$ m with $N = 450$ so that $h = 0.489$ m. The maximum velocity is $v_m = 30$ m/s and the maximum normalized density is 0.2, i.e., 20% of the maximum density a length of road can take. The initial traffic density distribution is $\rho_0(x) = 0.09 \exp^{\left(\frac{-x^2}{50}\right)}$ and is the same for both the LWR and improved

LWR models. The initial density interval $\Delta\rho$ is set to 0.0004 to evaluate $|q'(\rho)|_{max}$, and this is used in (3.24) to determine k. The boundary conditions are such that vehicles can move beyond the 200 m point. The traffic density distribution evolves with time over the length of road according to the technique presented in Section 3.3. Transitions are observed from average transition velocities of $v_a = 0$ and 10 m/s to the equilibrium velocity distribution (1.1) having $v_m = 30$ m/s.

Figure 3.1 shows the traffic density evolution with the LWR model at 0 s, 1.5 s and 3 s. Figures 3.2, 3.3 and 3.4 show the corresponding results for the improved LWR model. The initial density is shown in blue. The LWR model can only characterize traffic moving with the equilibrium velocity distribution, as it ignores the inhomogeneous traffic flow. Thus, Figure 3.1 shows the traffic flow at the equilibrium velocity with a maximum velocity of 30 m/s.

Figures 3.2 and 3.3 show the improved LWR model for safe velocities of 20 m/s and 10 m/s, respectively, with $v_a = 10$ m/s. The safe distances for these velocities are assumed to be 20 m and 10 m, respectively. During the transitions, traffic adapts its velocity from $v_a = 10$ m/s to the equilibrium velocity distribution having a maximum velocity of 30 m/s. The results in these figures show that traffic moves slower with a 20 m/s safe velocity compared to a 10 m/s safe velocity. At 1.5 s, the traffic density in Fig. 3.2 spans from 23 to 83 m, whereas in Fig. 3.3 it spans from 65 to 155 m. Thus the traffic density has a greater variance at lower safe velocities, and this velocity has a significant effect on traffic behaviour. This variance is greater than with the LWR model, as shown in Figure 3.1. The average distance covered is higher at lower safe velocities as vehicles maintain small safe distance. Figure 3.4 shows the improved LWR model behavior with traffic adapting from a velocity of 0 m/s to the equilibrium velocity distribution having a maximum velocity of 30 m/s with a safe velocity of 20 m/s. There is no significant difference between Figures 3.2 and 3.4, which shows that the average transition velocity has little effect on traffic behaviour.

3.5 Summary

It has been observed that the LWR model cannot accurately model vehicle traffic as it only considers homogeneous flow conditions [44]. Thus it does not capture variations in the flow of traffic, and does not incorporate the safe distance and time. It also does not account for transitions when abrupt changes in the density occur. To overcome

Table 3.1: Simulation Parameters

Name	Parameter	Value
average transition velocity	v_a	0, 10 m/s
equilibrium velocity distribution	$v(\rho)$	Greenshields equation
maximum velocity	v_m	30 m/s
initial density distribution	$\rho_0(x)$	$0.09\exp^{\left(\frac{-x^2}{50}\right)}$
length of road	x	220 m
number of road steps	N	450
segment length	h	$220/450 = 0.489$ m
safe velocity	v_s	10, 20 m/s
normalized maximum density	ρ_m	0.2
initial density interval	$\Delta\rho$	0.0004
time step for the LWR model	k	0.0067 s
time step for the improved LWR model, $v_a = 10$ m/s, $v_s = 20$ m/s	k	0.0102 s
time step for the improved LWR model, $v_a = 0$ m/s, $v_s = 20$ m/s	k	0.0091 s
time step for the improved LWR model, $v_a = 10$ m/s, $v_s = 10$ m/s	k	0.0051 s
Total simulation time	t_M	3 s

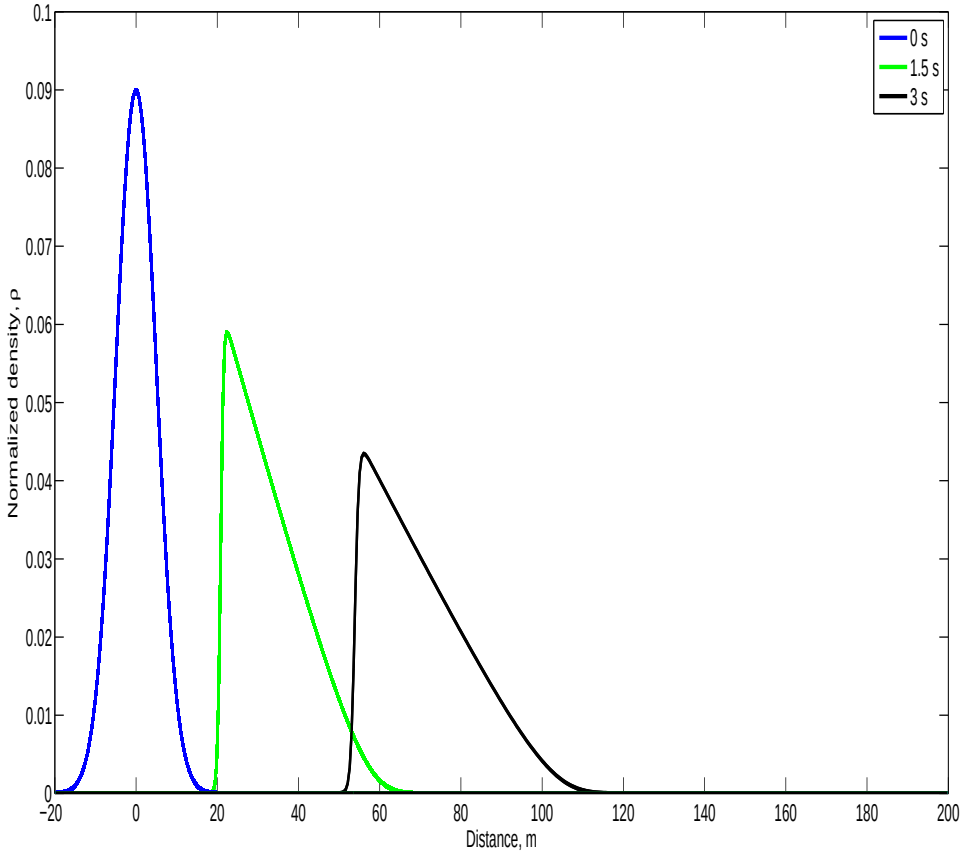

Figure 3.1: Traffic behavior with the LWR model with $v_m = 30$ m/s.

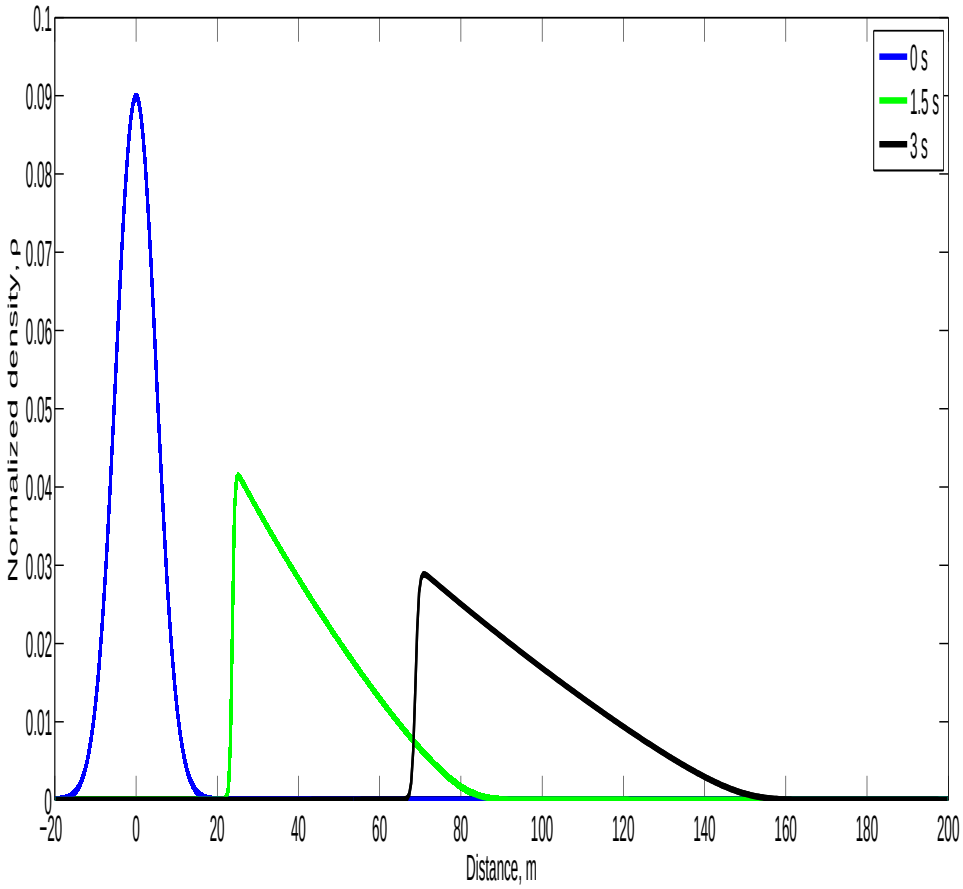

Figure 3.2: The improved LWR model behavior with $d_s = 20$ m, $v_s = 20$ m/s and $v_a = 10$ m/s.

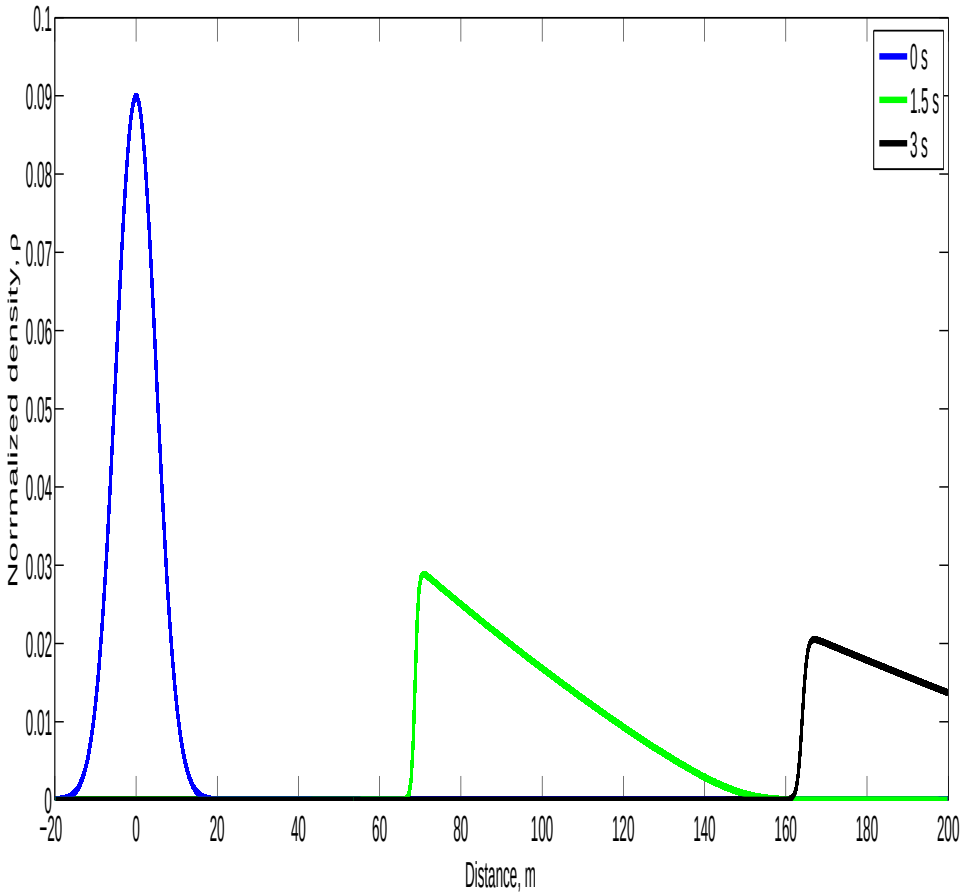

Figure 3.3: The improved LWR model behavior with $d_s = 10$ m, $v_s = 10$ m/s and $v_a = 10$ m/s.

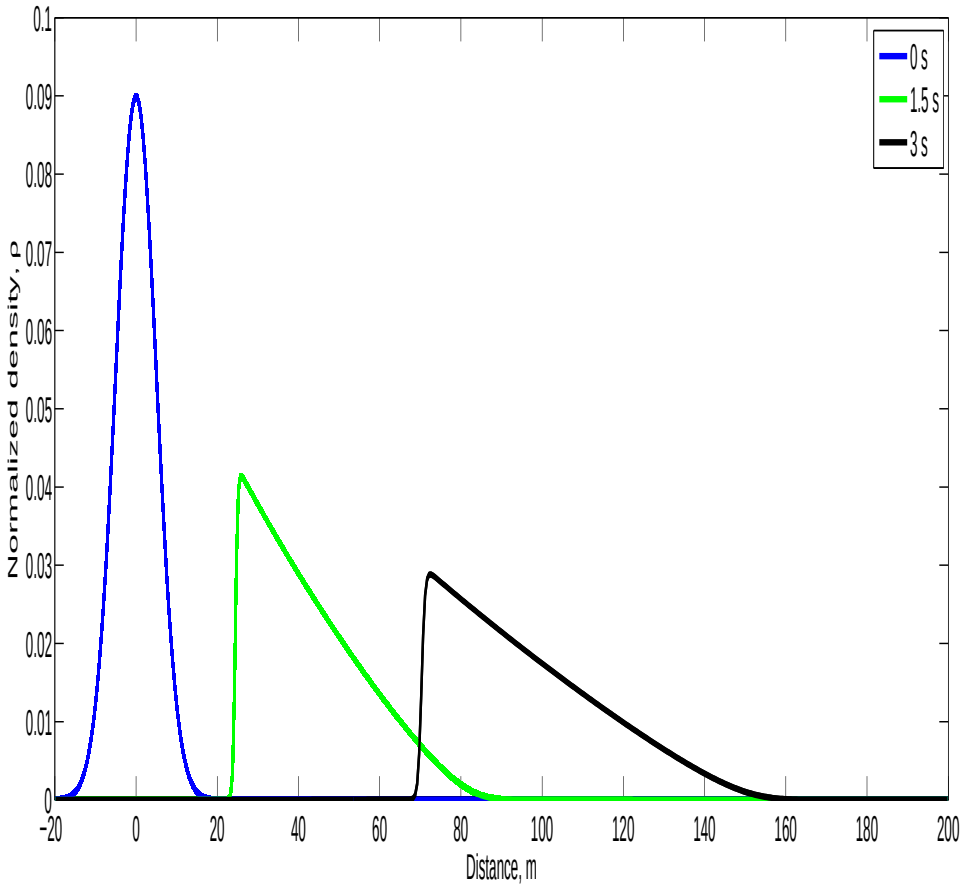

Figure 3.4: The improved LWR model behavior with $d_s = 20$ m, $v_s = 20$ m/s and $v_a = 0$ m/s.

these drawbacks, an improved LWR model was developed which incorporates changes in the velocity behavior during traffic transitions based on the safe time and distance. Performance results were presented which show that this model provides a more realistic characterization of traffic behaviour. Therefore it will provide more realistic results which can be used to reduce fuel consumption and improve the quality of air.

Chapter 4

Traffic Flow Model based on Alignment

This chapter considers the behavior of vehicles as they align to forward traffic conditions. The time for traffic alignment is based on the front traffic stimuli, i.e. the time to react and align to the forward traffic. The time required to react is known as the reaction time, and the time for traffic alignment is known as the transition time. The reaction distance is the distance travelled during the reaction time, while the transition distance is the distance covered during the transition time. The sum of the transition and reaction times is known as the safe time. This is the time required for the safe adjustment of velocity and can be considered the minimum time needed to avoid accidents. The distance travelled during the safe time is known as the safe distance.

Drivers adjust their velocity when a change in traffic flow is observed to achieve the equilibrium velocity distribution. This distribution depends on the traffic density as well as driver behavior and road characteristics, and will result in a homogeneous traffic flow [4]. The traffic flow will evolve into clusters with a large safe distance and small safe time. Conversely, a small safe distance and large safe time will produce a more uniform flow. The goal of this chapter is to develop a simple, realistic model to characterize the traffic flow. This will lead to better control of traffic behavior to mitigate congestion, reduce pollution levels, and improve public safety.

Khan and Gulliver [50] improved the PW model using the fact that driver anticipation is based on the velocity of the forward traffic, so that traffic behavior depends on the velocity during transitions. It was shown that this model provides more realistic

traffic flow and density. The sensitivity of traffic is the rate at which alignment occurs. The limitation of the Khan-Gulliver (KG) model is that this sensitivity depends only on the relaxation time τ. For high velocities, τ is small, so traffic alignment can occur too quickly, whereas with low velocities, τ is large so alignment can be very slow. As a consequence, this model does not have sufficient flexibility to properly characterize traffic behavior.

In this chapter, an improved KG model is proposed to provide more realistic traffic behavior ranging from vehicle clusters to a uniform flow. Transitions in the flow occur when vehicles enter or leave at connecting roads, or when there are obstructions or bottlenecks on the road. The resulting alignment is affected by the safe velocity and the flow behaviour. The safe velocity is the ratio of safe distance to safe time

$$v_s = \frac{d_s}{t_s}.$$

The traffic density distribution has a greater variance at lower safe velocities [49], and changes in this distribution during alignment depend on the velocity adjustments required to adapt to the equilibrium velocity distribution. In the proposed model, a parameter is introduced to regulate traffic flow behaviour so these adjustments are appropriate. With a large flow regulation value, the flow evolves into a large number of small clusters. Conversely, the traffic flow is more uniform with a small value. This value can be chosen based on real traffic data to accurately model traffic behavior. The effect of this parameter is examined in Section 4.3.

The remainder of this chapter is organized as follows. Section 4.1 presents the KG and the improved KG models. In Section 4.2, the well-known Roe decomposition technique is used to implement these models, and performance results are presented for a circular road in Section 4.3. Finally, some concluding remarks are given in Section 4.4.

4.1 Traffic Flow Models

The KG model [50] was developed to characterize traffic flow behavior according to forward velocity conditions. The KG model in conservation form is given by

$$\rho_t + (\rho v)_x = 0 \tag{4.1}$$

$$(\rho v)_t + \left(\frac{(\rho v)^2}{\rho} + \left(\frac{v^2(\rho) - v^2}{2d_{tr}} \right) \rho \right)_x = \rho \left(\frac{v(\rho) - v}{\tau} \right), \tag{4.2}$$

where the subscripts t and x denote the temporal and spatial derivatives, respectively. ρ and v are the traffic density and average velocity, respectively, so that ρv is the flow. $v(\rho)$ is the equilibrium velocity distribution and d_{tr} is the transition distance. A large average velocity results in a small relaxation time and thus the alignment can be very quick and produce unrealistic behaviour.

The source term in (4.2) is

$$\rho \left(\frac{v(\rho) - v}{\tau} \right), \tag{4.3}$$

which indicates that traffic alignment occurs according to the difference between the average velocity and the equilibrium velocity distribution. In reality, alignment is faster at higher velocities, so it should not be a function of only this difference. After alignment, the source term is zero ($v = v(\rho)$), and the traffic flow is smooth. The sensitivity of this term is given by

$$\zeta_1 = \frac{1}{\tau}, \tag{4.4}$$

and this determines how quickly alignment will occur given the other parameters in (4.3). Thus it can have a significant effect on traffic behavior. However, ζ_1 only depends on the relaxation time τ, which may not be sufficient to produce appropriate traffic behavior.

The following traffic model based on the forward traffic stimuli was presented in [49]

$$\rho_t + \left(\rho \left(\frac{v(\rho)^2 - v^2}{2v_s} \right) \right)_x = 0. \tag{4.5}$$

This model has been used to characterize traffic behavior during transitions as well as when the flow is smooth [49]. The RHS of (4.5) is zero because the traffic is considered to be on a long infinite road with no transitions due to the egress or ingress of vehicles to the flow. The anticipation term of this model

$$\rho \left(\frac{v^2(\rho) - v^2}{2v_s} \right), \tag{4.6}$$

characterizes the driver presumption of changes in the forward traffic. With this model, traffic alignment is a quadratic function of velocity. Further, the sensitivity

of (4.6) is

$$\zeta_2 = \frac{1}{2v_s}, \tag{4.7}$$

so it is also a function of the safe distance and safe time, and alignment occurs according to the inverse of the safe velocity.

In this chapter, an improved KG model is proposed for the egress and ingress to the traffic flow, by characterizing the driver response using (4.6). If the equilibrium velocity $v(\rho)$ is greater than the average velocity v, acceleration occurs and alignment will occur at a velocity greater than v. Conversely, if $v(\rho)$ is smaller than v, deceleration occurs, and alignment will occur at a velocity smaller than v. This can be characterized by the numerator of (4.6). Further, alignment depends on the physiological and psychological response of the drivers. This behavior can be characterized using the denominator of (4.6). To provide flexibility in the proposed model, the number 2 in (4.6) is replaced with a flow regulation value b. A small value of b will produce a more uniform flow, while a large value will result in clustered traffic. The new source term is then

$$\rho\left(\frac{v^2(\rho) - v^2}{b\frac{d_s}{t_s}}\right). \tag{4.8}$$

The safe distance consists of the reaction distance d_r and transition distance d_{tr} so that

$$\zeta_3 = \frac{1}{b\left(\frac{d_r + d_{tr}}{t_s}\right)}. \tag{4.9}$$

The psychological response of a driver is characterized by the transition distance, and the physiological response by the reaction distance. A tamed driver responds slowly and takes more time to perceive and process forward traffic conditions. Thus, they will have large reaction and transition distances to align to the traffic. An extreme example of a tamed driver is a person who is intoxicated and so has a very slow response. For a tamed or distracted driver b should be large. Conversely, an excited or aggressive driver will have small reaction and transition distances, so b should be small.

Replacing the source term in the KG model (Improved PW model in Chapter 2) with (4.8) gives the new model

$$(\rho v)_t + \left(\frac{(\rho v)^2}{\rho} + \left(\frac{v^2(\rho) - v^2}{2d_{tr}}\right)\rho\right)_x = \rho\left(\frac{v^2(\rho) - v^2}{bv_s}\right). \tag{4.10}$$

Note that (4.1) is not changed.

4.2 The Decomposition of Traffic Flow Models

To evaluate the performance, Roe decomposition technique is used to implement the KG and improved KG models. This technique is presented in section 1.2.

The Jacobian matrices of both the models are found with the help of Roe's technique. These matrices, average velocity and density are found to be the same as in section 2.2.

In the next section, performance results are presented.

4.3 Performance Results

The performance of the proposed model is evaluated in this section and compared with the KG model over a circular road of length $x_M = 100$ m. A discontinuous density distribution ρ_0 at $t = 0$ with periodic boundary conditions is employed. ρ_0 is shown in blue in the figures. Greenshields equilibrium velocity distribution given in (1.1) is used with $v_m = 34$ m/s and maximum density $\rho_m = 1$. The safe distance is 28 m, the safe time is $t_s = 1.4$ s, and d_{tr} is 20 m. For the KG model, $\tau = 1$ s. The total simulation time is 30 s. Based on $\delta x = 1$ m, the time step is chosen as $\delta t = 0.01$ s to satisfy the CFL condition [46]. The number of time steps and road steps are 3000 and 100, respectively, for both the KG and improved KG models. The flow regulation parameters considered for the improved model are $b = 1$ and 2. The simulation parameters are summarized in Table 4.1.

Figure 4.1 presents the normalized traffic density with the KG model at four different time instants. This shows that the traffic evolves into two clusters of vehicles. At 5 s the density behavior is slightly oscillatory. However, at 15 s the traffic density beyond 50 m has an almost uniform level of 0.09, and there are two clusters of vehicles between 0 and 50 m. The traffic density of these clusters ranges from 0.1 to 0.21. Both the clusters span a distance of approximately 20 m. At 30 s, the traffic density between 0 and 40 m has an almost uniform density of 0.09, while beyond 40 m there are two clusters. The clusters still span a distance of about 20 m, so they have just moved over time. The first cluster has a maximum density of 0.25 at 50 m, and the second a maximum density 0.2 at 78 m.

Table 4.1: Simulation Parameters

Name	Parameter	Value
road step	δx	1 m
equilibrium velocity	$v(\rho)$	Greenshields velocity distribution
maximum velocity	v_m	34 m/s
road step	δx	1 m
time step	δt	0.01 s
safe distance	d_s	28 m
transition distance	d_{tr}	20 m
safe time	t_s	1.4 s
safe velocity	v_s	$\frac{28}{1.4} = 20$ m/s
normalized maximum density	ρ_m	1
total simulation time	t_M	30 s
flow regulation parameter	b	1,2
relaxation time constant	τ	1 s
number of time steps	M	3000
number of road steps	N	100

Figure 4.2 presents the normalized traffic density with the improved KG model and $b = 1$ s at four different time instants. This shows that with a small value of b, the traffic becomes quite smooth over time. At 5 s, the variation in traffic density ranges from 0.07 to 0.17, while at 15 s this variation is 0.1 to 0.14, and at 30 s the range is only 0.12 to 0.13.

Figure 4.3 presents the normalized traffic density behavior with the improved KG model and $b = 2$ s at four different time instants. There are larger variations in the density than with $b = 1$, but smaller than with the KG model. The traffic evolves into two clusters with a smooth density between them. The variation in density is between 0.09 and 0.16 at 15 s, and between 0.1 and 0.15 at 30 s.

Figure 4.4 presents the traffic density behavior with the KG model over a time span of 30 s (3000 time steps) for 100 road steps. This shows that the traffic evolves into clusters over time. Figure 4.5 presents the density behavior with the proposed model and $b = 1$. In this case, the traffic becomes more uniform over time. The traffic density behavior for the proposed model with $b = 2$ is given in Figure 4.6. The density variations are smaller than with the KG model, but there are still two clusters. Further, they are larger than with the improved KG model and $b = 1$.

The traffic velocity behavior with the KG model is given in Figure 4.7 at four different time instants. The similarity with the density shown in Figure 4.1 indicates that the velocity is density dependent, with greater velocities observed at lower densities. The greatest fluctuations in velocity occur at 5 s. At 15 s, the traffic has a nearly uniform velocity beyond 50 m of 31 m/s. There are two clusters of vehicles from 0 to 50 m. The velocity in these clusters varies from 27 m/s to 30.2 m/s. At 30 s, between 0 and 40 m the traffic has a near uniform velocity of 31 m/s, and the two clusters are located beyond 40 m. The first cluster is between 40 and 70 m and has a velocity which varies from 26 to 30.2 m/s, while in the second cluster is located between 70 and 90 m and has a velocity which varies from 28 to 30.2 m/s. Comparing the traffic at 15 and 30 s, the velocity in the second cluster increases by 1 m/s, whereas the velocity of the first cluster decreases by 2 m/s.

Figure 4.8 presents the velocity behavior at four different time instants for the improved KG model with $b = 1$. This corresponds to the density shown in Figure 4.2. At 5 s, the variations in velocity are the greatest, ranging from 29 to 31 m/s. At 15 s, this variation is 29.5 to 31.5 m/s, while at 30 s, it is less than 1 m/s. These variations are smaller than with the KG model. Figure 4.9 presents the velocity behavior at four different time instants for the improved KG model with $b = 2$. This corresponds

to the density shown in Figure 4.3. The fluctuations in velocity are greatest at 5 s, with a range of 28 to 31 m/s, At 15 s, the range is 29 to 30.5 m/s, while at 30 s it is only 29 to 30.2 m/s. Thus the velocity fluctuations are larger than with $b = 1$, but smaller than with KG model.

The velocity behavior on the road over a time span of 30 s with the KG model and the improved KG model with $b = 1$ and 2 is given in Figures 4.10, 4.11, and 4.12, respectively. These figures also illustrate that the fluctuations in velocity are density dependent, but the variations in the velocity reduce over time in all cases. However, the velocity is more oscillatory with the KG model than with the improved KG model, particularly with $b = 1$.

The traffic flow behavior with the KG model is presented in Figure 4.13 at four different time instants. The change in flow follows the changes in density and velocity as it is the product of these two parameters. At 5 s, the flow is more oscillatory, whereas at 15 s, the flow evolves into two clusters between 0 and 50 m. The flow in the first cluster varies from 6 veh/s to 3.5 veh/s, while in the second cluster it varies from 6 veh/s to 2.8 veh/s. The flow beyond 50 m aligns to a uniform level of 2.8 veh/s. At 30 s, the two clusters have moved beyond 40 m. The flow in the first cluster now varies from 2.8 to 7 veh/s, while in the second cluster it varies from 3 to 5.2 veh/s. The minimum flow between the clusters is 3 veh/s at 65 m. In the first 40 m, the flow has an approximately uniform level of 2.8 veh/s.

Figure 4.14 presents the traffic flow behavior at four different time instants with the improved KG model and $b = 1$. At 5 s, the flow varies from 2.5 to 4.5 veh/s. The maximum and minimum flows occur at 50 m and 40 m, respectively. At 15 s, the flow varies from 3.2 to 4.2 veh/s, which is less than at 5 s. The maximum and minimum flows now occur at 70 m and close to 60 m, respectively. At 30 s, the flow is only in the range 3.5 to 4 veh/s, and the maximum flow occurs at 40 m. Figure 4.15 presents the corresponding traffic flow behavior with the proposed model and $b = 2$. The behavior is more oscillatory at 5 s, and the flow varies from 2.5 to 6 veh/s, which is greater than with $b = 1$. At 15 s, the flow varies from 3 to 4.5 veh/s, and it is almost the same at 30 s. However, the locations of the maximum and minimum traffic flows are different.

Traffic flow over a time span of 30 s with the KG model and the improved KG model with $b = 1$ and 2 is given in Figures 4.16, 4.17 and 4.18, respectively. The flow variations reduce with time in all cases. These figures demonstrate that the flow is more oscillatory with the KG model, while the variations are lowest (the flow is

more uniform), with the improved KG model and $b = 1$. With $b = 2$, there are small oscillations in the flow which are smaller than with the KG model.

The results in this section show that the flow regulation parameter b in the proposed model can be used to adjust traffic oscillations and cluster behavior. For smaller values of b, traffic becomes more uniform. Thus, unrealistic oscillations can be eliminated with this parameter, and cluster behavior can be properly characterized.

4.4 Summary

In this chapter, improved KG model was proposed to characterize the physiological and psychological response of drivers to changes in the traffic flow. For a slow response, the traffic becomes clustered, while for a fast response the traffic flow is more uniform. A regulation parameter was introduced to further refine the driver response to forward conditions. This allows for a more realistic traffic characterization than with other models in the literature, The use of this improved KG model will lead to better results which can be used to reduce fuel consumption and pollution.

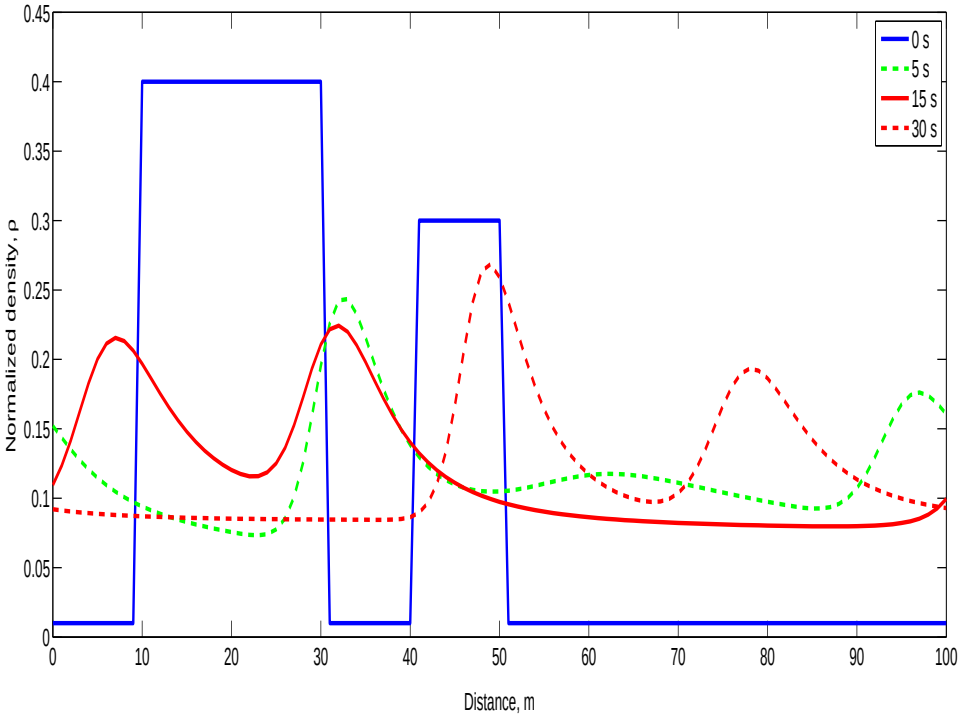

Figure 4.1: The KG model density behavior with $\tau = 1$ s.

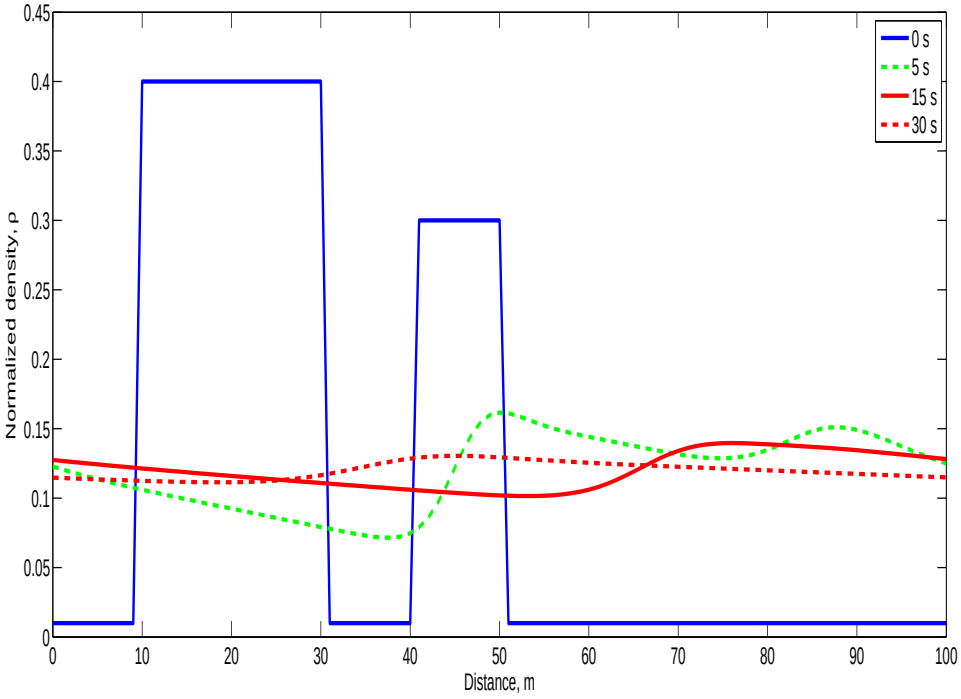

Figure 4.2: The improved KG model density behavior with aggresive drivers having $b = 1$.

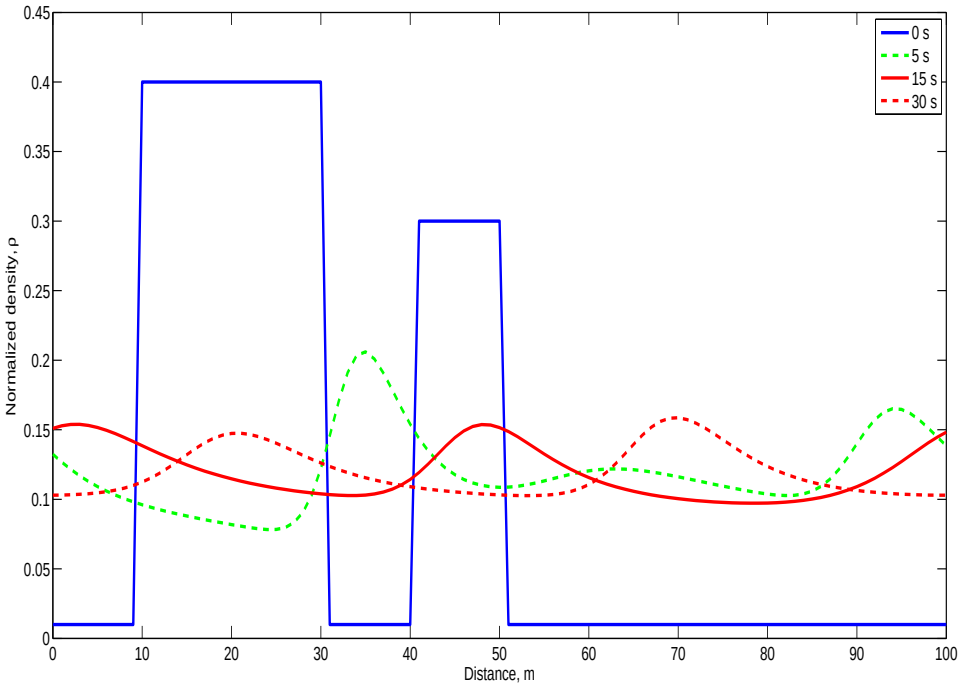

Figure 4.3: The improved KG model density behavior with slow drivers having $b = 2$.

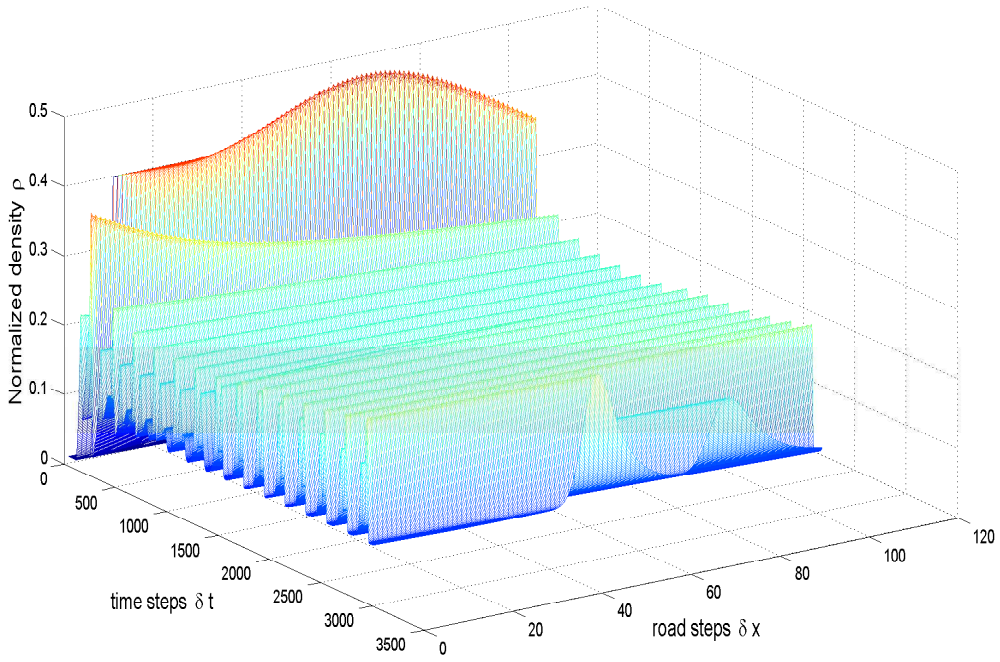

Figure 4.4: The KG model density behavior with $\tau = 1$ s.

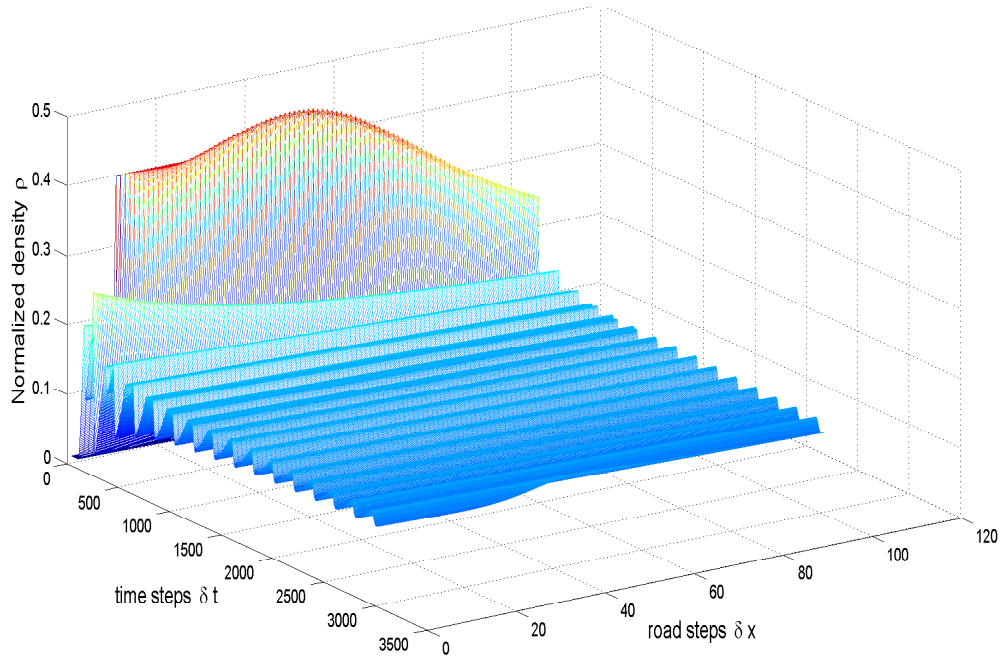

Figure 4.5: The improved KG model density behavior with aggresive drivers having $b = 1$.

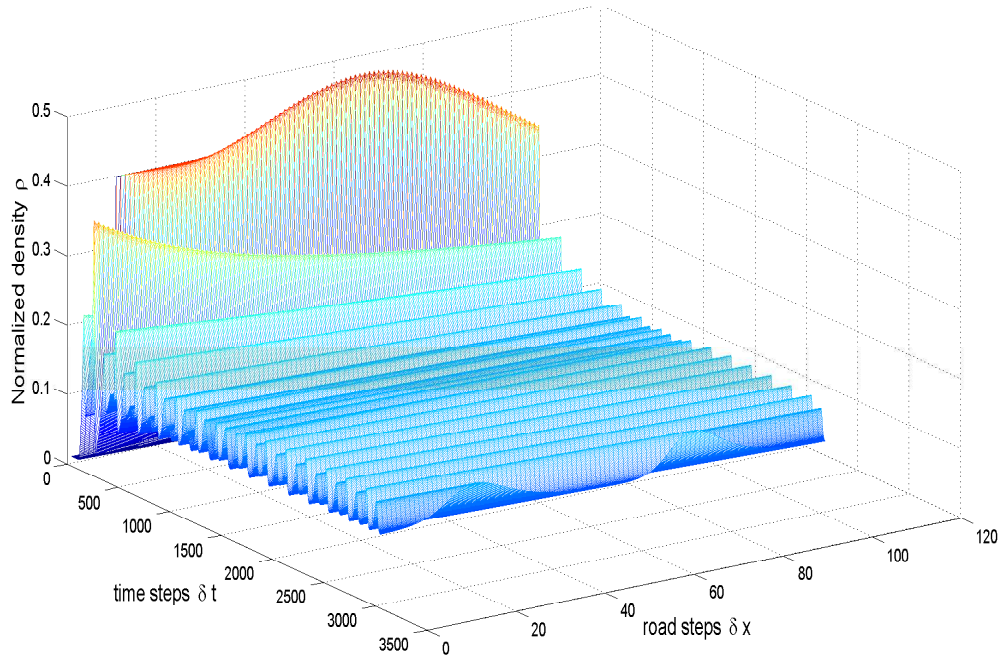

Figure 4.6: The improved KG model density behavior with slow drivers having $b = 2$.

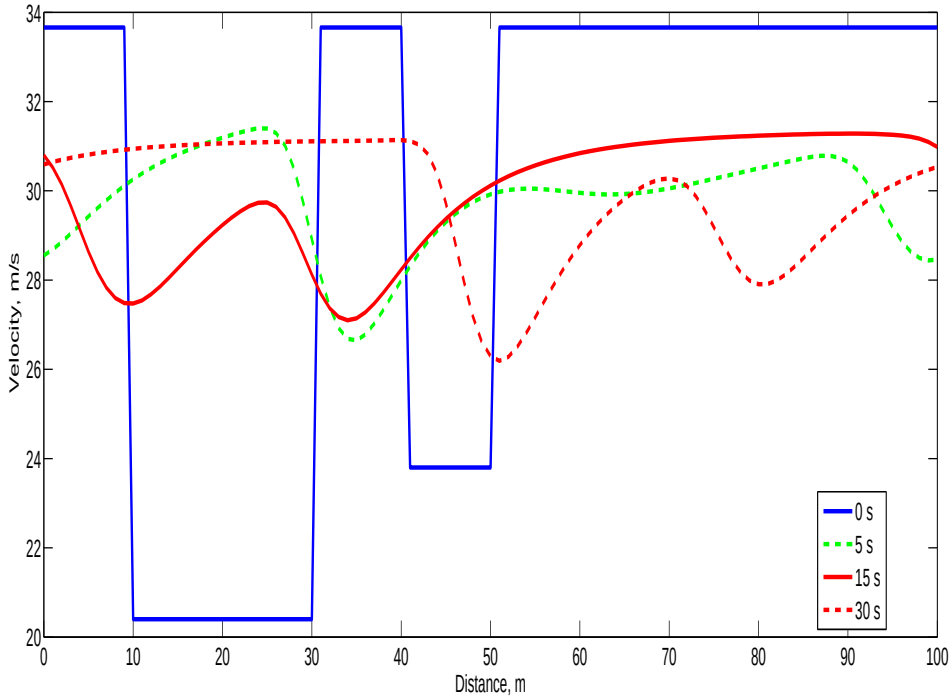

Figure 4.7: The KG model velocity behavior with $\tau = 1$ s.

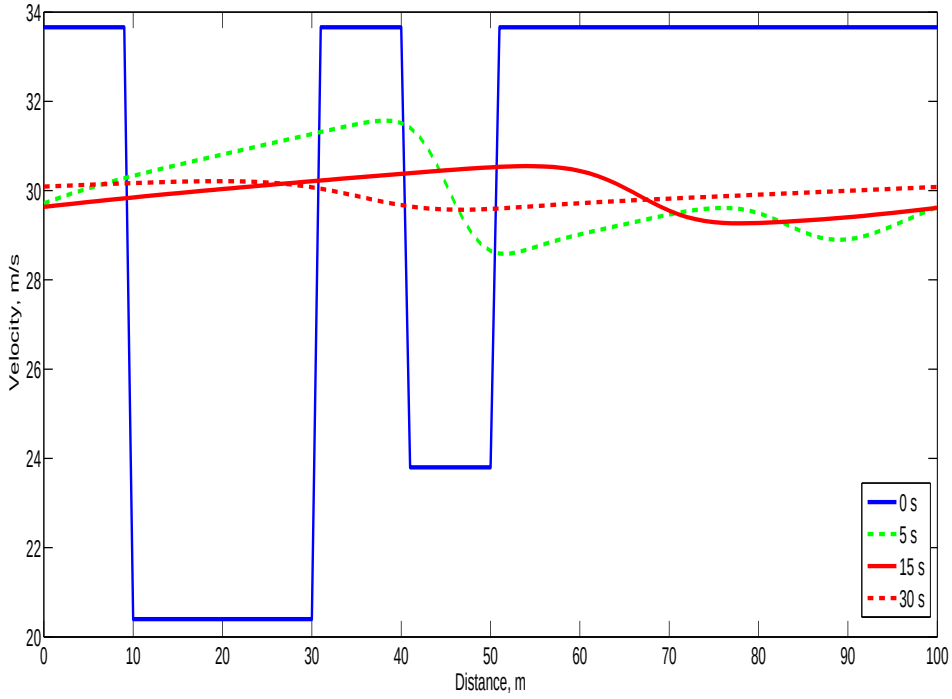

Figure 4.8: The improved KG model velocity behavior with aggressive drivers having $b = 1$.

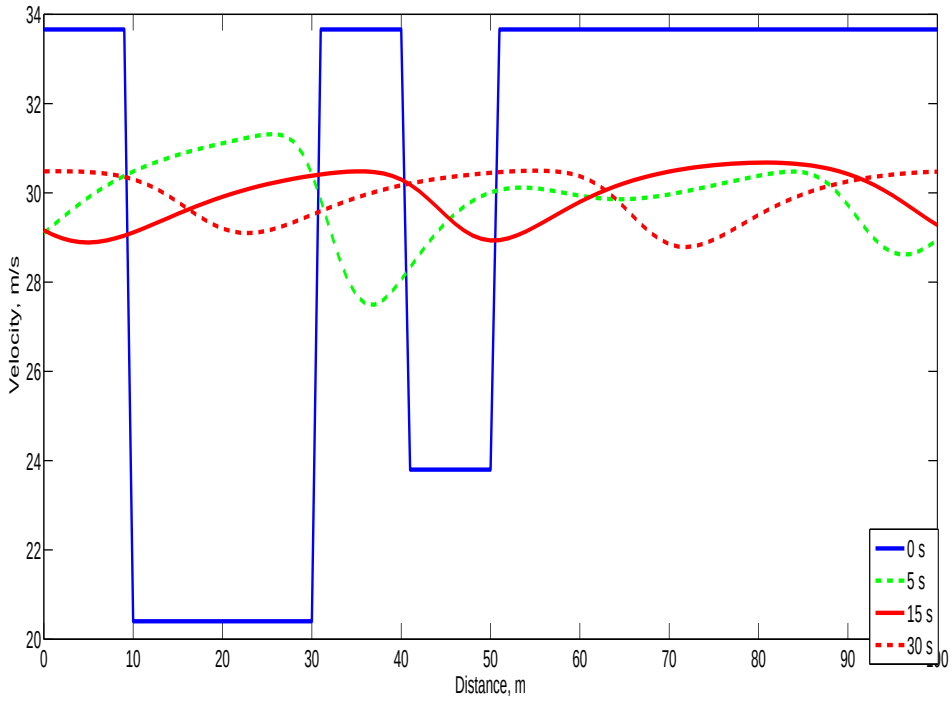

Figure 4.9: The improved KG model velocity behavior with slow drivers having $b = 2$.

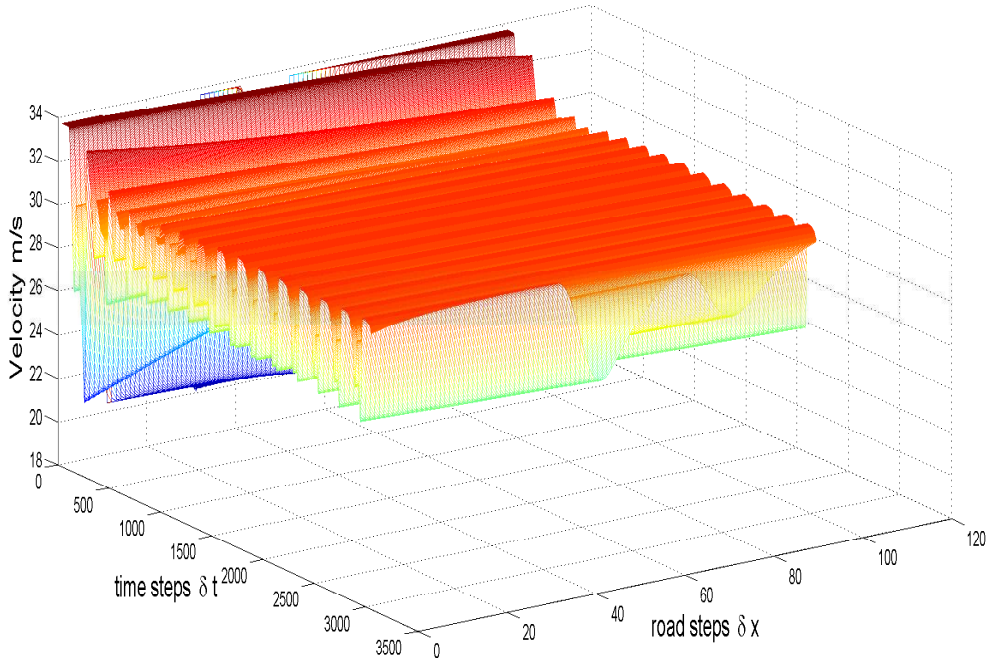

Figure 4.10: The KG model velocity behavior with $\tau = 1$ s.

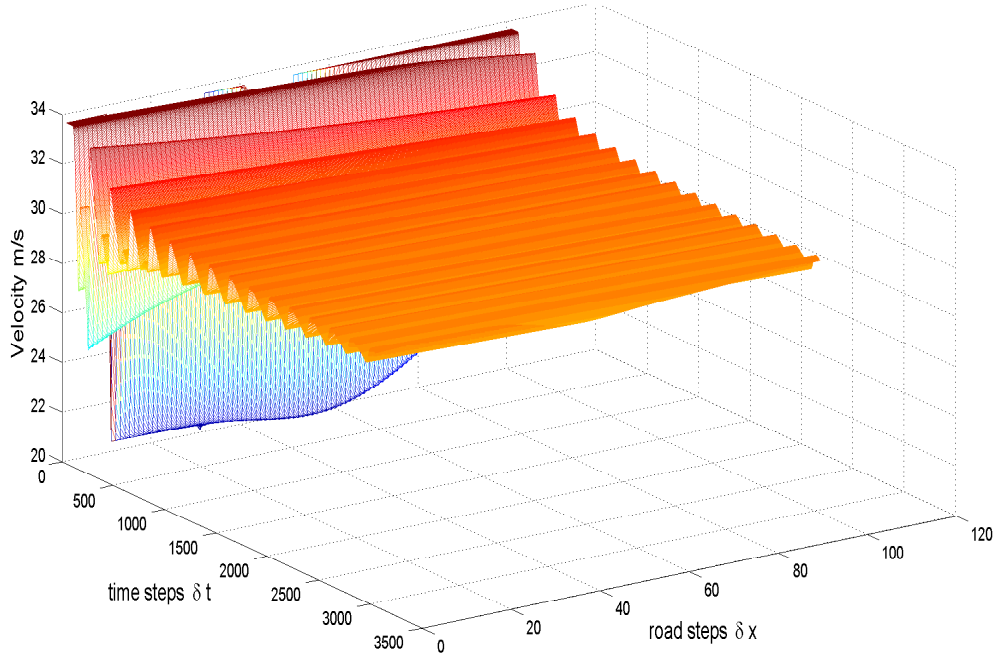

Figure 4.11: The improved KG model velocity behavior with aggressive drivers having $b = 1$.

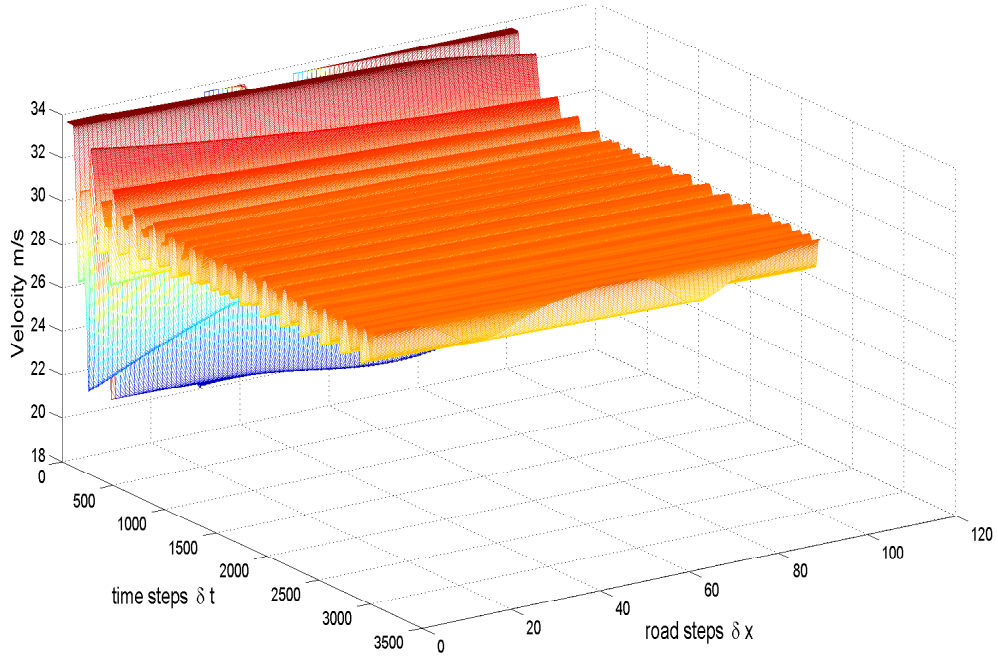

Figure 4.12: The improved KG model velocity behavior with slow drivers having $b = 2$.

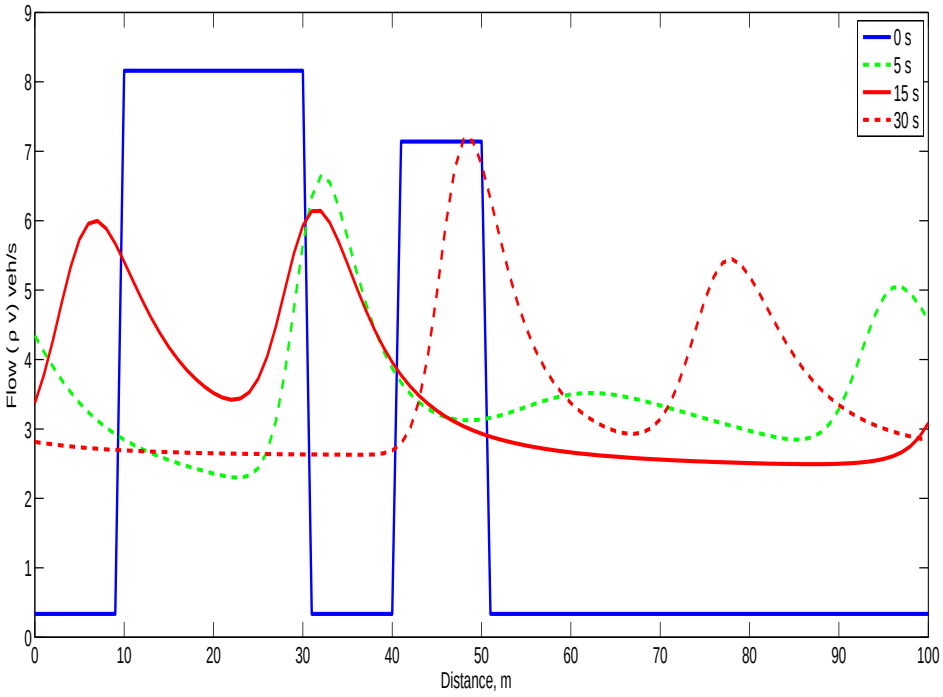

Figure 4.13: The KG model flow with $\tau = 1$ s.

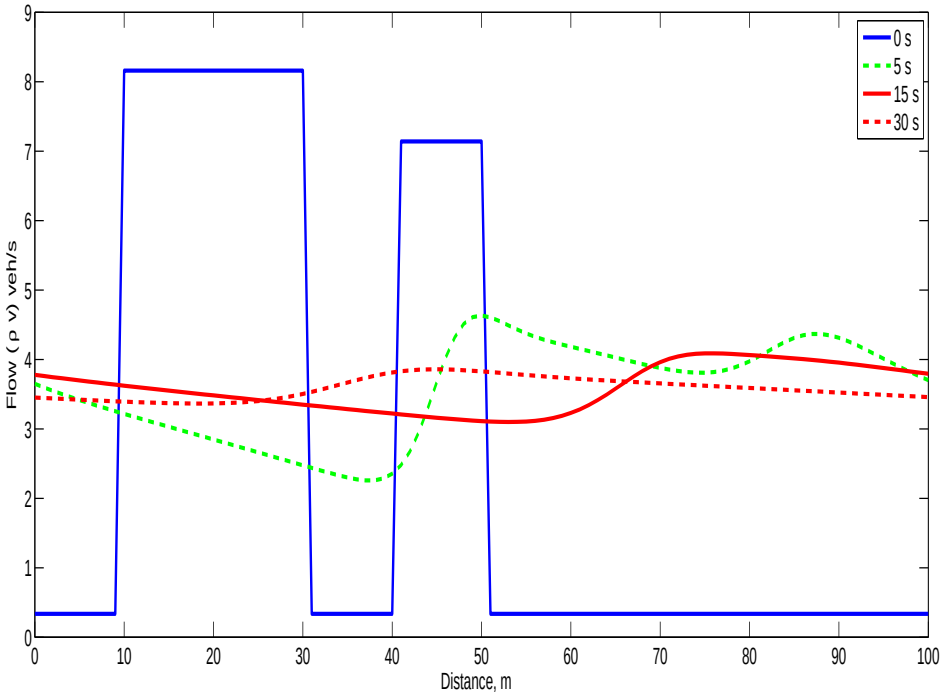

Figure 4.14: The improved KG model flow with aggressive drivers having $b = 1$.

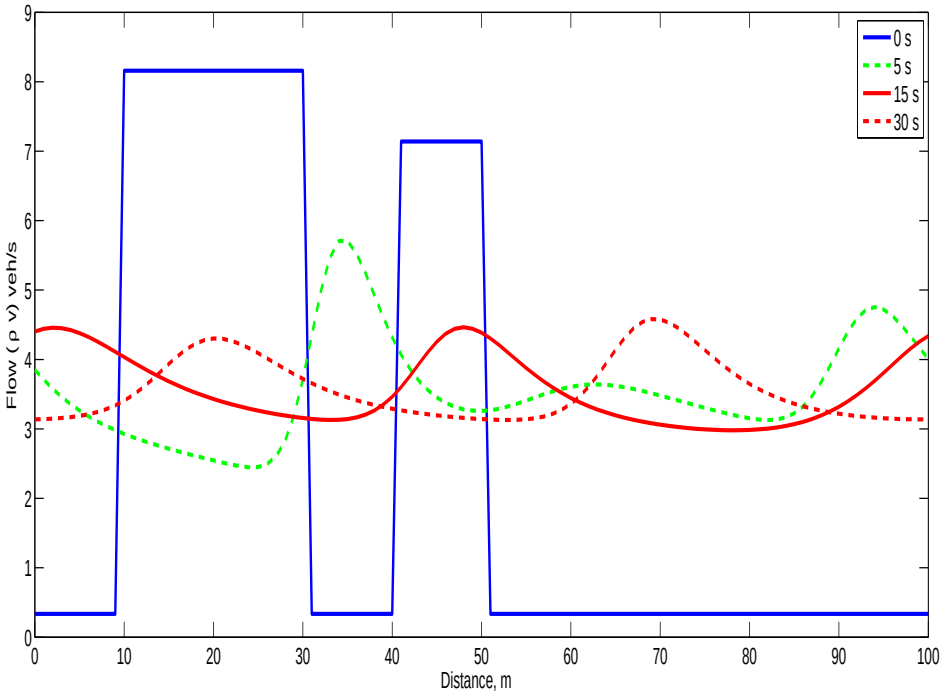

Figure 4.15: The improved KG model flow with slow drivers having $b = 2$.

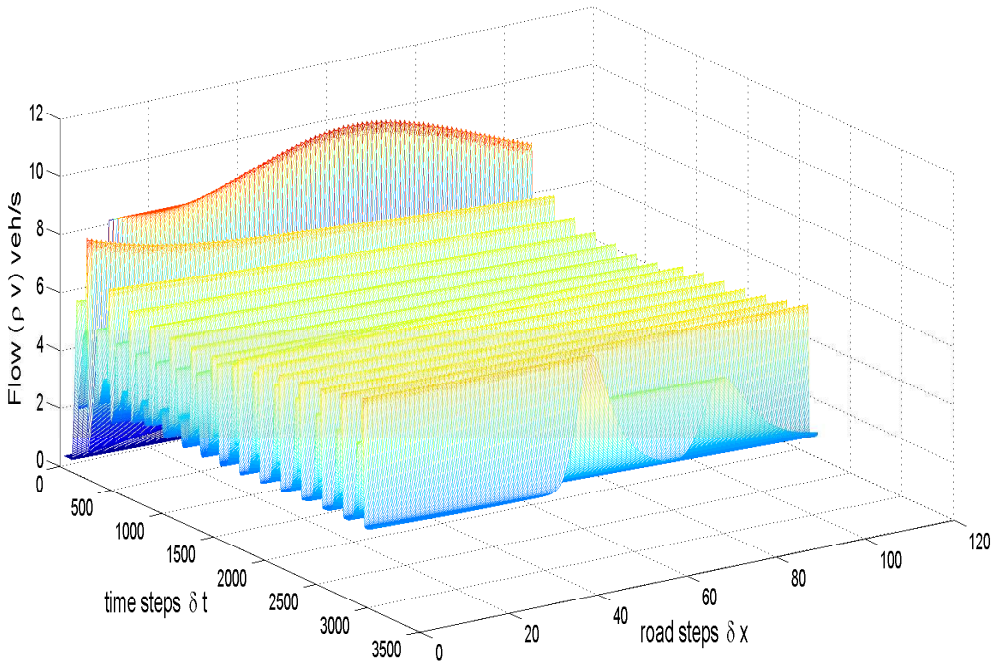

Figure 4.16: The KG model flow with $\tau = 1$ s.

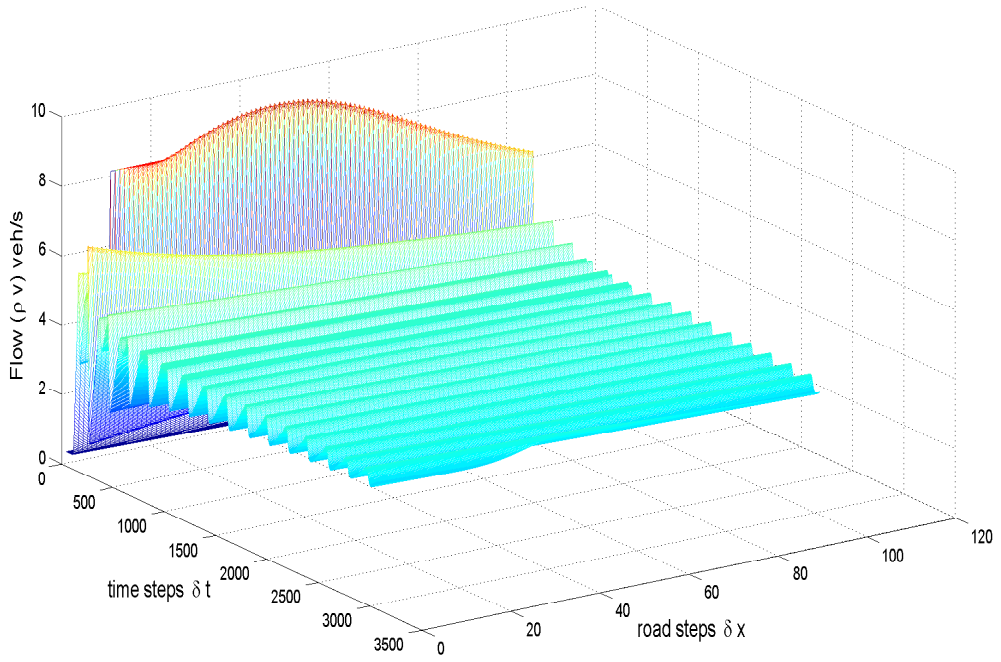

Figure 4.17: The improved KG model flow with aggressive drivers having $b = 1$.

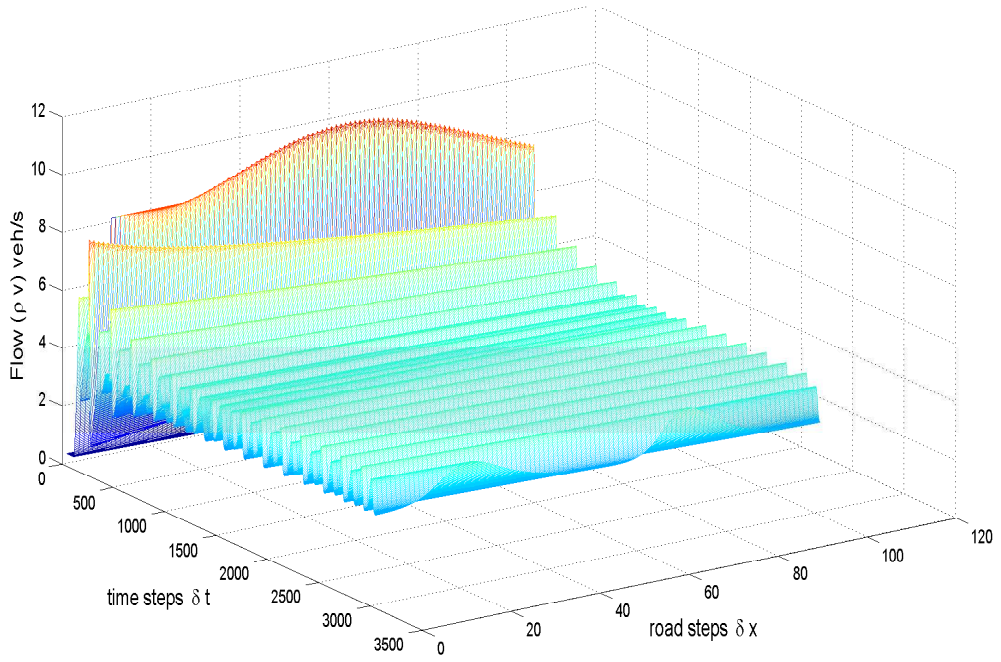

Figure 4.18: The improved KG model flow behavior with slow drivers having $b = 2$.

Chapter 5

Traffic Flow Model based on Driver Response

5.1 Introduction

A new macroscopic flow model is proposed to accurately predict traffic behavior. This model includes the characterization of traffic density and velocity during alignment with forward conditions. This alignment should be based on the physiological and psychological response of the drivers. Further, for large traffic densities traffic moves at smaller velocities, whereas traffic moves faster at low traffic densities. The average distance between vehicles is proportional to the traffic density and so there will be significant interaction between vehicles at large densities, which indicates congestion. Driver response is typically fast during congestion because conditions are more predictable and distances between vehicles are small. Conversely, traffic with a low density is typically free flow and thus response is small. However, driver response can deviate from typical behavior and be slow or aggressive.

In this chapter, a new macroscopic traffic flow model is proposed based on analogies developed from the ideal gas law. This law specifies that the density of gas changes with temperature for a given pressure. For traffic, the density changes with velocity. When there is congestion, the traffic density is high and the velocities are small, while during free flow, the density is low and the velocities can be high. Analogous to the specific gas constant, a traffic constant is introduced to characterize the driver response. These conditions include the traffic headway, safe time and velocity. Headway is the distance between the centers of adjacent vehicles and is a function of

traffic density. The interaction between vehicles is large when the headway is small (and the density is high). The minimum time required for traffic alignment to avoid accidents is known as the safe time and is related to the velocity. The traffic flow model proposed in this paper has an anticipation term which is based on this traffic constant. Conversely, the PW model has an anticipation term based on a constant driver response for all traffic conditions.

Driver response includes both physiological and psychological behavior. The physiological behavior includes the time taken to perceive and process traffic situations and the resulting actions. The psychological behavior is the response to a situation based on awareness and attitude. Traffic can be characterized more realistically if the model incorporates both types of behavior. Therefore, in this chapter driver perception, awareness, reaction and attitude are considered.

Traffic model performance is examined on a circular road with a transition caused by an inactive bottleneck. An inactive bottleneck is congestion resulting from a higher density ahead. It is shown that the PW model can produce unrealistic results in this situation because it cannot adequately characterize driver behavior. Conversely, the proposed model is shown to provide realistic results.

The rest of the chapter is organized as follows. Section 5.2 presents the proposed model. In Section 5.3 Roe's decomposition technique is used to characterize the proposed and PW models, and the traffic performance using this method is presented in Section 5.4. Finally, some concluding remarks are given in Section 5.5.

5.2 The Proposed Model

In this section, analogies between gas and traffic behavior are considered in developing a new traffic model. The ideal gas law is given by

$$pV = nRT, \tag{5.1}$$

where p is pressure, V is volume, n is the number of moles of gas, R is the ideal gas constant, and T is temperature. The number of moles is

$$n = \frac{m}{z}, \tag{5.2}$$

where m is the mass and z is the molar mass. Substituting (5.2) in (5.1) gives

$$p = \frac{m}{V}\frac{R}{z}T. \tag{5.3}$$

The density is $\rho = \frac{m}{V}$ and the specific gas constant is $R_s = \frac{R}{z}$, so that

$$p = \rho R_s T, \tag{5.4}$$

which shows that pressure is proportional to density.

Traffic pressure can be considered as the desire to achieve the equilibrium velocity. The traffic pressure is high in congestion due to the high density. This effect is similar to the behavior of gas given by (5.4). Further, the average traffic velocity, v, is analogous to gas temperature, as an increase in velocity results in a greater pressure.

The specific gas constant relates pressure, density and temperature. In this paper, a traffic constant denoted by L_d is introduced which relates traffic pressure, density and velocity based on the driver response and so is a function of their physiological and psychological behavior. The physiological response of a driver includes driver perception of and reaction to traffic conditions ahead, whereas the psychological response includes driver awareness and attitude. Thus, the traffic constant incorporates driver perception, attitude, awareness and reaction, and analogous to (5.4) we have

$$p = \rho L_d v, \tag{5.5}$$

The time taken by a driver to perceive and process traffic conditions is collectively called the perception time, and is a function of density, so it is denoted by $\tau(\rho)$. In congested traffic, the perception time is large and the alignment of the vehicles flow is slow. Conversely, during free flow perception time is small and vehicle alignment is fast. Driver attitude can be characterized as the ratio of the safe time and perception time

$$\beta = \frac{\tau_s}{\tau(\rho)}, \tag{5.6}$$

where τ_s is the safe time. Driver behavior is considered normal if the perception time is similar to the safe time. If the perception time is larger than the safe time, the behavior can be considered slow (such as with an intoxicated driver). Conversely, if the perception time is much smaller than the safe time, the driver behavior can be

considered to be aggressive. Thus, for a normal driver

$$\beta \approx 1,$$

for a slow driver

$$\beta \ll 1,$$

and for an aggressive driver

$$\beta \gg 1.$$

The safe time τ_s is inversely proportional to the spatial rate of change in velocity v_x (acceleration), and so can be expressed as

$$\tau_s = \frac{1}{v_x}, \tag{5.7}$$

where the subscript x denotes the derivative with respect to distance. Thus the lower the acceleration or deceleration, the greater the safe time.

The perception time $\tau(\rho)$ is small during free flow as vehicles align quickly, and is large during congestion. Thus, the perception time due to fluctuations in the density can be characterized as

$$\tau(\rho) = \frac{1}{v(\rho)_\rho} \tag{5.8}$$

where $v(\rho)$ denotes the equilibrium velocity distribution and the subscript ρ denote the derivative with respect to density. Substituting (5.7) and (5.8) in (5.6) gives

$$\beta = \frac{v(\rho)_\rho}{v_x}. \tag{5.9}$$

In the literature, driver reaction has been characterized as a constant [1], and also as a linear [55] or exponential function of the density. While using a constant results in a simple model, it may not provide realistic results. With a linear relationship, the response is too similar with high and low densities. Conversely, with an exponential relationship, significant acceleration and deceleration can occur with high densities, and very low acceleration and deceleration at low densities, which can produce unrealistic behavior. Thus in this chapter, the driver reaction is characterized by

$$\rho^2. \tag{5.10}$$

This square law relationship provides a smooth change in traffic flow with variations in density, which is desirable.

Driver awareness increases with greater interaction between vehicles, and so can be characterized by the traffic headway S. The headway is small during congestion, which increases the acceleration and deceleration, and thus results in a more discontinuous traffic flow. With an increase in traffic density, driver awareness increases as the surrounding vehicles must be observed more carefully. Conversely, free flow traffic has a low density, so the headway is large and awareness tends to be low. The traffic headway S can then be expressed as

$$S = \frac{1}{\rho}. \tag{5.11}$$

Combining (5.9), (5.10), and (5.11), the traffic constant which characterizes driver response is given by

$$L_d = \frac{v(\rho)_\rho \rho_x^2}{v_x \rho}. \tag{5.12}$$

Several models have been proposed for the equilibrium velocity distribution $v(\rho)$ [32]. The Greenshields model [60] is commonly employed [33] and is given by

$$v(\rho) = v_m \left(1 - \frac{\rho}{\rho_m}\right), \tag{5.13}$$

where ρ_m and ρ are the maximum and average traffic densities, respectively, and v_m is the maximum velocity on the road. Therefore, (5.13) is used here to evaluate the traffic models.

From (5.5), the rate of change in pressure with respect to density is

$$\frac{dp}{d\rho} = L_d v. \tag{5.14}$$

The spatial change in pressure is a function of the temporal change in velocity [31], so that

$$\frac{dp}{dx} = -\rho \frac{dv}{dt}. \tag{5.15}$$

Further

$$\frac{dp}{dt}\frac{dt}{dx} = -\rho \frac{dv}{dt}, \tag{5.16}$$

and substituting $v = \frac{dx}{dt}$ gives

$$\frac{dp}{dt} = -v\rho\frac{dv}{dt}. \tag{5.17}$$

The temporal change in pressure can also be expressed as

$$\frac{dp}{dt} = \frac{dp}{d\rho}\frac{d\rho}{dt}, \tag{5.18}$$

and substituting (5.14) and (5.17) gives

$$-v\rho\frac{dv}{dt} = L_d v\frac{d\rho}{dt}. \tag{5.19}$$

The rate of change in ρ and v with distance and time is given by

$$\frac{d\rho}{dt} = \frac{\partial\rho}{\partial t} + \frac{\partial\rho}{\partial x}\frac{dx}{dt} \text{ and } \frac{dv}{dt} = \frac{\partial v}{\partial t} + \frac{\partial v}{\partial x}\frac{dx}{dt}, \tag{5.20}$$

respectively, which can be expressed as

$$\frac{d\rho}{dt} = \frac{\partial\rho}{\partial t} + v\frac{\partial\rho}{\partial x} \text{ and } \frac{dv}{dt} = \frac{\partial v}{\partial t} + v\frac{\partial v}{\partial x}. \tag{5.21}$$

Then substituting $\frac{d\rho}{dt}$ and $\frac{dv}{dt}$ from (5.21) in (5.19) gives

$$-\rho\left(v_t + vv_x\right) = L_d\left(\rho_t + v\rho_x\right), \tag{5.22}$$

where the subscripts t and x denote the derivatives with respect to time and distance, respectively. Adding and subtracting $L_d\rho v_x$ to the RHS of (5.22) gives

$$-\rho\left(v_t + vv_x\right) = L_d\left(\rho_t + v\rho_x + \rho v_x - \rho v_x\right), \tag{5.23}$$

and substituting

$$(v\rho)_x = v\rho_x + \rho v_x,$$

results in

$$-\rho\left(v_t + vv_x\right) = L_d\left(\rho_t + (v\rho)_x - \rho v_x\right). \tag{5.24}$$

The conservation of vehicles on the road is given by [2]

$$\rho_t + (\rho v)_x = 0, \tag{5.25}$$

which models the smooth flow of traffic on a long idealized road. Substituting (5.25) in the RHS of (5.24) gives

$$-\rho\left(v_t + vv_x\right) = L_d\left(0 - \rho v_x\right), \tag{5.26}$$

which can be simplified to

$$v_t + \left(v - L_d\right)v_x = 0. \tag{5.27}$$

This represents the homogeneous traffic flow as there are no transitions in the flow. The transitions in the flow are caused by the traffic control devices or egress and ingress to the flow. To include the effect of transitions which result in acceleration or deceleration in the flow, a relaxation term is added to the RHS of (5.27). According to the kinematic equation of motion, acceleration $a(\rho)$ is given by

$$a(\rho) = \frac{v(\rho) - v}{\tau}, \tag{5.28}$$

where τ is the relaxation time. Considering traffic transitions, (5.27) can be expressed as

$$v_t + \left(v - L_d\right)v_x = \frac{v(\rho) - v}{\tau}. \tag{5.29}$$

Multiplying by ρ, the traffic flow is obtained as

$$\rho v_t + \rho\left(v - L_d\right)v_x = \rho\frac{v(\rho) - v}{\tau}. \tag{5.30}$$

Then, the proposed model for traffic flow from (5.25) and (5.30) is

$$\begin{aligned} \rho_t + (\rho v)_x &= 0 \\ \rho v_t + \rho v v_x - \rho L_d v_x &= \rho\frac{v(\rho) - v}{\tau}, \end{aligned} \tag{5.31}$$

where

$$-\rho L_d v_x,$$

is the anticipation term. This term includes the traffic constant L_d which characterizes the driver response.

Table 5.1: Traffic Model Comparison

Term	PW model	Proposed model
anticipation term	$\rho C_0^2 \rho_x$	$-\rho L_d v_x$
relaxation term	$\rho \frac{v(\rho)-v}{\tau}$	$\rho \frac{v(\rho)-v}{\tau}$

The PW model [1], [7] is given by

$$\begin{aligned} \rho_t + (\rho v)_x &= 0 \\ \rho v_t + \rho v v_x + \rho C_0^2 \rho_x &= \rho \frac{v(\rho) - v}{\tau}, \end{aligned} \tag{5.32}$$

where C_0 is the anticipation constant which characterizes driver response. According to this model, driver response does not depend on the traffic conditions and is a constant. The relaxation term of the proposed model is the same as that in the PW model, as shown in Table 5.1.

5.3 The Decomposition of Traffic Flow Models

In order to evaluate the performance of the PW and proposed models, they are decomposed using Roe's technique to approximate the macroscopic traffic flow. This approach is described in Section 1.2.

5.3.1 Jacobian Matrix

The Jacobian matrix $A(G)$ is now obtained. Multiplying the first equation in (5.31) with v, the proposed model is

$$\begin{aligned} v\rho_t + v(\rho v)_x &= 0 \\ \rho v_t + \rho v v_x - \rho L_d v_x &= \rho \frac{v(\rho) - v}{\tau}, \end{aligned} \tag{5.33}$$

Combining these equations gives

$$v\rho_t + \rho v_t + v(\rho v)_x + \rho v v_x - L_d \rho v_x = \rho \left(\frac{v(\rho) - v}{\tau} \right), \tag{5.34}$$

As

$$(\rho v)_t = v\rho_t + \rho v_t,$$

and

$$(\rho vv)_x = v(\rho v)_x + \rho v v_x,$$

(5.34) becomes

$$(\rho v)_t + (\rho vv)_x - L_d \rho v_x = \rho \left(\frac{v(\rho) - v}{\tau} \right), \tag{5.35}$$

Substituting the traffic constant relation from (5.12) in (5.35) gives

$$(\rho v)_t + (\rho vv)_x - v(\rho)_\rho \rho_x^2 = \rho \left(\frac{v(\rho) - v}{\tau} \right), \tag{5.36}$$

Taking the derivative of the equilibrium velocity distribution $v(\rho)_\rho$ in Greenshields model (5.13) with respect to the traffic density gives

$$v(\rho)_\rho = -\frac{v_m}{\rho_m}, \tag{5.37}$$

where v_m is the maximum velocity and ρ_m is the maximum traffic density, so that

$$(\rho v)_t + \left(\frac{(\rho v)^2}{\rho} - v(\rho)_\rho \rho^2 \right)_x = \rho \left(\frac{v(\rho) - v}{\tau} \right), \tag{5.38}$$

Then the proposed model (5.31) is

$$G = \begin{pmatrix} \rho \\ \rho v \end{pmatrix}, f(G) = \begin{pmatrix} \rho v \\ \frac{(\rho v)^2}{\rho} - v(\rho)_\rho \rho^2 \end{pmatrix}, S = \begin{pmatrix} 0 \\ \rho \frac{v(\rho) - v}{\tau} \end{pmatrix}. \tag{5.39}$$

Further (5.39) in quasilinear form, i.e. $\rho \frac{v(\rho) - v}{\tau} = 0$, is

$$G = \begin{pmatrix} \rho \\ \rho v \end{pmatrix}, f(G) = \begin{pmatrix} \rho v \\ \frac{(\rho v)^2}{\rho} - v(\rho)_\rho \rho^2 \end{pmatrix}, S = \begin{pmatrix} 0 \\ 0 \end{pmatrix}. \tag{5.40}$$

The Jacobian matrix $A(G) = \frac{\partial f}{\partial G}$ from (5.40) is then

$$A(G) = \begin{pmatrix} 0 & 1 \\ -\frac{(\rho v)^2}{\rho^2} - v(\rho)_\rho 2\rho & \frac{2\rho v}{\rho} \end{pmatrix} \tag{5.41}$$

which gives

$$A(G) = \begin{pmatrix} 0 & 1 \\ -v^2 - 2v(\rho)_\rho \rho & 2v \end{pmatrix} \tag{5.42}$$

The eigenvalues λ_i of the Jacobian matrix are required to obtain the flux in (1.9), and are obtained from (5.42) as the solution of

$$\Big|A(G) - \lambda I\Big| = 0, \tag{5.43}$$

so that

$$\begin{vmatrix} -\lambda & 1 \\ -v^2 - 2v(\rho)_\rho \rho & 2v - \lambda \end{vmatrix} = 0, \tag{5.44}$$

and therefore

$$-\lambda(2v - \lambda) + v^2 + 2v(\rho)_\rho \rho = 0. \tag{5.45}$$

Letting $2v(\rho)_\rho \rho = D$

$$\lambda^2 - 2v\lambda + v^2 + D = 0, \tag{5.46}$$

and the solutions are

$$\lambda_{1,2} = \frac{2v \pm \sqrt{4v^2 - 4(v^2 + D)}}{2} = v \pm \sqrt{-D}, \tag{5.47}$$

which can be expressed as

$$\lambda_{1,2} = v \pm \sqrt{-(2v(\rho)_\rho \rho)}. \tag{5.48}$$

The equilibrium velocity distribution is a decreasing function of density and therefore

$$v(\rho)_\rho \leq 0, \tag{5.49}$$

which ensures that the eigenvalues and eigenvectors are real. Substituting $v(\rho)_\rho$ from (5.37) in (5.48) gives

$$\lambda_{1,2} = v \pm \sqrt{\frac{2v_m \rho}{\rho_m}}. \tag{5.50}$$

The eigenvectors are obtained by solving

$$|A(G) - \lambda I|x = 0 \tag{5.51}$$

where

$$x = \begin{pmatrix} 1 \\ x_2 \end{pmatrix}. \tag{5.52}$$

From (5.42) and $\lambda_1 = v + \sqrt{\frac{2v_m\rho}{\rho_m}}$ from (5.50), (5.51) takes the form

$$\begin{pmatrix} -v - \sqrt{\frac{2v_m\rho}{\rho_m}} & 1 \\ -v^2 + 2v(\rho)_\rho\rho & v - \sqrt{\frac{2v_m\rho}{\rho_m}} \end{pmatrix} \begin{pmatrix} 1 \\ x_2 \end{pmatrix} = 0, \tag{5.53}$$

so the eigenvectors are

$$e_1 = \begin{pmatrix} 1 \\ v + \sqrt{\frac{2v_m\rho}{\rho_m}} \end{pmatrix}, \tag{5.54}$$

and

$$e_2 = \begin{pmatrix} 1 \\ v - \sqrt{\frac{2v_m\rho}{\rho_m}} \end{pmatrix}. \tag{5.55}$$

To obtain the average velocity for the proposed model, using (1.6) and (5.42), Δf can be expressed as

$$\triangle f = A(G)\triangle G = \begin{pmatrix} \triangle f_1 \\ \triangle f_2 \end{pmatrix} = \begin{pmatrix} 0 & 1 \\ -v^2 - 2v(\rho)_\rho\rho & 2v \end{pmatrix} \begin{pmatrix} \triangle\rho \\ \triangle\rho v \end{pmatrix}, \tag{5.56}$$

so that

$$\triangle f_2 = \left(-v^2 - 2v(\rho)_\rho\rho\right)\triangle\rho + 2v\triangle\rho v. \tag{5.57}$$

Using $f(G)$ in (5.40)

$$\triangle f = \begin{pmatrix} \triangle f_1 \\ \triangle f_2 \end{pmatrix} = \begin{pmatrix} \triangle\rho v \\ \triangle\left(\frac{(\rho v)^2}{\rho} - v(\rho)_\rho\rho^2\right). \end{pmatrix}, \tag{5.58}$$

Equating (5.57) with Δf_2 in (5.58) gives

$$\left(-v^2 - 2v(\rho)_\rho\rho\right)\triangle\rho + 2v\triangle\rho v = \triangle\left(\frac{(\rho v)^2}{\rho} - v(\rho)_\rho\rho^2\right) \tag{5.59}$$

Considering that

$$2v(\rho)_\rho\rho\triangle\rho = \triangle\left(v(\rho)_\rho\rho^2\right), \tag{5.60}$$

(5.59) can be expressed as

$$\overline{v}^2 \triangle\rho - 2\overline{v}\triangle\rho v + \triangle(\rho v^2) = 0, \tag{5.61}$$

and taking the positive root gives the average velocity of the proposed model as

$$\overline{v} = \frac{\triangle\rho v + \sqrt{(\triangle\rho v)^2 - (\triangle\rho)(\triangle\rho v^2)}}{\triangle\rho}. \tag{5.62}$$

Substituting $\triangle\rho v = \rho_{i+1}v_{i+1} - \rho_i v_i$, $\triangle\rho v^2 = \rho_{i+1}v_{i+1}^2 - \rho_i v_i^2$, and $\triangle\rho = \rho_{i+1} - \rho_i$ in (5.62), the average velocity at the boundary of segments i and $i+1$ is

$$v_{i+\frac{1}{2}} = \frac{\sqrt{\rho_{i+1}}v_{i+1} + \sqrt{\rho_i}v_i}{\sqrt{\rho_{i+1}} + \sqrt{\rho_i}}. \tag{5.63}$$

The average density $\rho_{i+\frac{1}{2}}$ at the boundary of segments i and $i+1$ is given by the geometric mean of the densities in these segments

$$\rho_{i+\frac{1}{2}} = \sqrt{\rho_{i+1}\rho_i} \tag{5.64}$$

Using (5.63) and (5.64), the average eigenvalues and eigenvectors are

$$\lambda_{1,2} = v_{i+\frac{1}{2}} \pm \sqrt{\frac{2v_m\rho_{i+\frac{1}{2}}}{\rho_m}} \qquad e_{1,2} = \begin{pmatrix} 1 \\ v_{i+\frac{1}{2}} \pm \sqrt{\frac{2v_m\ \rho_{i+\frac{1}{2}}}{\rho_m}} \end{pmatrix} \tag{5.65}$$

The eigenvalues provide information about the rate of change in traffic flow. Equation (5.65) indicates that the eigenvalues at the boundary of segments i and $i+1$ can be interpreted as the average velocity plus the change in velocity due to transitions at the segment boundaries. This change in velocity is dependent on the maximum velocity, maximum density and the average density. The maximum density refers to the road capacity, and a road with a larger capacity will have the smaller changes in velocity than a road with smaller capacity. Changes in velocity will be higher with a larger v_m. Thus the faster the traffic flow, the larger the changes in the flow. The average density $\rho_{i+\frac{1}{2}}$ also affects the changes in velocity. These changes will be greater with a larger average density.

Using (5.43) and (5.51), the eigenvalues and eigenvectors of the PW model are

obtained. The eigenvalues

$$\lambda_{1,2} = v_{i+\frac{1}{2}} \pm C_0, \tag{5.66}$$

show that the change in traffic velocity with the PW model occurs at a constant rate. The corresponding eigenvectors are

$$e_{1,2} = \begin{pmatrix} 1 \\ v_{i+\frac{1}{2}} \pm C_0 \end{pmatrix} \tag{5.67}$$

The parameters $v_{i+\frac{1}{2}}$ and $\rho_{i+\frac{1}{2}}$ for the PW model are the same as those for the proposed model given in (5.63) and (5.64), respectively.

5.3.2 Entropy Fix

Entropy fix as described in Section 1.2.1 is applied to the Jacobian matrix of the proposed and PW models.

The Jacobian matrix of the proposed model is

$$e|\Lambda|e^{-1} = \begin{pmatrix} 1 & 1 \\ v_{i+\frac{1}{2}} + \sqrt{\frac{2v_m\rho_{i+\frac{1}{2}}}{\rho_m}} & v_{i+\frac{1}{2}} - \sqrt{\frac{2v_m\rho_{i+\frac{1}{2}}}{\rho_m}} \end{pmatrix} \times$$
$$\begin{pmatrix} \left| v_{i+\frac{1}{2}} + \sqrt{\frac{2v_m\rho_{i+\frac{1}{2}}}{\rho_m}} \right| & 0 \\ 0 & \left| v_{i+\frac{1}{2}} - \sqrt{\frac{2v_m\rho_{i+\frac{1}{2}}}{\rho_m}} \right| \end{pmatrix} \times \begin{pmatrix} v_{i+\frac{1}{2}} - \sqrt{\frac{2v_m\rho_{i+\frac{1}{2}}}{\rho_m}} & -1 \\ -v_{i+\frac{1}{2}} - \sqrt{\frac{2v_m\rho_{i+\frac{1}{2}}}{\rho_m}} & 1 \end{pmatrix} \frac{-1}{2\sqrt{\frac{2v_m\rho_{i+\frac{1}{2}}}{\rho_m}}},$$

and for the PW model is

$$e|\Lambda|e^{-1} = \begin{pmatrix} 1 & 1 \\ v_{i+\frac{1}{2}} + C_0 & v_{i+\frac{1}{2}} - C_0 \end{pmatrix} \times$$
$$\begin{pmatrix} \left| v_{i+\frac{1}{2}} + C_0 \right| & 0 \\ 0 & \left| v_{i+\frac{1}{2}} - C_0 \right| \end{pmatrix} \times \begin{pmatrix} v_{i+\frac{1}{2}} - C_0 & -1 \\ -v_{i+\frac{1}{2}} - C_0 & 1 \end{pmatrix} \frac{-1}{2C_0}.$$

The corresponding flux is obtained from (1.9) using $f(G_i)$ and $f(G_{i+1})$ and substituting $e|\Lambda|e^{-1}$ for $A(G_{i+\frac{1}{2}})$. The updated data variables, ρ and ρv, are then obtained at time m using (1.10).

5.4 Performance Results

The performance with the proposed and PW models are compared using the parameters shown in Table 5.2. The initial density distribution is

$$\rho_0 = \begin{cases} 0.01, \text{ for } x < 10, \\ 0.3, \text{ for } 10 \leq x \leq 30, \\ 0.1, \text{ for } 30 < x \leq 40, \\ 0.3, \text{ for } 40 < x \leq 50, \\ 0.2, \text{ for } x > 50, \end{cases} \tag{5.68}$$

which is considered a worst case traffic flow as there are two clusters with significant density changes. This ρ_0 is used to demonstrate traffic flow behavior on a circular road of length 100 m.

The velocity constants used in the literature for the PW model range between 2.4 m/s and 57 m/s to evaluate the performance for a variety of traffic densities [32, 34, 56]. Thus the velocity constants considered here are $C_0 = 5.83$ m/s as in [1] and $C_0 = 25$ m/s. The traffic target is the Greenshields equilibrium velocity distribution $v(\rho)$ as given in (5.13) with $v_m = 34$ m/s. The relaxation time is $\tau = 0.5$ s. The road has a maximum normalized density of $\rho_m = 1$. The road step is chosen as $\delta x = 1$ m so the total number of road steps is 100. The time step chosen for the proposed model is $\delta t = 0.01$ s to satisfy the CFL condition [46]. The number of time steps for the proposed model is 3000. For the PW model, the time step is $\delta t = 0.001$ s with $C_0 = 25$ m/s and 0.01 with $C_0 = 5.83$ m/s to satisfy the CFL condition [46]. The corresponding number of time steps is 30000 for $C_0 = 25$ m/s and 3000 for $C_0 = 5.83$ m/s. The total simulation time is 30 s.

Figure 5.1 gives the traffic density behavior with the proposed model. The traffic density is more oscillatory at 1.5 s than at 15 s and 30 s. The traffic density separates at 15 and 30 s into clusters. From 40 to 80 m, the traffic density at $t = 30$ s is approximately uniform at value of 0.17. There are also two clusters of vehicles. The first lies between 8 m and 40 m and has a density which increases from 0.21 at 8 m to 0.28 at 20 m, and then decreases to 0.18 at 40 m. The second cluster lies between 80 m and 100 m. The density of this cluster varies from 0.17 at 80 m to 0.21 at 100 m.

Figure 5.2 presents the density behavior of the PW model with $C_0 = 25$ m/s.

The PW model produces an oscillatory traffic behavior. Further, the traffic divides into ten small clusters of span approximately 9 m, which are very close. The average density within the clusters ranges from 0.08 to 0.3. The density is very small between the clusters.

The density behavior of the PW model with $C_0 = 5.83$ m/s is given in Figure 5.3. This shows that the abrupt changes in traffic density are smoothed at 1.5 s and 15 s. However, at 30 s the traffic exceeds the maximum density of $\rho_m = 1$ by a factor of 2.5, which is impossible.

The corresponding velocity behavior of the proposed model is shown in Figure 5.4. The traffic velocity is more oscillatory at 1.5 s than at 15 and 30 s. From 40 to 80 m, at $t = 30$ s the velocity is approximately uniform at 28 m/s. The velocity within the first cluster varies from 25 to 27 m/s, and within the second cluster varies from 27 to 28 m/s. This is realistic traffic behavior which is within the minimum and maximum velocities. As expected, the traffic velocity is fast where the density is low and vice versa.

The corresponding PW model velocity behavior with $C_0 = 25$ m/s is given in Figure 5.5. This shows that the traffic velocity oscillates at a lower frequency at 1.5 s than at at 15 s and 30 s. At 30 s, the velocity fluctuates from 22.5 to 45.5 m/s even though the maximum velocity is 34 m/s. There are also unrealistic abrupt changes in velocity. On average, within the clusters the velocity varies by 20 m/s within a distance of 8 m, which is not possible. The PW model velocity behavior with $C_0 = 5.83$ m/s is given in Figure 5.6. This shows that at 30 s, the velocity goes below zero to -14 m/s at 68 m, which is impossible.

The proposed model traffic density and velocity behavior over a distance of 100 m for 30 s is given in Figures 5.7 and 5.8, respectively. These shows that the traffic density and velocity with the proposed model is well behaved and has only small variations. Traffic moves faster or slower at locations where the traffic density is low or high, respectively, as expected. The velocity stays within the range of 0 to 34 m/s, and the density between 0 and 1.

The PW model velocity and density behavior with $C_0 = 25$ m/s is shown in Figures 5.9 and 5.10 over a distance of 100 m for 30 s. Figure 5.9 shows that the velocity ranges from 0 m/s to 160 m/s at 0.3 s, which is impossible. Further, Figure 5.10 shows that the traffic evolves into 10 clusters having widths of 9 m over the 100 m distance, which is not realistic. The PW model velocity and density behavior with $C_0 = 5.83$ m/s over the 100 m distance for 30 s is given in Figures 5.11 and 5.12,

Table 5.2: Simulation Parameters

Name	Parameter
maximum velocity	$v_m = 34$ m/s
equilibrium velocity distribution	$v(\rho)$
relaxation time	$\tau = 0.5$ s
anticipation coefficient	$C_0 = 25$ m/s and 5.83 m/s
road length	$x = 100$ m
time step for the proposed model	$\delta t = 0.01$ s
number of time steps for the proposed model	$M = 3000$
time step for the PW model with $C_0 = 25$ m/s	$\delta t = 0.001$ s
number of time steps for $C_0 = 25$ m/s	$N = 30000$
time step for the PW model with $C_0 = 5.83$ m/s	$\delta t = 0.01$ s
total time steps for $C_0 = 5.83$ m/s	$N = 3000$
road step	$\delta x = 1$ m
number of road steps	$N = 100$
simulation time	$t_M = 30$ s
Maximum normalized density	$\rho_m = 1$

respectively. Degradation in traffic velocity and density behavior is developed with the evolution of time over the distance.

The results in this section show that the proposed model provides realistic behavior which is smooth, unlike the PW model. The PW model produces oscillatory traffic behavior with $C_0 = 25$ m/s, whereas with $C_0 = 5.83$ m/s the PW model produces unrealistic behavior.

5.5 Summary

A model has been proposed based on gas behavior. Analogies of traffic density, velocity and traffic constant are developed. The traffic constant is based on the physiological and psychological response of a driver. The proposed model performance are compared with the PW model on a circular road having a traffic bottleneck. The transitions in density at a bottleneck are realistically captured by the proposed model. As expected, the transitions smeared out with the passage of time. The density and velocity stayed with in the limits of maximum and minimum. The PW model adapts unrealistic oscillatory behavior although C_0 has been changed from a high to low value. The traffic density overflows and as a result velocity goes into negative. The proposed

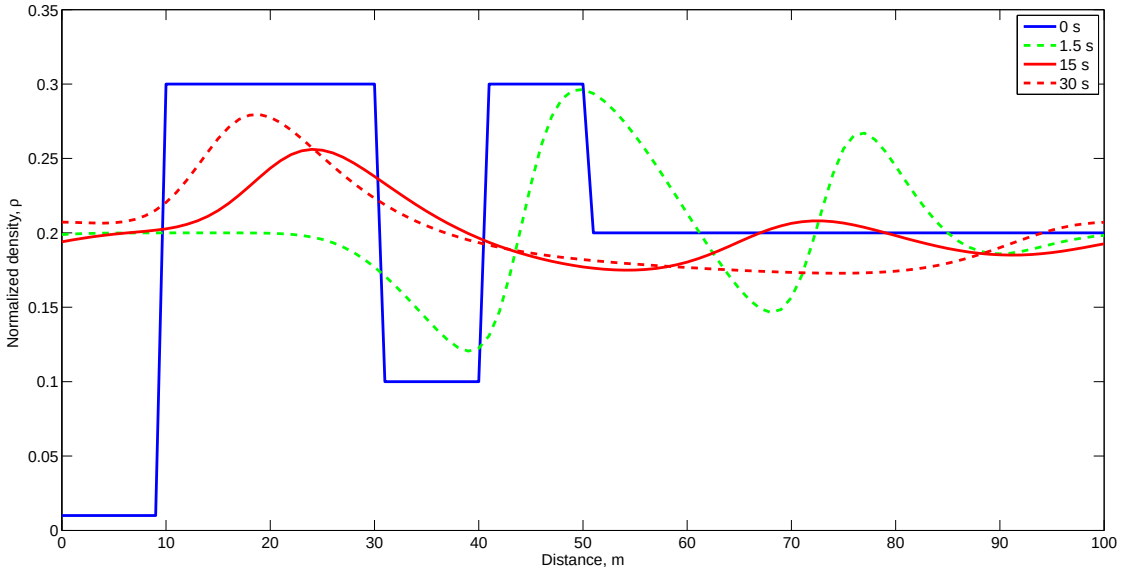

Figure 5.1: The proposed model density behavior at 0 s, 1.5 s, 15 s and 30 s.

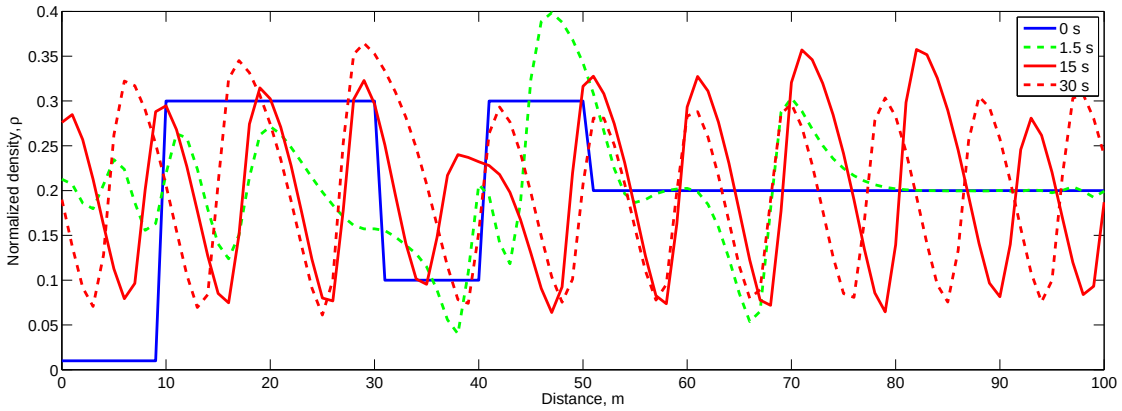

Figure 5.2: The density behavior of the PW model with $C_0 = 25$ m/s.

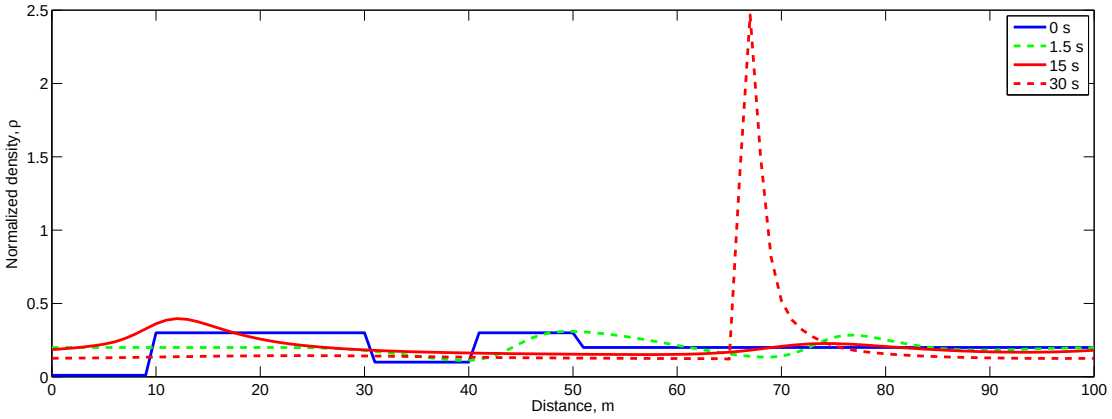

Figure 5.3: The density behavior of the PW model with $C_0 = 5.83$ m/s.

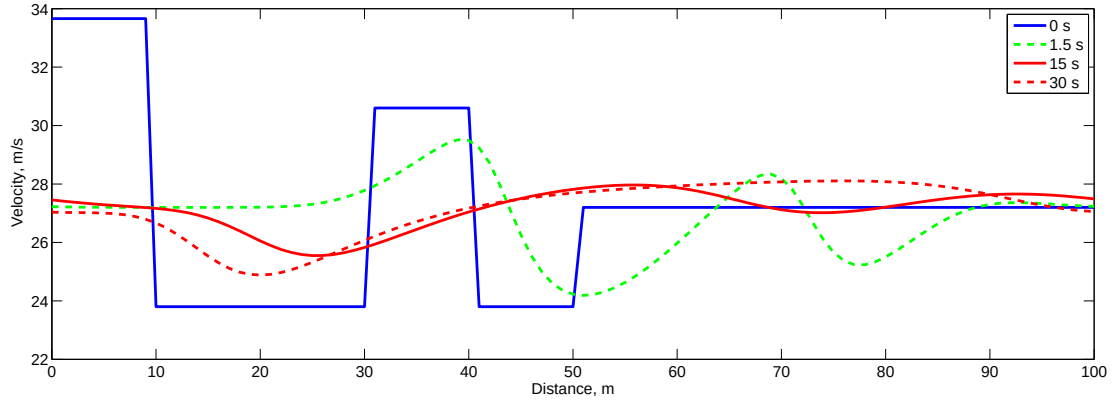

Figure 5.4: The proposed model velocity behavior at 0 s, 1.5 s, 15 s and 30 s.

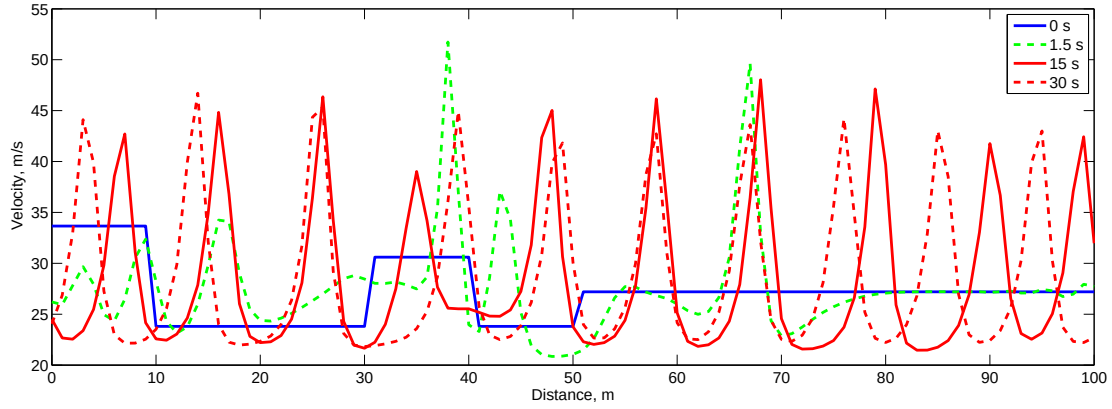

Figure 5.5: The velocity behavior of the PW model with $C_0 = 25$ m/s.

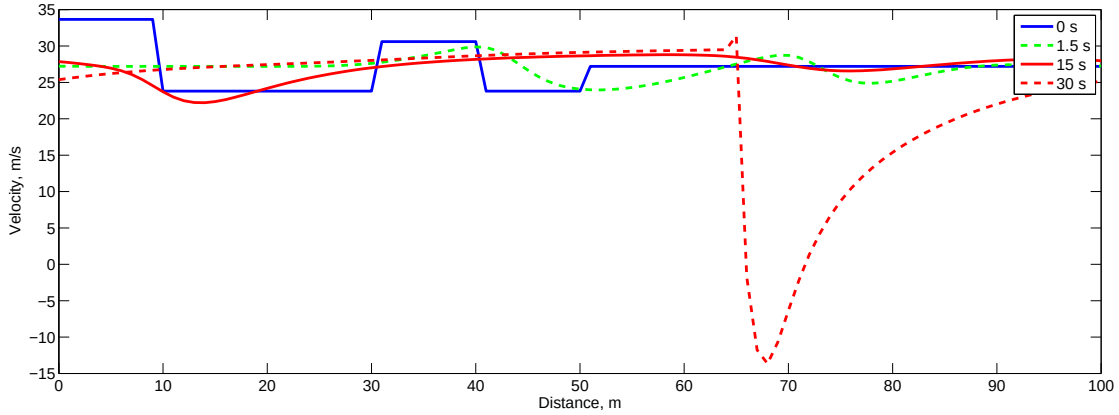

Figure 5.6: The velocity behavior of the PW model with $C_0 = 5.83$ m/s.

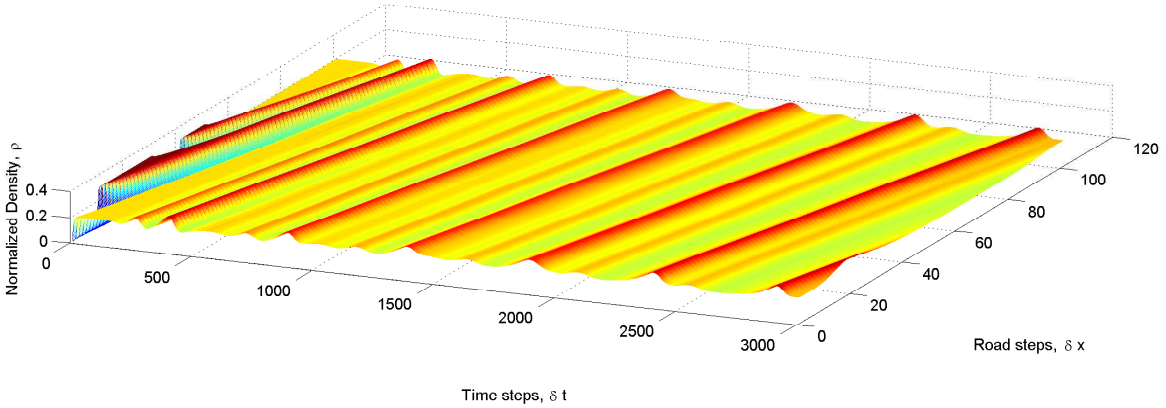

Figure 5.7: The proposed model density behavior from 0 to 30 s.

model provides promising results as evident from the performance evaluation.

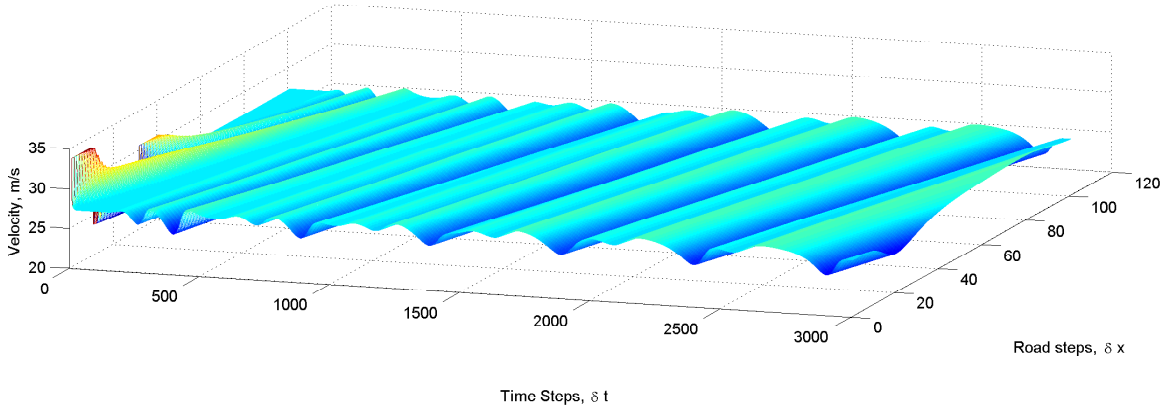

Figure 5.8: The proposed model velocity behavior from 0 to 30 s.

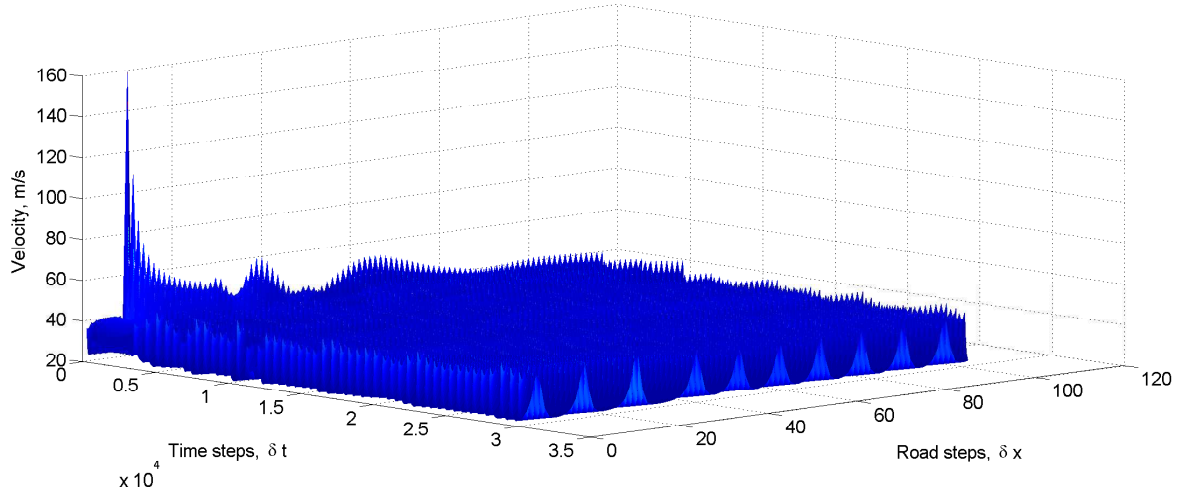

Figure 5.9: The velocity behavior of the PW model with $C_0 = 25$ m/s.

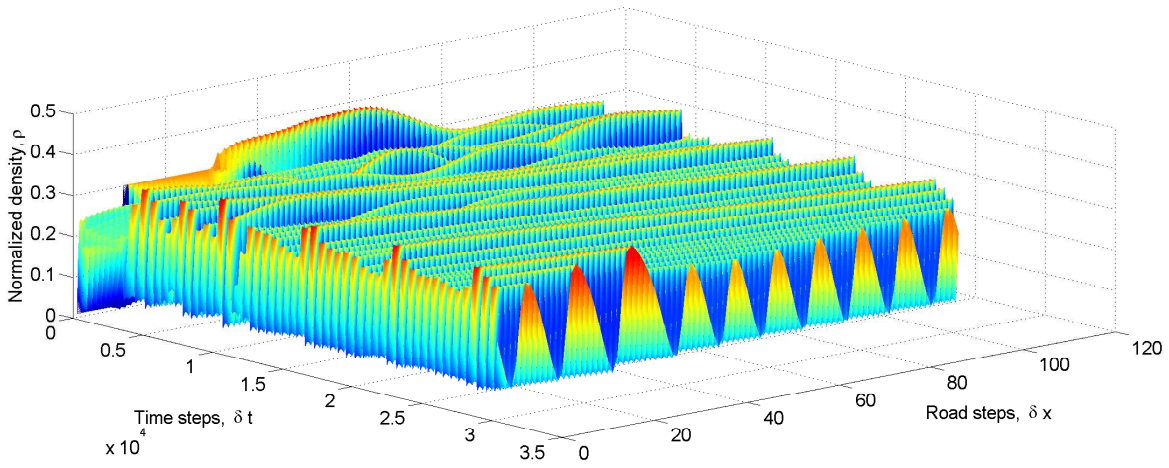

Figure 5.10: The density behavior of the PW model with $C_0 = 25$ m/s.

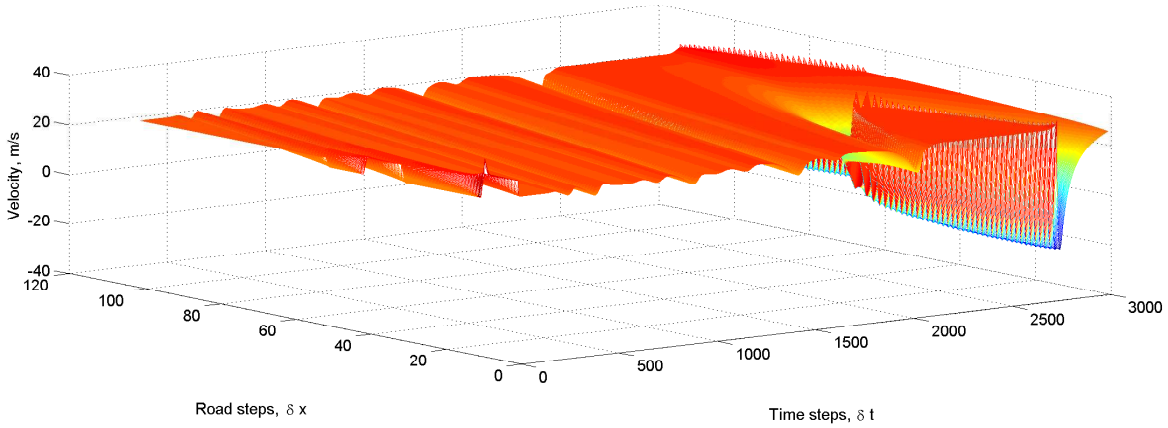

Figure 5.11: The velocity behavior of the PW model with $C_0 = 5.83$ m/s.

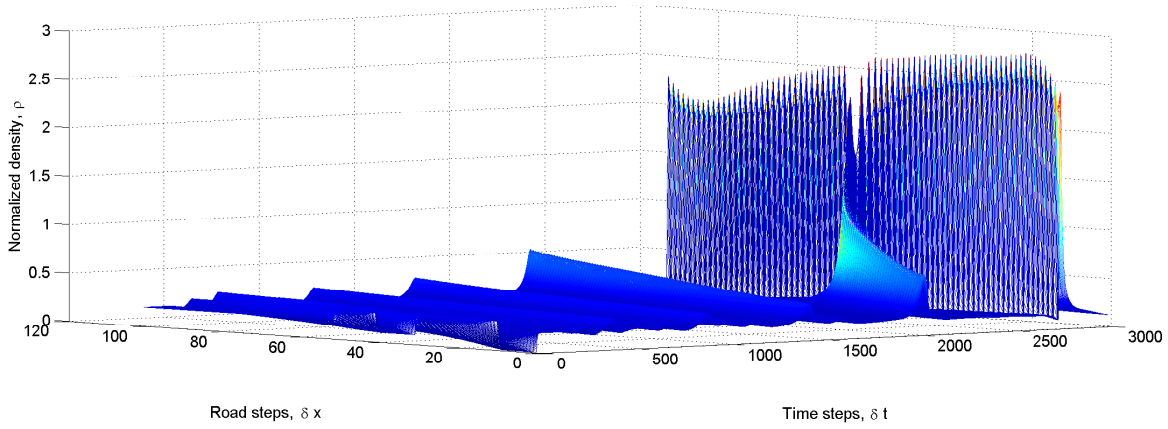

Figure 5.12: The density behavior of the PW model with $C_0 = 5.83$ m/s.

Chapter 6

Route Merit Models for Traffic Flow

6.1 Introduction

Route merit is a decision criterion which influences drivers to follow a path. In this chapter, route merit based on traffic velocity, density and relaxation time are proposed. Traffic velocity aligns during the relaxation time. In congestion, the traffic density has a low variance. The interaction between vehicles is large which increases the fluctuations in velocity and ultimately a higher rate of fuel consumption. With large number of fluctuations in velocity, traffic can take a large time to reach their destinations. The emission of CO_2, hydrocarbons and the consumption of the fuel are high with the fluctuation in velocity. In free flow, the traffic density has a large variance. The distance between vehicles is large and their interactions are largely independent. Therefore there are less fluctuations in traffic velocity in free flow and ultimately there is less fuel consumption.

Route merit is based on the shortest period of time [24, 26], shortest distance [27], flow region, familiarity of a route, degree of difficulty, tool cost, attraction points, location of a road, geometry, traffic lamps, road surface, quality of service of a network and road capacity. The route merit is also proposed as a trade off between distance, time, congestion, difficulty and toll [24]. Some strategies include dynamic traffic sign management, automatic cruise control, high tolls for congested routes, automatic traffic flow, and dynamic route selection to influence drivers behavior and improve the trip time [21]. These measures improve the road network utilization, and reduces

congestion. However, an integrated model is required to control the flow and emissions of the traffic [20].

In this chapter, route merit based on the Mach number, relative trip time and traffic resistance are proposed to minimize the trip time, improve fuel consumption and smooth the traffic flow. The Mach number is an analogous term to that used in air traffic. In the air traffic, it indicates the utilization of air space. In this chapter, the Mach number is used as an indicator of velocity fluctuation.

Trip time is the time taken by the traffic to reach a destination from an origin. Trip time on a route is smaller with a larger velocity. Relative trip time gives the comparison of trip time of a route when followed with different velocities.

The traffic resistance is a hindrance in achieving a larger velocity. Based on the traffic resistance, route merit is proposed to select a route with minimum trip time. The traffic on the route with minimum traffic resistance will have the minimum trip time. In this chapter, traffic resistance is developed from analogies with fluid pressure. Traffic resistance depends on acceleration and density. For a large acceleration, the traffic faces large resistance due to fluctuations in velocity. For a low variance density distribution on the road, traffic resistance will be large. The distance between vehicles is smaller and the reduced ability to react to transitions, so the interaction between the vehicles will be high. For a smooth flow, the traffic has a large variance density distribution and the vehicles have less interaction between them. The fluctuations in velocity are low and the traffic has the shortest trip time to reach the destination. Further, route merit for a group of routes running between an origin and distination is analogous to electrical resistance. An example is given in this chapter to determine the route merit based on electrical resistance.

The rest of the chapter is organized as follows. The formulation of Mach number is given in Section 5.2. Then the relative trip time is explained in Section 5.3. Section 5.4 gives the details of traffic resistance. We then calculate the traffic resistance based on electric resistance in Section 5.5. Finally, Section 5.6 concludes the chapter.

6.2 Mach Number

Mach number is a parameter used for objects moving in fluids. This number compares the velocity of an object to the velocity of sound through a medium [22]. Mach number Mn is given as

$$Mn = \frac{e}{w}, \tag{6.1}$$

where e and w are the velocities of an object and sound, respectively. It is a dimensionless quantity.

Mach number is applied to macroscopic road traffic theory such that it provides the information of the relative velocities. e is analogous to the average velocity v of the traffic and w to the maximum velocity v_m. Then Mn for road traffic is given as

$$Mn = \frac{v}{v_m} \tag{6.2}$$

For traffic moving with maximum velocity $v = v_m$

$$Mn = 1 \tag{6.3}$$

The traffic with velocity lower than the maximum velocity will have Mn less than 1. For bumper to bumper traffic having zero velocity

$$Mn = 0.$$

Therefore, the limits of Mn are

$$0 \leq Mn \leq 1. \tag{6.4}$$

$Mn = 1$ indicates that traffic flow conditions are ideal, that is, the traffic has free flow behavior and there are less fluctuations in velocity. The interactions between the vehicles are minimum and the flow is smooth as desired. The utilization of the road infrastructure is maximized as traffic will have minimum trip time. As Mn reduces, the trip time will increase. The traffic conditions are worse for M_n close to zero, which indicates congestion. The distance between the vehicles is smaller than free flow and more interaction between the vehicles. There will be large fluctuations experienced in velocity. It is a good criterion to estimate the delay in reaching a destination.

6.3 Relative Trip Time

The relative trip time is the time taken by the traffic moving from origin to destination with velocity other than the maximum velocity. It helps in the selection of a route.

It is calculated from a well known distance relation which is given as

$$d = vT_{tr}, \tag{6.5}$$

where v, T_{tr} and d are velocity, relative trip time and distance, respectively. If the distance d be covered during the minimum time t_m with maximum velocity v_m then

$$d = v_m t_m, \tag{6.6}$$

Comparison (6.5) and (6.6) gives

$$T_{tr} = \frac{v_m t_m}{v}, \tag{6.7}$$

From (6.2), the Mach number is

$$Mn = \frac{v}{v_m},$$

then T_{tr} takes form as

$$T_{tr} = \frac{t_m}{Mn}, \tag{6.8}$$

For $Mn = 1$, the trip time is minimum and the relative trip time is then given as

$$T_{tr} = t_m. \tag{6.9}$$

That is, the traffic will have minimum trip time to reach the destination. This is evident in the case of free flow where the traffic moves with maximum velocity. Whereas for $Mn = 0$, the trip time becomes undefined as an uncertain time starts adding to the trip time. Such situation takes place during congestions.

Figure 6.1 illustrates the trip time behavior with fluctuations in average velocity, v based on (6.7). Maximum velocity v_m is chosen as 33.33 m/s. Based on this v_m, the minimum trip time is $t_m = 0.03$ s/m. It is shown that as velocity reduces with reference to the maximum velocity, the trip time increases.

6.4 Traffic Resistance R

The traffic resistance is defined as the hindrance in achieving the maximum velocity. In this section, the traffic resistance is developed from the fluid pressure analogies.

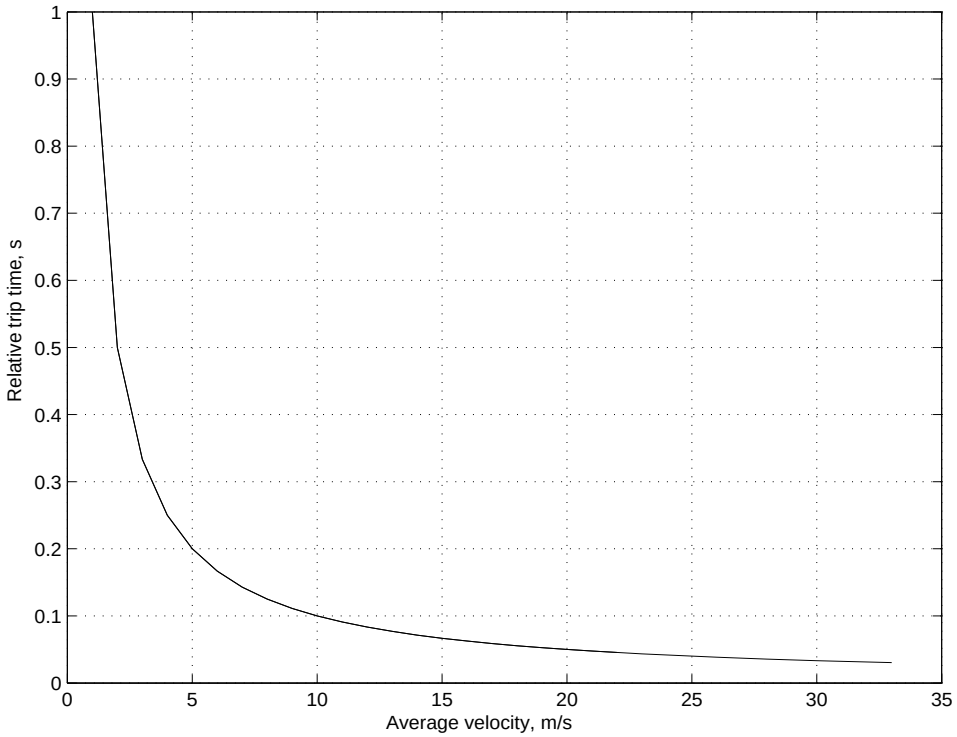

Figure 6.1: Relative trip time behavior with fluctuations in velocity.

The fluid pressure expression per unit length is given as

$$p = \rho a, \tag{6.10}$$

where p is the fluid pressure, a is acceleration and ρ is the density. Fluid pressure fluctuates with the changes in acceleration and density. There is a large traffic resistance when the traffic acquires to accelerate to a large velocity in congestion. This traffic resistance reduces with low density as interactions between vehicles are less due to the large headway between them. In other words, interactions are largely independent. It is easier for the traffic to acquire large velocity and the tendency of free flow is large. Therefore, the traffic resistance changes with fluctuations in velocity and density. In this section, traffic resistance R is introduced which relates traffic density and acceleration and is given as

$$R = \rho a, \tag{6.11}$$

Traffic develops acceleration at the transitions due to change in velocity. Then, from well known kinematic equation of motion, acceleration is given as

$$a = \frac{v_m - v}{\tau}, \tag{6.12}$$

where v_m is the maximum velocity attained by traffic while moving from velocity v during a transition. v_m is achieved during transition time τ. The transition time is also known as relaxation time. Therefore substituting (6.12) in (6.11), gives

$$R = \rho \left(\frac{v_m - v}{\tau} \right) \tag{6.13}$$

For a smooth flow, R will be zero and the traffic will reach the destination in minimum trip time, that is

$$v = v_m.$$

For a traffic, to start with zero velocity ($v = 0$), faces the maximum resistance.

Multiplying and dividing the numerator in (6.13) by v_m, we get

$$R = \rho v_m \left(\frac{1 - \frac{v}{v_m}}{\tau} \right), \tag{6.14}$$

Applying Mach number theory, that is $Mn = \frac{v}{v_m}$, we get (6.14) as

$$R = \rho v_m \left(\frac{1 - Mn}{\tau} \right), \tag{6.15}$$

For $Mn = 0$, that is $v = 0$, (6.15) gives

$$R = \frac{\rho v_m}{\tau}. \tag{6.16}$$

Thus in congestion, resistance is the maximum momentum per unit time, which is required to completely mobilize the traffic to smooth flow. For $Mn = 1$, the traffic moves with maximum velocity ($v = v_m$), then (6.15) gives

$$R = 0. \tag{6.17}$$

Thus, traffic having maximum velocity will have the minimum resistance and the trip time to the destination will be minimum.

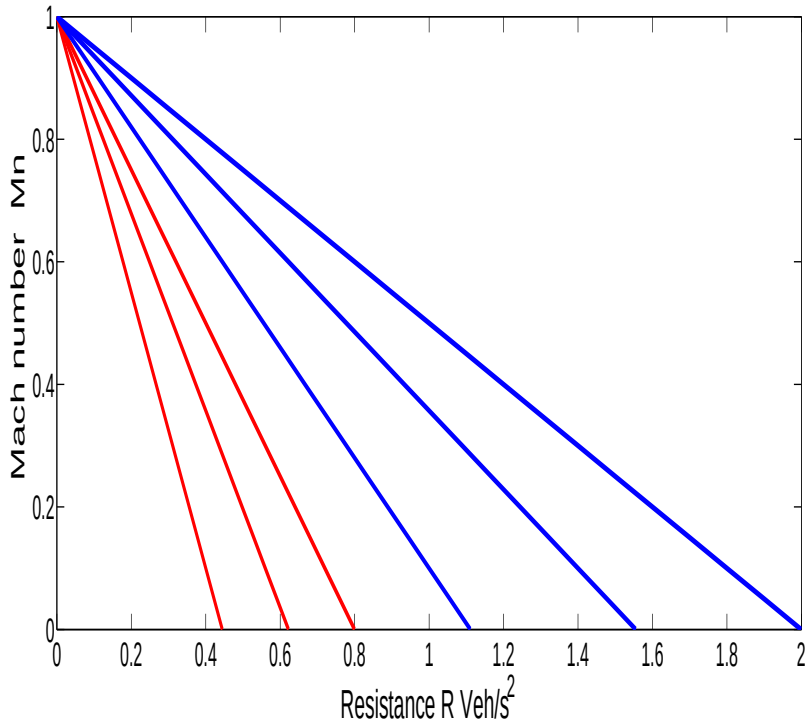

Figure 6.2: Variation in traffic resistance with changes in mach number.

Figure 6.2 and 6.3 illustrates the traffic resistance behavior with changes in Mach number and relaxation time. The traffic resistance behavior is based on the expression (6.15). Figure 6.2 demonstrates the traffic resistance behavior with Mach number ranging from 0 to 1. There are two groups of curves with distinct relaxation time. The red curves has $\tau = 25$ s, whereas for blue curves $\tau = 10$ s. Each curve in a group corresponds to the normalized density. The left and right most curves respectively in a group corresponds to 0.5 and 0.9 normalized density. Whereas the middle curve corresponds to 0.7 normalized density. The maximum velocity for both the groups is assumed as $v_m = 22.22$ m/s. As expected, resistance is minimum for $Mn = 1$ and maximum for $Mn = 0$. At $\tau = 25$ s, the resistance for 0.5 density is 0.45 veh/s^2, 0.7 is 0.62 veh/s^2 and for 0.9 is 0.8 veh/s^2. At $\tau = 10$ s, the resistance for 0.5 density is 1.1 veh/s^2, 0.7 is 1.55 veh/s^2 and for 0.9 is 2 veh/s^2. As τ reduces, resistance increases and is evident from these results. Further, as the density rises, the traffic resistance becomes larger.

Figure 6.3 demonstrates the traffic resistance behavior with changes in relaxation time. The maximum velocity is assumed as $v_m = 22.22$ m/s and average velocity

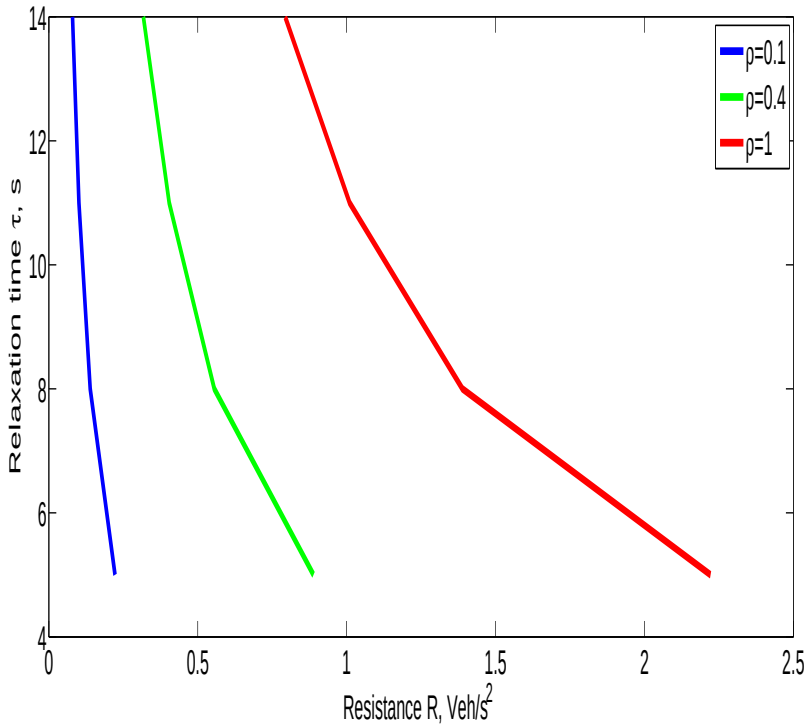

Figure 6.3: Variation in traffic resistance with changes in relaxation time.

v = 11.11 m/s. The relaxation time τ is varied from 5 to 14 s. The variation in traffic resistance is demonstrated with normalized densities. For a large density, the fluctuation in traffic resistance is larger with the change in relaxation time. For an individual case of density, the resistance is higher at smaller values of relaxation time. This is more evident in the high density curves. That is, traffic required to reach the maximum velocity in a short period of time will face high resistance. At normalized density 1, R = 2.25 veh/s^2 at τ = 5 s, whereas at τ = 14 s, R is 0.62 veh/s^2. For 0.1 normalized density, R = 0.25 veh/s^2 at τ = 5 s, whereas at τ = 14 s, R is 0.05 veh/s^2. The traffic resistance has small variations for low density.

6.5 Traffic Resistance based on Electric Circuit Theory

In this section, traffic resistance is calculated based on the electric circuit theory. In electric circuit theory, the electrical resistance offered to the flow of current is calculated in series and parallel combinations [28]. For a number of series resistances

from R_1 to R_n in an electric circuit, the total resistance R_t is given as

$$R_t = R_1 + R_2 + ... + R_n \tag{6.18}$$

The total resistance R_t in series is the sum of all resistances in a circuit. The total electric resistance for the resistances installed in parallel is given as

$$\frac{1}{R_t} = \frac{1}{R_1} + \frac{1}{R_2} + ... + \frac{1}{R_n} \tag{6.19}$$

Most of the current will pass through the least resistance R_{le} in parallel combinations, that is,

$$R_{le} = \min(R_1, R_2, ..., R_n) \tag{6.20}$$

The traffic resistance on the road is analogous to electrical resistance. For a large traffic resistance on a road, less number of vehicles will pass through. The traffic velocity is analogous to the electric current. Velocity is slow with high traffic resistance. The road is viewed as electric conductor. Therefore, the traffic resistance offered to the flow at multiple locations on a long infinite road from origin to destination is given by (6.18). The traffic resistance for multiple roads running between the origin and destination is given by (6.20). The destination is considered as datum node. This concept is applied to a road network with the traffic resistance mentioned in Figure 6.4. There are three routes leading to the destination. one is a direct route, and the other two are having two and three branches. The choice of a route depends on the traffic resistance of a network or a direct route. The direct route is having resistance R_9. The other two routes total resistances are calculated with the help of (6.18) and (6.20) for the comparison. For the route with three branches, is having all the branches in parallel. Parallel branches are solved according to (6.20) as

$$\frac{1}{R_{2eq}} = \frac{1}{R_2} + \frac{1}{R_9} + \frac{1}{R_{10}}. \tag{6.21}$$

The final total resistance for this branch will be the summation of resistances and solved according to (6.18) as

$$R_{1eq} = R_1 + R_{2eq} + R_3. \tag{6.22}$$

For the route with two branches, route merit is calculated as

$$\frac{1}{R_{6eq}} = \frac{1}{R_6} + \frac{1}{R_7}, \tag{6.23}$$

and have the final total resistance as

$$R_{5eq} = R_5 + R_{6eq} + R_8 \tag{6.24}$$

The traffic resistances of the three routes, that is R_9 from the direct route, R_{1eq} from (6.22), and R_{5eq} from (6.24), are then compared for the minimum as

$$R_r = \min\left(R_{1eq}, R_9, R_{5eq}\right) \tag{6.25}$$

R_r is the minimum resistance of the route and traffic traversing on this route will have the minimum trip time. There will be less fluctuations in the traffic flow.

The probability of a route is the reciprocal of the route resistance. A route having lowest resistance will be having the highest probability to be followed. The probability of a route is given as

$$P_r = \frac{1}{R_r}, \tag{6.26}$$

where P_r denotes the probability of a route. The probabilities of a route can be defined at different intersections for different routes. The route with minimum resistance will have the highest probability to be followed.

6.5.1 Range of Traffic Resistance and Time Delay

The traffic resistance exists when there are fluctuations in flow. The maximum traffic resistance occurs at bumper to bumper density. The bumper to bumper density is a complete congestion and this is the maximum density a road can take. Traffic resistance is minimum for the traffic flow at equilibrium velocity.

Time delay is the time spent additional to the minimum trip time due to the fluctuations in flow and denoted by Y. The decision to follow a route can be made by comparing the traffic resistances of the routes. Let the traffic resistance for the route 1 be R, for route 2 be $2R$ and for route 3 be $4R$ as shown in Table 6.1. Then by the comparison of the traffic resistances of the three routes, it can be noted that route 3 will take 4 times travelling time as that of route 1 and 2 times as that of route 2.

Table 6.1: Traffic Resistance and Time Delay of Routes

Name	Parameter	Value
traffic resistance of route 1	R_1	R
traffic resistance of route 2	R_2	$2R$
traffic resistance of route 3	R_3	$4R$
time delay of route 1	Y_1	1
time delay of route 2	Y_2	2
time delay of route 3	Y_3	4

The fluctuations in flow will be minimum in route 1, as there will be less fluctuations in velocity. The density on route 1 will be minimum among the three routes.

6.6 Summary

Since the trip time is dependent on the velocity profile, therefore a route merit was proposed based on the fluctuations in velocity. The air pollution level and consumption of fuel improve with the minimum fluctuations in traffic velocity. The Mach number, relative trip time and traffic resistance were used to evaluate route merit to realistically predict traffic behavior. The route merit can either be used as soft or hard data for a road network selection. The simplicity of route merit calculation in a road network based on electric resistance is noteworthy.

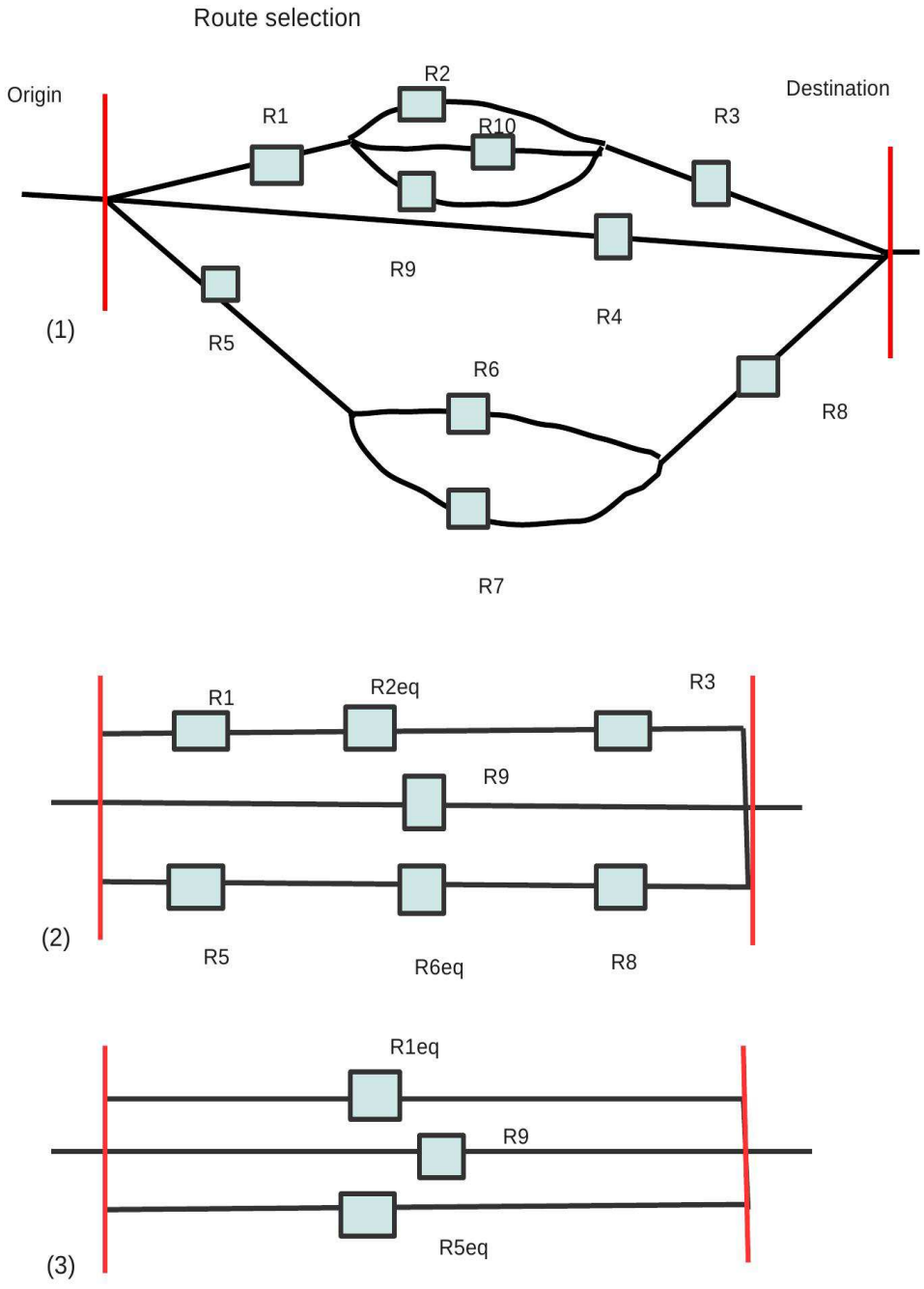

Figure 6.4: Selection of a route.

Chapter 7

Conclusions

This chapter summarizes the contributions to traffic flow models presented in this dissertation. A brief outline of the accomplishments are given with comments on their importance.

7.1 Contributions

In this dissertation, vehicle traffic modelling for intelligent transportation systems was investigated. The goal was to develop realistic traffic flow models. Five subproblems were formulated to characterize the traffic flow such that congestion and pollution are mitigated. The following traffic modelling problems were studied.

1. The study was started by investigating the PW model for its unrealistic stop and go behavior at discontinuities. The traffic flow changes according to the conditions ahead. Based on this property, a new model was proposed such that traffic velocity and density adjust in proportion to the change ahead. This model mitigates the deficiencies of the PW model.

2. The transition behavior of traffic flow with the LWR model was investigated. The LWR characterizes the traffic flow on a long idealized road. The flow adjustment to the traffic ahead depends on the safe velocity. Based on this property, a new model was proposed which included the realistic parameters to predict the traffic flow during transitions.

3. A new model was proposed to characterize the physiological and psychological response of driver to changes in the traffic flow. For a slow response, the traffic

becomes clustered, while for a fast response the traffic flow is more uniform. A regulation parameter was introduced to further refine the driver response to forward conditions. This allows for a more realistic traffic characterization than with other models in the literature.

4. A new model was proposed to characterize the distribution of traffic flow on the basis of safe time, vehicles interaction, velocity and driver response. The model was compared with the PW model and it was found that traffic clusters with the new model span a large distance. The proposed model avoids congestion and tends to produce a smooth traffic flow behavior.

5. Route merits were proposed based on the velocity profile of a route. The route merit can be determined on the basis of real-time or pre-recorded data. The simplicity of selection of a road network or a road is noteworthy.

Solutions to the above problems are proposed to realistically characterize the traffic flow to mitigate congestion and improve public safety.

7.2 Future Work

There are some interesting future research problems for traffic flow modelling for intelligent transportation systems.

- A noteworthy problem is to develop a distribution for the safe distance. Different traffic flow situations have different safe distances due to drivers response. This safe distance affects the traffic flow dissemination and distribution.

- Another important problem is to develop a realistic equilibrium density distribution. This distribution should be based on the psychological and physiological response of drivers.

- An interesting problem is the development of a distribution for the regulation value of the model proposed in Chapter 4. This distribution should be based on the driver response.

- All of the developed models can be extended to crowd modeling to effectively disseminate crowd traffic in case of emergency evacuation.

Bibliography

[1] H. J. Payne, "Models of freeway traffic and control," *Simulation Council Proc.,* vol. 1, no. 1, pp. 51–61, Jan. 1971.

[2] M. J. Lighthill and J. B. Whitham, "On kinematic waves II: A theory of traffic flow on long crowded roads," *Proc. Royal Soc. A,* vol. 229, pp. 317–345, May 1955.

[3] C. F. Daganzo, "Requiem for second-order fluid approximations of traffic flow," *Transpn. Res. B,* vol. 29, no. 4, pp. 277–286, Aug. 1995.

[4] J. M. Del Castillo, P. Pintado, and F. G. Benitez, "The reaction time of drivers and the stability of traffic flow," *Transpn. Res. B,* vol. 28, no. 1, pp. 35–60, Feb. 1994.

[5] M. Papageorgiou, "Some remarks on macroscopic traffic modelling," *Transpn. Res. A,* vol. 32, no. 5, pp. 323–329, Sept. 1998.

[6] M. Papageorgiou, J.-M. Blosseville, and H. Hadj-Salem, "Modelling and real-time control of traffic flow on the southern part of Boulevard Peripherique in Paris, Part-1: Modelling," *Transpn. Res. A,* vol. 24, no. 5, pp. 345–359, Sept. 1990.

[7] G. B. Whitham, *Linear and Nonlinear Waves,* New York: Wiley, 1974.

[8] A. Aw and M. Rascle, "Resurrection of "second order" models of traffic flow," *SIAM J. Appl. Math.,* vol. 60, no. 3, pp. 916–938, Feb. 2000.

[9] B. S. Kerner and P. Konhuser, "Cluster effects in initially homogeneous traffic flow," *Phys. Rev. E,* vol. 48, no. 4, pp. 2335–2338, Oct. 1993.

[10] P. Berg, A. Mason, and A. Woods, "Continuum approach to car-following models," *Phys. Rev. E,* vol. 61, no. 2, pp. 1056–1066, Feb. 2000.

[11] P. L. Roe, "Approximate Riemann solvers, parameter vectors, and difference schemes," *J. Comput. Phys.,* vol. 43, no. 2, pp. 357–372, Oct. 1981.

[12] R. Herman and I. Prigogine, "A two-fluid approach to town traffic," *Science, New Series* vol. 204, no. 4389, pp. 148–151, Apr., 1979.

[13] S. Ardekani and R. Herman, "A comparison of the quality of traffic in downtown networks of various cities around the world," *Traffic Eng. Control,* vol. 26, pp. 574–581, 1985.

[14] S. Ardekani and R. Herman, "Urban network-wide traffic variables and their relations," *Transpn. Sci.,* vol. 21, pp. 1–16, 1987.

[15] R. Herman, L. Malakhoff and S. Ardekani, "Trip time-stop time studies of extreme driver behaviors," *Transpn. Res. A,* vol. 22, pp. 427-433, 1988.

[16] I. Prigogine and R. Herman, *Kinetic Theory of Vehicular Traffic,* Elsevier: New York, 1971.

[17] H. Mahmassani, J. C. Williams and R. Herman, "Performance of urban traffic networks", *Proc. Symp. on Transpn. and Traffic Theory,* Elsevier, 1987.

[18] S. Y. Hong, S. B. Chung, C. Lee and S. Y. Kho, "Analysis of two-fluid model using GPS data," *J. Eastern Asia Soc. for Transpn. Stud.,* vol. 6, pp. 560 - 572, 2005.

[19] M. Treiber, A. Kesting and C. Thiemann, "How much traffic congestion increase fuel consumption and emissions? Applying fuel consumption model to NGSIM trajectory data," *Proc. Annu. Meeting of the Transpn. Res. Board,* 2008.

[20] S. L. Hallmark, R. Guensler and I. Fomunung, "Characterizing on road variables that affects passengers vehicle modal operation," *Transpn. Res. D,* vol. 7, pp. 81-98, 2002.

[21] S. Chiquetto, "The environmental impacts from the implementation of a pedestrian scheme," *Tranpn. Res. D,* vol. 2, pp. 133-46 1997.

[22] *www.grc.nasa.gov/WWW/K-12/airplane/mach.html.*

[23] Z. Shenpel and Y. Xinping, "Driver's route choice model based on traffic signal control," *IEEE Proc. Conf. on Indust. Electron. and Applicat.,* pp. 2331-2334, June 2008.

[24] P. Grantham and C. Ming-Hei, "Route selection for vehicle navigation and control," *IEEE Proc. Conf. on Indust. Electron. Soc.,* pp. 2586–2591, Nov. 2007.

[25] N.B. Hounsell, M. Mcdonald and R. A. Lambert, "The integration of scoot and dynamic route guidance," *IEEE Proc. Conf. on Road Traffic Monitoring and Control,* pp. 168-172, April 1992

[26] G. Hoffmann and J. Janko, "Travel times as a basic part of the LISB guidance strategy," *IEE Proc. Conf. on Road Traffic Control,* pp. 6-10, May 1990.

[27] T. Saito, J. Shima, H. Kanemitsu and Y. Tanaka, "Automobile navigation system using beacon information," *Proc. Conf. on Vehicle Navigation and Inform. Syst.,* pp. 139-144, 1989.

[28] W. H. Hayt and J. E. Kemmerly, *Engineering Circuits Analysis,* McGraw Hill, 1971.

[29] A. A. Trani, *Transportation systems analysis modelling,* lectures, Dept. Civil Eng., Univ. Virginia Tech., Blacksburg, VA, Nov 2011.

[30] F. Durst, *Fluid Mechanics: An Introduction to the Theory of Fluid Flows,* Springer, Berlin, 2008.

[31] A. Nakrachi, S. Hayat and D. Propescu, "An energy cocept for maroscopic traffic flow modeling." *Eur. Transp. Res. Rev.,* vol. 4, pp. 57-66, 2012.

[32] J. V. Morgan, "Numerical methods for macroscopic traffic models," Ph.D. dissertation, Dept. Math., Univ. Reading, Berkshire, UK, 2002.

[33] A. Muralidharan, "Tools for modelling and control of freeway networks," Ph.D. dissertation, Dept. Mech. Eng., Univ. California, Berkeley, USA, 2012.

[34] W., Jin, "Traffic flow models and their numerical solutions," Ph.D. dissertation, Dept. Math., Univ. California, Davis, CA, 2003.

[35] A. K. Gupta and V. K. Katiyar, "A new anisotropic continuum model for traffic flow," *Phys. Rev. A,* vol. 368, no. 2, pp. 551–559, Jan. 2006.

[36] T. Li, "Instability and formation of clustering solutions of traffic flow," *Bull. Inst. of Math. Academia Sinica (New Series)*, vol. 2, no. 2, pp. 281–295, 2007.

[37] T. Q. Tang, H. J. Huang, Z. Y. Gao, and S. C. Wong, "Interaction of waves in the speed-gradient traffic flow model," *Physica A,* vol. 380, no. 1, pp. 481–489, July 2007.

[38] S. Fengchum, W. Hui, and L. Hong, "A mesoscopic model for bicycle flow," *Proc. Chinese Control Conf.,* pp. 5574–557, July 2011.

[39] H. M. Zhang, "A non-equilibrium traffic model devoid of gas-like behaviour," *Transpn. Res. B,* vol. 36, no. 3, pp. 275–290, Mar. 2002.

[40] G. Strang, *Introduction to Applied Mathematics*, 4th Ed. Wellesley-Cambridge Press: Wellesley, MA, 2009.

[41] P. I. Richards, "Shock waves on the highway," *Operations Res.,* vol. 4, no. 1, pp. 42–51, Feb. 1956.

[42] N. Bellomo and C. Dogbe, "On the modelling of traffic and crowds: A survey of models, speculations, and perspectives," *SIAM Rev.,* vol. 53, no. 3, pp. 409–463, Nov. 2011.

[43] A. Klar and R. Wegener, "Kinetic derivation of macroscopic anticipation models for vehicular traffic," *SIAM J. Appl. Math.,* vol. 60, no. 5, pp. 1749–1766, May 2000.

[44] D. Helbing, "Improved fluid dynamic model for vehicular traffic," *Phys. Rev. E,* vol. 51, no. 4, pp. 3164–3169, Apr. 1995.

[45] P. Kachroo, "Optimal and feedback control for hyperbolic conservation laws," Ph.D. dissertation, Univ. Virginia Tech., Blacksburg, VA, 2007.

[46] R. J. LeVeque, *Numerical Methods for Conservation Laws*, 2nd. Ed., Lectures in Math., ETH Zürich, Birkhäuser: Basel, Switzerland, 1992.

[47] E. F. Toro, *Riemann Solvers and Numerical Methods for Fluid Dynamics,* Berlin: Springer, 2009.

[48] Y. Yokoya, Y. Asano, and N. Uchida, "Qualitative change of traffic flow induced by driver response," *IEEE Conf. on Syst., Man and Cybernetics,* pp. 2315–2320, Oct. 2008.

[49] Z. Khan and T. A. Gulliver, "A macroscopic traffic model based on front traffic stimuli," submitted.

[50] Z. Khan and T. A. Gulliver, "A macroscopic traffic model based on anticipation," submitted.

[51] Z. Khan and T. A. Gulliver, "A macroscopic traffic model based on driver response," *J. Modern Traffic and Transpn. Eng. Research*, accepted.

[52] M. J. Kermani and E. G. Plett, "Modified entropy correction formula for the Roe scheme," *J. Amer. Inst. Aeronautics and Astronautics,* vol. 83, 2001.

[53] P. Benedetto and T. Andrea, "Vehicular traffic: A review of continuum mathematical models," *Math. of Complexity and Dynamical Syst.,* pp. 1748–1770, 2011.

[54] Z. Li and S. Qi, "Intelligent vehicle headway distance control system design," *Symp. on Intell. Inform. Technology Applicat.,* vol. 1, pp. 529–532, 2009.

[55] H. Zhang, "A theory of non-equilibrium traffic flow," *Transpn. Res. B,* vol. 32, no. 7, pp. 485–498, Sept. 1998.

[56] W. Jin, and H. M. Zhang, "Solving the Payne-Whitham traffic flow model as a hyperbolic system of conservation laws with relaxation," Technical Report UCD-ITS–Zhang–2001–1, Davis, 2001.

[57] B. Kakali et al., "Modelling reaction time with in a traffic simulation model," *IEEE Conf. on Intell. Transp. Syst.,* pp. 302–309, 2013.

[58] W. Jin, "Traffic flow models and their numerical solutions," Masters thesis, Dept. Math., Univ. California, Davis, CA, 2000.

[59] A. Harten and J. M. Hayman, "Self adjusting grid methods for one dimensional hyperbolic conservation laws," *J. Comput. Phy.,* vol. 50, pp. 253–269, 1983.

[60] B. D. Greenshields, "A study in highway capacity," *Proc. Highway Res. Board,* vol. 14, pp. 448–477, 1935.

[61] B. V. Leer, J. L. Thomas, P. L. Roe and R. W. Newsome, "A comparison of numerical flux formulas for the Euler and Navier-Stokes equations," *J. Amer. Inst. Aeronautics and Astronautics,* pp. 36–41, 1987.